Phenotypic and Functional Heterogeneity of Intermediate Monocytes in Healthy Adults

Eanna Connaughton

Regenerative Medicine Institute (REMEDI)

College of Medicine, Nursing and Health Sciences

National University of Ireland, Galway

A thesis submitted to National University of Ireland, Galway for a

Degree of Doctor of Philosophy

September 2015

Supervisors: Professor Matthew Griffin and

Professor Rhodri Ceredig

Table of Contents

Declaration

This thesis describes work that I undertook between 2011 and 2015 at the Regenerative Medicine Institute, National University of Ireland, Galway. This work was supervised and mentored by Professors Matthew Griffin (Transplant Biology) and Rhodri Ceredig (Immunology).

I declare that the results presented herein are from original experimental work which has been carried out by me for the purpose of this thesis. The work described within this thesis has not been submitted for degree, diploma or other qualification at any other University.

I have no conflict of interest pertaining to the subject matter of this work.

Funding Authorities

This work was funded by Molecular Medicine Ireland (MMI) Clinical & Translational Research Scholars Programme, which is funded under the Programme for Research in Third Level Institutions (PRTLI) Cycle 5, and co-funded under the European Regional Development Fund (ERDF).

Acknowledgements

Firstly, I am immensely grateful to my supervisors, Matt Griffin and Rhodri Ceredig, for the mentorship and advice over the past four years. Your doors were never closed, and the time and effort you invested in me over the years has contributed immensely to the scientist I am today. I would also like to thank Conall Dennedy for his advice throughout the years.

I would like to thank the members of the immunology group for their advice and friendship over the years. I would especially like to thank Stephanie Slevin, Senthil Alagesan, Joana Cabral and Andreia 'are you kidding me' Ribeiro for their scientific advice and opinions. I would also like to thank Ronan Downey from the Prostate Cancer group for his advice and expertise towards the end of my study. I am grateful to Shirley Hanley for her expertise in cell sorting and advice on flow cytometry matters.

I am thankful to the staff within REMEDI for their assistance throughout the years, especially Siobhan Gaughan, Kieran Ryan, Noreen Ryan, Robert Giblin and Enda O'Connell.

I would like to thank my family, girlfriend and friends for all their support, belief and patience throughout the years. Without this I would not be where I am today. Thanks to Steph, Martina, Enda, Rose, Seamus, Grainne and last but not least, Bridgie.

Finally, to Wesley, it was a pleasure to be your colleague and friend over the past years. You will be sadly missed.

'*To sleep: perchance to dream: ay, there's the rub; for in that sleep of death what dreams may come'*

Wesley van Oeffelen RIP

Dedicated to my parents

Enda and Martina Connaughton.

Abstract

Human blood monocytes are currently classified into three subsets: $CD14^{++}CD16^{-}$ "Classical", $CD14^{++}CD16^{+}$ "Intermediate" and $CD14^{+}CD16^{++}$ "Non-Classical". Distinct functional differences between Classical and Non-Classical have been described but the role of Intermediate monocytes is less clear.

In profiling monocytes from healthy adults by multi-colour flow cytometry, we observed that Intermediate monocytes exhibit dichotomous surface expression of the Class II major histocompatibility protein HLA-DR, with separate sub-populations expressing mid- (DR^{mid}) and high-levels (DR^{hi}). Further profiling of cell surface markers demonstrated that, compared to the DR^{hi} subset, DR^{mid} Intermediate monocytes express higher levels of CCR2 and CD62L, and lower levels of CD45, CX3CR1, LFA-1, VLA-4 and Mac-1, indicating heterogeneity for multiple functionally-relevant proteins.

We assessed how the newly described Intermediate sub-populations interact with and migrate through endothelium in in vitro assays. Results indicated both the DR^{mid} and DR^{hi} subsets are highly adherent to resting and activated primary human aortic endothelium, with adherence of the DR^{mid} subset being partially mediated by CD11a. Both sub-populations exhibited poor CCL2-induced transmigration in contrast to the highly migratory $CCR2^{+}$ Classical monocytes, despite the fact that DR^{mid} and DR^{hi} subset expressing $CCR2^{+}$ and $CCR2^{int}$ phenotypes respectively.

Further experiments revealed reduced intracellular calcium release and filamentous actin polymerisation, suggesting early termination of the CCL2-CCR2 signal. Chemokine receptors are G-protein coupled receptors (GPCRs), and GPCR signalling may be regulated by Regulator of G-Protein Signalling (RGS) proteins. We quantified mRNA levels of RGS1, 2, 12 and 18 in the monocyte subsets. Interestingly, elevated RGS1 was detected in the newly-described Intermediate monocyte subpopulations. RGS1 has been implicated as a negative regulator of CCR2 signalling in monocytes. Therefore, the results are consistent with a role for RGS1 up-regulation in the blunted CCL2-induced signalling and migration of the DR^{mid} and DR^{hi} intermediate monocytes.

Overall, the results of this project add novel details to current knowledge regarding human Intermediate monocytes provide further evidence for heterogeneity within this monocyte subset and indicate that changes in the intracellular regulation of chemokine receptor signalling may contribute to DR^{mid} intermediate monocyte expansion in the circulation during inflammatory disorders.

List of Figures

List of Tables

Abbreviations

[^{3}H]-thymidine	3HT
Acetylated-Low Density Lipoprotein	ac-LDL
Analysis of Variance	ANOVA
Angiotensin Converting Enzyme	ACE
Antigen Presenting Cell	APC
Apolipoprotein E	APOE
B-cell Lymphoma 2	BCL-2
Becton Dickinson	BD
Bone Marrow	BM
Bovine Serum Albumin	BSA
Chemokine Ligand	CCL
Chronic Kidney Disease	CKD
c-Jun N-terminal kinase	JNK
Colony Stimulating Factor-1	CSF-1
Common Monocyte Precursor	cMoP
Complementary DNA	cDNA
Counter Current Centrifugal Elutriation	CCE
CXCL12 Abundant Reticular Cells	CARs
Dendritic Cells	DCs
Deoxyribonucleic Acid	DNA
Diaglycerol	DAG
Diethylpyrocarbonate	DEPC
Dulbecco's Phosphate Buffered Saline	D-PBS
Ethidium Bromide	EtBr

Ethylenediaminetetraacetic Acid	EDTA
Filamentous Actin	F-actin
Fluorescence Minus One	FMO
Fluorescent Activated Cell Sorting	FACS
Foetal Calf Serum	FCS
Forward Scatter	FSC
Glycosaminoglycans	GAGs
G-Protein Coupled Receptor	GPCR
G-Protein Receptor Kinases	GRKs
Granulocyte-Colony Stimulating Factor	G-CSF
Green Fluorescent Protein	GFP
Guanine Exchange Factors	GEFs
Guanosine Diphosphate	GDP
Guanosine Triphosphate	GTP
Herpes Simplex Virus-1	HSV-1
Highly Active Antiretroviral Therapy	HARRT
Human Aortic Endothelial Cells	HAECs
Human Immunodeficiency Virus	HIV
Inositol 1,4,5-trisphosphate	IP3
Interferon Beta 1	IFN-β
Interleukin	IL
Intracellular Adhesion Molecule-1	ICAM-1
Junctional Adhesion Molecule	JAM
Leukaemia Inhibitory Factor	LIF
Lipopolysaccharides	LPS

Lipoteichoic Acid	LTA
Lymphocyte Function Associated Antigen-1	LFA-1
Macrophage-1 Antigen	MAC-1
Magnetic Activated Cell Sorting	MACs
Major Histocompatibility Complex	MHC
Mannose Receptor	MR
Median Fluorescent Intensity	MFI
Mesenchymal Stem Cells	MSCs
Mitogen-Activated Protein Kinase	MAPK
Mixed Lymphocyte Reaction	MLR
Monoclonal Antibody	mAb
Monocyte Chemotactic Protein	ova
Oxidised Low-Density Lipoprotein	oxLDL
Paraformaldehyde	PFA
Peripheral Blood Mononuclear Cells	PBMCs
Phosphate Buffered Saline	PBS
Phosphatidylinositide 3-Kinase	PI3K
Phosphatidylinositol 4,5-bisphosphate	PIP2
Phospholipase C	PLC
Platelet Endothelial Cell Adhesion Molecule	PECAM-1
Polymerase Chain Reaction	PCR
Polymorphonuclear Cells	PMNs
Protein Kinase C	PKC
P-selection Glycoprotein Ligand-1	PSGL-1
Quantitative RT-PCR	qRT-PCR

Reactive Oxygen Species	ROS
Real Time Polymerase Chain Reaction	RT-PCR
Red Blood Corpuscles	RBCs
Regulated on activation, normal T cell Expressed and secreted	RANTES
Regulator of G-Protein Signalling	RGS
Relative Centrifugal Force	RCF
Revolutions per Minutes	RPM
Ribonucleic Acid	RNA
Serum Alanine aminotransferase	ALT
Side Scatter	SSC
Single Stain	SS
Sodium Azide	NaN3
Sphingosine-1-phosphate receptor 5	S1PR5
Staphylococcal Enterotoxin B	SEB
Stem Cell Factor	SCF
Stromal Cell-Derived Factor 1	SDF-1
Toll Like Receptor	TLR
Tropomyosin Receptor Kinase A	TrkA
Tumour Necrosis Factor	TNF
Vascular Cell Adhesion Molecule-1	VCAM-1
Very Late Antigen-4	VLA-4
Vesiculo-vacular Organelles	VVOs
Wild Type	WT
Yellow Fluorescent Protein	YFP

Chapter 1

Introduction 1.0

Monocyte Subsets and their Classification 1.1

Monocytes represent a heterogeneous population of myeloid cells, comprising 5-10% of peripheral blood mononuclear cells (PBMCs) in humans. Evidence of monocyte heterogeneity is observed in cell size, granularity and morphology (Gordon and Taylor, 2005). They are multifunctional cells with roles in immune defence, tissue repair and homeostasis. Monocytes are involved in the innate immune response to viral, bacterial and fungal infections and represent a key link between the innate and adaptive arms of the immune system (Cros et al., 2010). Current knowledge indicates a variety of roles for monocytes in humans, including but not limited to: Phagocytosis and antigen presentation, production of cytokines and chemokines, patrolling of vasculature and tissue for inflammation, and differentiation/phenotypic change into tissue macrophages and dendritic cells (DCs). Monocytes are non-dividing cells arising in the bone marrow (BM) from common myeloid progenitor cells which migrate to the circulation for a short period (1-3 days) and then either die via sequestration in the spleen or extravasate to tissues and organs via a co-ordinated engagement of chemokine signals and endothelial adhesion receptors to serve various effector functions. In 2010, an international agreement on human monocyte nomenclature acknowledged three distinct sub-populations of human monocytes based on cell surface expression of CD14 and CD16 (**Figure 1.1**), namely $CD14^{++}CD16^{-}$ "Classical", $CD14^{++}CD16^{+}$ "Intermediate" and $CD14^{+}CD16^{++}$ "Non-Classical" subsets (Ziegler-Heitbrock et al., 2010). Of particular interest are the newly classified Intermediate monocytes which may have been overlooked in previous monocyte studies.

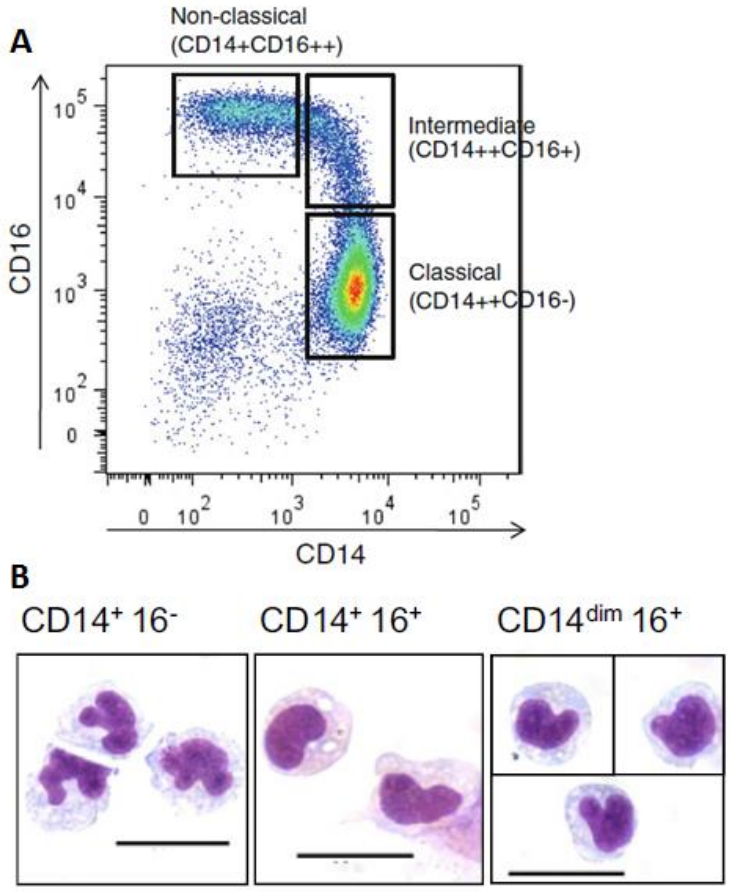

Figure 1. 1 Phenotypic and morphological characterisation of human monocytes

(**A**) Using flow cytometry, human monocytes can be classified into 3 distinct subtypes based on cell surface expression of CD16 and CD14, producing $CD14^{++}CD16^{-}$ "Classical", $CD14^{++}CD16^{+}$ "Intermediate" and $CD14^{+}CD16^{++}$ "Non-Classical" subsets. (**B**) Morphological characteristics of human monocyte subsets. Image **A** is adapted from Wong et al. *Blood*, 118(5):e16-31 2011. Image **B** is adapted from Cros et al. *Immunity*, 33(3):375-86, 2010.

Murine monocytes are divided into two distinct subsets based on cell surface expression of Ly6C, namely $Ly6C^{hi}$ and $Ly6C^{lo}$ monocytes. These are considered to represent the human equivalents of Classical and Non-Classical monocytes respectively. To date, there is no murine population that has been identified as being representative of the human Intermediate monocytes. The murine and human subsets also share similar cell surface expression of defining chemokine receptors CCR2 and CX3CR1 with Classical/$Ly6C^{hi}$ monocytes being $CCR2^{high}/CX3CR1^{low}$ and Non-Classical/$Ly6C^{lo}$ monocytes being

$CCR2^{low}/CX3CR1^{high}$ (Sunderkotter et al., 2004, Geissmann et al., 2003). Of note, human Intermediate monocytes reportedly express CCR2 and CX3CR1 at intermediate levels in comparison of the Classical and Non-Classical subsets. Additionally, genomic profiling of human and murine Classical and Non-Classical counterparts indicates similar gene expression characteristics between the species, suggesting that information obtained using mouse models may be applicable to human monocytes (Ingersoll et al., 2010, Ziegler-Heitbrock, 2014, Cros et al., 2010).

Functions of monocyte subsets 1.2

Monocytes perform a broad array of functions throughout the body and display remarkable functional and migratory plasticity. Monocytes contribute to localised and systemic inflammation, but also mediate regulatory functions in a physiological (steady-state) setting. As a result, monocyte phenotype and function is greatly shaped by cues and stimuli within their immediate environment. In vitro and in vivo studies of both murine and human monocytes have provided strong evidence of functional diversity among monocytes subsets.

Classical Monocytes 1.2.1

Classical monocytes represent approximately 85% of total monocytes in the circulation during health with Intermediate monocytes typically comprising 5% and Non-Classical monocytes 10% (Cros et al., 2010). Classical monocytes are phenotypically defined as $CD14^{+}$, $CD16^{-}$, $CCR2^{hi}$, $CX3CR1^{lo}$, $CD62L^{hi}$ in human and $Ly6C^{+}$, $CCR2^{hi}$, $CX3CR1^{lo}$, $CD62L^{hi}$ in mouse. Classical monocytes are commonly viewed as being pro-inflammatory and highly phagocytic. For example, Classical monocytes avidly phagocytose latex beads (Cros et al., 2010, Zawada et al., 2011) and concurrently display high levels of reactive oxygen species (ROS) and mRNA for myeloperoxidase and lysozyme enzymes (Cros et al., 2010). Intermediate monocytes also display high levels of bead phagocytosis, although less so than Classical monocytes while Non-Classical monocytes phagocytose beads relatively poorly (Zawada et al., 2011, Cros et

al., 2010). Both Intermediate and Non-Classical subsets are reported to produce low amounts of ROS along with low levels of myeloperoxidase and lysozyme (Cros et al., 2010). Human Classical monocytes respond strongly to TLR4 agonist LPS, producing distinct high amounts of interleukin (IL) -10, IL-8, IL-6, RANTES (regulated on activation, normal T cell expressed and secreted), chemokine ligand (CCL)2, CCL3 (Cros et al., 2010, Wong et al., 2011) and moderate amounts of tumour necrosis factor alpha (TNF-α) (Cros et al., 2010).

In contrast, Classical monocytes stimulated proliferation in allogeneic mixed lymphocyte reactions (MLR) as measured by [^{3}H]-thymidine (3HT) incorporation to a lesser degree than Intermediate and Non-Classical monocytes (Cros et al., 2010). To more specifically investigate the ability of human monocytes to process and present antigens to T cells, highly purified monocyte subsets and autologous T cells from tetanus-vaccinated donors were co-cultured in the presence of tetanus toxoid, with DC/T cell co-culture used as a positive control (Cros et al., 2010). In contrast to DCs, none of the monocyte subsets stimulated significant antigen-dependent T cell proliferation (Cros et al., 2010). In a separate study, staphylococcal enterotoxin B (SEB) was added to isolated monocyte subsets and $CD4^+$ T cell co-cultures. In this case, the Intermediate subset produced the greatest T-cell proliferation (52.4±10.8%), followed by Classical (45.4±7.9%) and Non-Classical subsets (42.2±16.1%), as assessed by cytoplasmic dilution of a fluorescent dye (Zawada et al., 2011). In this study, however, there was no presentation of negative control data (T cells without monocytes or SEB) and no comparison with the effects of professional antigen presenting cell, such as DCs (Zawada et al., 2011). Another study used highly purified monocyte subsets isolated from diseased livers to present *m. tuberculosis* antigenic peptides to autologous $CD4^+$ T cells. This study revealed weak T cell proliferation induced by Classical monocytes and relatively higher proliferation induced by Intermediate and Non-Classical monocytes which was comparable to that induced by isolated liver DCs (Liaskou et al., 2013). Thus, although results have varied to date, there is evidence that Classical monocytes have relatively weaker primary antigen presenting capacity compared to other monocyte subsets.

Monocytes have long been thought to replenish tissue macrophages, as evidenced by the landmark studies of van Furth and Cohn in which 3HT labelling was used to track the fate of blood monocytes and indicated that they replenish tissue resident-macrophages (van Furth and Cohn, 1968). This paradigm was further strengthened by the propensity of monocytes to transform into macrophages under the influence of varying stimuli in vitro. However, while monocytes and tissue macrophage development have long been considered to be inextricably linked, emerging evidence indicates an alternative paradigm for tissue macrophage development in the steady state. For example, recent studies revealed that tissue macrophages are embryonically derived and that progenitors exist in that compartment and are constantly replenishing by self-renewal. Definitive cell lineage tracing studies indicated microglia (brain macrophages) are primarily derived from yolk-sac progenitors and that alveolar macrophages (Hashimoto et al., 2013), Kupffer cells (Yona et al., 2013) , splenic macrophages (Yona et al., 2013, Hashimoto et al., 2013), and Langerhans cells (Hoeffel et al., 2012) are all seeded before birth with minimal contribution from blood monocytes in the steady state during adulthood. Nonetheless, in the steady state, blood monocytes, particularly $Ly6C^+$ (Classical) monocytes have been shown in mouse to contribute to macrophage populations in tissues with high macrophage turnover and exposure to microbiota such as the gut (Zigmond and Jung, 2013) and skin (Jakubzick et al., 2013). Furthermore, recent studies also indicate that $Ly6C^+$ monocytes in mouse are the main contributors to the accumulation of macrophages during localised inflammation (Wynn et al., 2013, Jakubzick et al., 2013, Yona et al., 2013).

Importantly, however, it is not obligatory for Classical monocytes to differentiate into macrophages following tissue transmigration, and, rather, their fate is determined by tissue-specific signals. For example, in the steady state (with the exception of the gut and skin) $Ly6C^+$ monocytes have been observed to enter tissue with minimal differentiation toward a macrophage phenotype (Jakubzick et al., 2013), preserving their mononuclear functional identity. In the absence of inflammation, $Ly6C^+$ monocytes have been shown

to be present in the skin, lung and lymph nodes, and genetic profiling of Ly6C$^+$ monocytes isolated from these sources resulted in tissue-derived monocytes clustering with the genetic profile of Ly6C$^+$ blood monocytes and not with isolated CD11b$^-$ and CD11b$^+$ lung macrophages populations, indicating minimal post-migration differentiation. However, among the transcripts that were found to be up-regulated in tissue versus blood-derived monocytes were *Ptgs2* (COX-2), *Il1b* (IL-1β), Tnfaip3 (A20) and *Itgax* (CD11c). In a parabiosis model between a CD45.1 WT and CD45.2 *Ccr2*$^{-/-}$ partners, WT monocytes efficiently populated the *Ccr2*$^{-/-}$ host. At 1 year, macrophages in the skin of *Ccr2*$^{-/-}$deficient mice were fully replenished by CD45.1 macrophages, demonstrating that monocytes contribute significantly to skin macrophage population. In contrast, there was no contribution of CD45.1 monocytes to the lung macrophages compartment when examined at the same time point, confirming the lack of a role for Classical monocytes in maintaining tissue macrophage populations in this tissue (Hashimoto et al., 2013) and suggesting alternative roles for lung monocytes (Jakubzick et al., 2013). Ly6C$^+$ monocytes depend somewhat on CD62L to enter tissue and lymphatic vessels, as evidenced by a disadvantage of CD62L-deficient (*Sell*$^{-/-}$*)* Ly6C$^+$ monocyte migration to skin and lymph nodes in CD45.1 WT mouse lethally irradiated and BM reconstituted with CD45.2 *Sell*$^{-/-}$ BM (Jakubzick et al., 2013). In this study, intra-nasally administered FITC-ovalbumin (ova) was acquired by lung monocytes, and approximately 6% of lymph node monocytes were FITC$^+$ 24 hours after administration. In the absence of inflammation, this points to an antigen-searching role for tissue monocytes with subsequent migration to the lymph nodes, although FITC$^+$ DCs outnumbered monocytes tenfold in the lymph nodes. When a FITC-ova source known to cause inflammation was administered, the number of FITC$^+$ monocytes in the lymph nodes were doubled, but remained substantially lower than the number of FITC$^+$ DCs (Jakubzick et al., 2013). This evidence points toward Ly6C$^+$ 'Classical' monocytes possessing a tissue-specific antigen surveying role without obligation for macrophage differentiation in the steady state.

Non-Classical Monocytes 1.2.2

Non-Classical monocytes are phenotypically defined as $CD14^{dim}$, $CD16^{++}$, $CCR2^{lo}$, $CX3CR1^{hi}$, $CD62L^{lo}$ in human and $Ly6C^{-}$, $CCR2^{lo}$, $CX3CR1^{hi}$, $CD62L^{lo}$ in mouse. Of note, human Non-Classical monocytes can be further subdivided into Slan $(M\text{-}DC8)^{+}$ and $Slan^{-}$ populations, however there have not been any distinct characteristics assigned to these Slan-based subs-populations (Cros et al., 2010). Non-Classical monocytes are considered to represent a more mature cell in contrast to the other monocyte subsets and have a longer half-life in the circulation (Yona et al., 2013). A defining feature of Non-Classical monocytes in both human and mouse is their manifestation of a crawling or patrolling behaviour on endothelial surfaces. In mouse, this endothelial crawling by $Ly6C^{-}$ monocytes was shown to be critically mediated by interaction of the integrin lymphocyte function-associated antigen-1 (LFA-1) with ICAM-1 (Auffray et al., 2007, Carlin et al., 2013, Sumagin et al., 2010). LFA-1 and other integrins are conserved between species (Vidovic et al., 2003). In a study by Cros et al, purified Non-Classical human monocytes were labelled with a fluorescent tag and injected intravenously into immune deficient *Rag2*$^{-/-}$ *Il2rg*$^{-/-}$ mice (Cros et al., 2010). Using intra-vital microscopy, transferred human Non-Classical monocytes were seen to rapidly adhere to and crawl along the endothelium of vessels in the ear dermis for extended periods of time. When a LFA-1 blocking antibody was administered, it completely neutralised Non-Classical monocyte crawling behaviour (Cros et al., 2010). This patrolling behaviour was also exhibited in vitro when Non-Classical human monocytes were perfused over micro- and macrovascular endothelium, and long range-crawling was inhibited by blocking ICAM-1, CX3CR1 and VCAM-1 interactions. Of note, Non-Classical monocytes adhered more strongly to microvascular compared to macrovascular endothelium (Collison et al., 2015). In contrast, Classical monocytes adhered more strongly to macrovascular endothelium and their long-range crawling was specifically dependant on ICAM-1 and was accompanied by transmigration through the endothelium (Collison et al., 2015). In contrast, Intermediate monocytes adhered to microvascular endothelium and remained static, exhibiting no crawling behaviour (Collison et

al., 2015). In another study, in which monocytes subsets were perfused over human hepatic sinusoidal endothelial cells in vitro, Intermediate and Non-Classical monocytes rolled, adhered and transmigrated in contrast to Classical monocytes which largely remained adherent (Liaskou et al., 2013). Although more studies are required, these observations indicate that individual monocyte subsets exhibit distinctive interactions with endothelium in tissue-specific fashion.

In regard to innate immune functions, purified human Non-Classical monocytes were found to respond poorly to TLR4 (LPS) and TLR2 (PAM3CK4) agonists producing small to no amounts of pro-inflammatory mediators (IL-1β, CCL2, IL-10, IL-8, IL-6, CCL3), while producing large amounts of the anti-inflammatory IL-1 receptor antagonist in overnight, un-stimulated culture (Cros et al., 2010). This evidence might suggest a primary anti-inflammatory phenotype. However, Non-Classical monocytes have also been shown to strongly produce a distinct set of cytokines in response to intact viruses and viral agonists via TLR7 and TLR8. When exposed to measles (ssRNA[-]) and herpes simplex virus 1 (HSV-1) (dsDNA), Non-Classical monocytes produced high amounts of CCL3 and pro-inflammatory cytokines TNF-α and IL-1β. In contrast, Classical monocytes produced high amounts of T cell, B cell and granulocyte helper chemokines and cytokines IL-6 and IL8 in response to these ligands while Intermediate monocytes produced the same cytokines as Classical and Non-Classical monocytes but at an 'intermediate' levels (Cros et al., 2010). It was postulated that divergent downstream signalling pathways may account for the distinct responses observed in Classical and Non-Classical monocytes in response to TLR7 and TLR8 agonists (**Figure 1.2**). In evidence of this, p38 mitogen-activated protein kinase (MAPK) was rapidly phosphorylated in $CD14^{+}$ monocytes following TLR8 stimulation while Non-Classical monocytes exhibited phosphorylation of p42 mitogen-activated protein kinase 1 (MEK1) followed by Jun N-terminal kinases (JNK) phosphorylation (Cros et al., 2010). Using pharmacological inhibitors, it was found that Non-Classical monocyte production of TNF-α, CCL3 and IL-1 following TLR7/8 stimulation was strongly

inhibited by MEK1 inhibitor but not p38 MAPK inhibition. Conversely, p38 MAPK inhibitor reduced IL-6 and IL-8 cytokine production by $CD14^+$ monocytes.

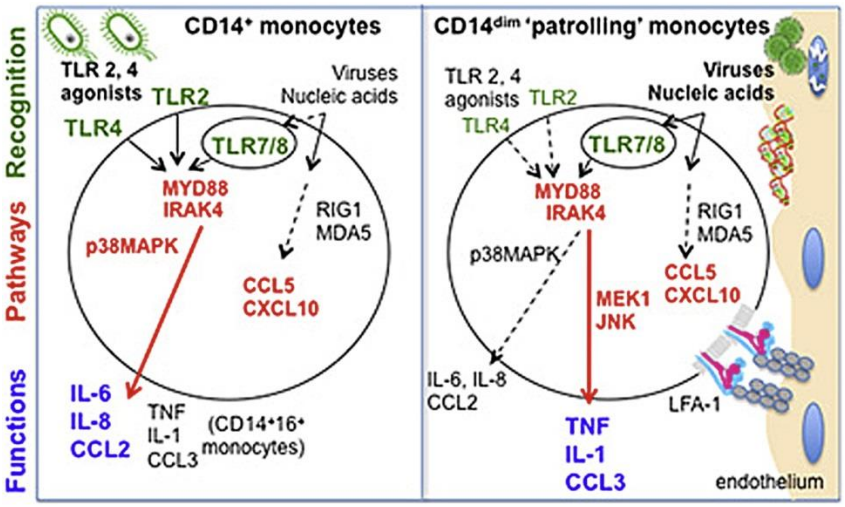

Figure 1. 2: Summary of distinctive responses of $CD14^+$ (Classical and Intermediate) and $CD14^{dim}$ (Non-Classical) human monocyte response to bacterial and viral stimuli

$CD14^+$ and $CD14^{dim}$ monocytes respond to viral stimuli via TLR7/TLR8. $CD14^{dim}$ monocytes signal through p42 (MEK) MAP kinase pathway to produce TNF-α, CCL3 and IL-1 in response to viral stimuli, suggesting a pro-inflammatory role upon viral recognition. In contrast, $CD14^+$ monocytes produce IL-6, IL-8 and CCL2 via p38 MAPK activation alongside classical NF-κB pathway. Image adapted from adapted from Cros et al. *Immunity*, 33(3):375-86, 2010.

To investigate the physiological role of Non-Classical monocyte sensing of nucleic acid danger signals via TLR7, a murine model in which homeostatic disruption of the kidney cortex was experimentally induced using the TLR7 ligand R848 ligand (Carlin et al., 2013). In *Cx3cr1*$^{gfp/+}$ mice, GFP^+ (Non-Classical) monocytes were observed by intra-vital microscopy to patrol and crawl along the kidney microvasculature under steady-state independent of *Cx3cr1* and *Ccr2* but critically mediated by LFA-1 interaction with ICAM-1 and ICAM-2 (Carlin et al., 2013). Painting of the kidney capsule with R848 resulted in increased Non-Classical monocyte adherence, crawling and retention along kidney capillaries mediated by CX3CR1 and integrin receptor Mac-1 (Sumagin et al., 2010). Neutralising antibodies to Mac-1 and genetic absence of CX_3CR_1

mice prevented accumulation of Non-Classical monocytes in TLR7-treated kidney capillaries (Carlin et al., 2013). Of note, TLR7 is ubiquitously expressed (Gunzer et al., 2005) and is present on kidney endothelium. Engagement of endothelial TLR7 by R848 results in up regulation of fractalkine (CX3CL1) and subsequent monocyte adhesion. Kidney endothelium exhibited severe focal damage at areas where Non-Classical monocytes had adhered and monocytes were observed to scavenge cellular debris and organelles. Furthermore, neutrophils clustered around the monocytes that had adhered to damaged areas of endothelium. Bone marrow chimeric mice, in which monocytes but not endothelium was TLR7 deficient revealed that endothelial TLR7 expression was required for monocyte recruitment (Carlin et al., 2013). However, TLR7 expression on monocytes was essential for neutrophil recruitment to the site, with Non-Classical monocytes producing CXCL1, a known neutrophil chemokine along with pro-inflammatory cytokines IL-1β, CCL3, IL-6 and TNF-α (Carlin et al., 2013). Importantly, this cytokine profile of murine Non-Classical monocytes is similar to the cytokine profile of their human counterparts in response to TLR7/TLR8 stimulation in vitro (Cros et al., 2010). The experimental evidence of this mouse study points towards a unique role for Non-Classical monocytes to survey endothelium in the steady state in a LFA-1/ICAM1-2 dependent manner and to respond to viral infection or tissue damage by sensing endothelial activation, adhering strongly and potentially mustering neutrophilic inflammation (**Figure 1.3**).

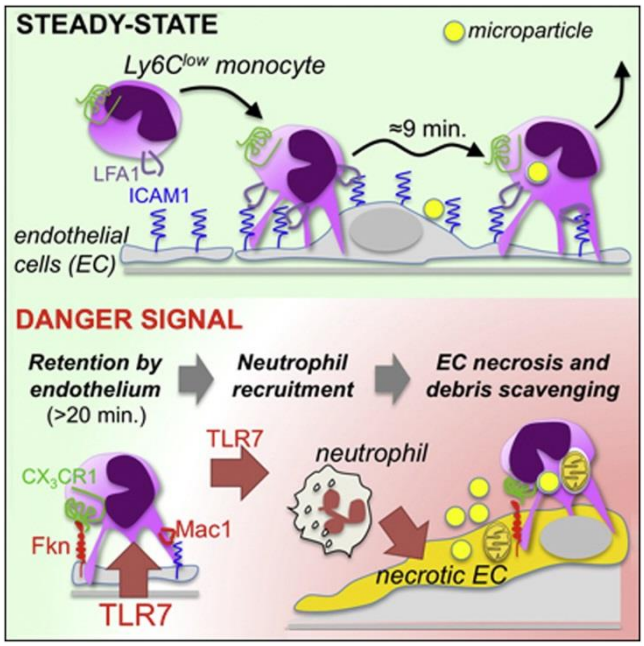

Figure 1. 3 Non-Classical monocytes mediate disposal of endothelial cells via neutrophil recruitment

Mouse Ly6C^{lo} 'Non-Classical' Monocytes crawl along endothelium sampling and scavenging micro-particles on the luminal surface in the steady state. When endothelial cells are damaged, upregulation of CX3CL1 on the cell surface retains the monocyte at this area. 'Danger signals' such as self-nucleic acids presented by the endothelium are sensed through monocyte TLR7, promoting cytokine production and neutrophil migration to the area. The neutrophils mediate endothelial necrosis and Ly6C^{lo} 'Non-Classical' monocytes dispose of cellular debris. Image adapted from Carlin et al. *Cell*, 153(2):362-75, 2013.

In contrast, a murine model of peritoneal infection using *L. monocytogenes* injection into the peritoneum indicated that Ly6C^{lo} monocytes extravasate quickly to the site of infection, peaking at 2 hours after injection (Auffray et al., 2007). This was in contrast to Ly6C^{hi} monocytes extravasation to the peritoneum which occurred several hours later. Furthermore, Ly6C^{lo} monocytes accounted for the early stage of inflammation through TNF-α production and also upregulation of chemokines including *Ccl7* (MCP-3, strong migratory chemokine for Ly6C^{hi} monocytes) and *Cxcl1*. Eight hours after Ly6C^{lo} extravasation, TNF-α and chemokine production was markedly reduced and an upregulation of genes associated with tissue remodelling [Arginase1, Fizz1, Mgl2, mannose receptor (MR)] was observed. This was accompanied by a switch to a 'typical' macrophage phenotype evidenced by upregulation of

transcription factors cMaf and MafB. Ly6C^{+} monocytes which appeared in the peritoneal cavity at a later time appeared to adopt a 'DC like' differentiation phenotype exhibited by up-regulation of transcription factors Pu.1 and RelB (Auffray et al., 2007). In keeping with Carlin et al, Ly6C^{-} patrolling monocyte extravasation to the site of infection was significantly disrupted in *Cx3cr1*$^{-/-}$ mice and was shown to be LFA-1 dependant (Auffray et al., 2007).

Overall, the current experimental evidence from human and mouse points toward a patrolling, 'house keeper' role for Non-Classical monocytes within the vasculature, which, in the steady state, is mediated by LFA-1. Under conditions of infection, disease or tissue injury, damaged endothelium upregulates CX3CL1 expression on its surface, interacting with CX3CR1 to 'hold' Non-Classical monocytes in place. Subsequently, it appears likely that Non-Classical monocytes make a decision to remain adhered to endothelium or to extravasate to the tissue depending on different stimuli received. Due to their patrolling behaviour within the bloodstream, Non-Classical monocytes are likely to represent first responders to localised inflammation, with their initial production of chemokines leading to recruitment of other inflammatory effector cells, including Classical monocytes and neutrophils, to the area.

Intermediate Monocytes 1.2.3

The function of human Intermediate monocytes has been the focus of a number of recent studies and is a major theme for this thesis. Elucidating their roles in vivo has been complicated by the fact, based upon current knowledge, that there is no equivalent to the Intermediate subset in the mouse. Human Intermediate monocytes are defined as CD14^{+}, CD16^{+}, CCR2^{mid}, CX3CR1^{mid}, CD62L^{mid}, with a number of other cell surface markers expressed at levels that are intermediate between those of Classical and Non-Classical monocytes. Separate gene profiling studies found similar genes to be most highly expressed in Intermediate monocytes. These included genes involved in antigen processing and presentation such *HLA-DR*, *CD74*, *CD40* (Zawada et al., 2011, Wong et al., 2011) and oxidative stress. Related to the latter process, upregulation of *CYBA*, *TSPO*, *NCF2* (involved in superoxide production) and

downregulation of *SOD2*, *PRDX1*, *GPX4* (involved in detoxification of superoxide radicals) have been reported (Zawada et al., 2011). In vitro testing of spontaneous oxidative stress revealed that Intermediate monocytes contained the highest amounts of spontaneous ROS (as measured by flow cytometry using carboxy-H_2DFFDA reagent) reflecting the described genetic profile (Zawada et al., 2011). The ability of Intermediate monocytes to process and present antigen (already discussed, see **Section 1.2.1**) was tested in vitro by quantifying their ability to stimulate proliferation of T-cells. In this case, one study reported that Intermediate monocytes provide the greatest T-cell proliferation among the subsets (Zawada et al., 2011) while another revealed weak monocyte-induced T-cell proliferation for all subsets (Cros et al., 2010). Intermediate monocytes also express high levels of the pro-angiogenic markers endoglin, TEK tyrosine kinase (angiopoietin receptor), and VEGFR2 (Zawada et al., 2011). In Matrigel® assays, Intermediate monocytes failed to produce a typical cord-like HUVEC structure but did selectively co-locate to clusters, unlike Classical and Non-Classical monocytes (Zawada et al., 2011).

As previously described, Intermediate monocytes have been shown to be quite phagocytic in various in vitro settings. Intermediate monocytes avidly phagocytosed 1µm latex beads in a similar fashion to Classical monocytes, albeit at a slightly decreased level (Cros et al., 2010). An in-vitro assay for modified lipid uptake assessed by Bodipy® staining and flow cytometric analysis revealed that Intermediate monocytes scavenge oxidised low-density lipoprotein (oxLDL) more avidly than Classical or Non-Classical monocytes and this scavenging associated with Intermediate monocyte production of inflammatory cytokines TNF-α, IL-1β and IL-6 (assessed by intracellular flow cytometry) (Rogacev et al., 2014). This observation of greater scavenging of modified lipids was accompanied by reduced cholesterol efflux capacity of the Intermediate monocytes in contrast to the other subsets (Rogacev et al., 2014). These results were from monocytes taken from chronic kidney disease (CKD) patients, and, as such, may not reflect steady-state Intermediates. However, work from our own research group using monocytes isolated from healthy individuals is consistent with this concept. Specifically, Intermediate

monocytes were found to most avidly ingest oxLDL as well as acetylated (ac) LDL in a scavenger receptor (CD36 and SRA-1) dependent manner (MC Dennedy, EP Connaughton and M Griffin, unpublished observations).

A recent study has implicated Intermediate monocytes in phagocytosis of malarial infected red blood corpuscles (RBCs). Blood from healthy controls was exposed to ethidium bromide (EtBr)-stained purified trophozoite-stage *P. falciparum* infected RBCs and phagocytosis was measured by monocyte EtBr signal assessed by flow cytometry with ingestion confirmed by imaging cytometry. Intermediate monocytes significantly internalised infected RBCs while Classical and Non-Classical monocytes exhibited minimal uptake (Zhou et al., 2015). Additionally, phagocytosis of infected RBCs resulted in increased production of TNF-α by Intermediate monocytes in contrast to the other monocyte subsets. Intermediate monocyte phagocytosis was found to be dependent on antibody opsonisation and the complement component C3. Blockade of the FcR component CD16 abrogated phagocytosis (Zhou et al., 2015).

Intermediate monocytes are primarily considered to be pro-inflammatory cells. A large number of studies have examined blood monocyte subset phenotype and proportions in inflammatory diseases such as Crohn's disease (Grip et al., 2007), sepsis (Poehlmann et al., 2009), chronic kidney disease (Rogacev et al., 2014), obesity and diabetes mellitus (MC Dennedy, EP Connaughton and M Griffin, unpublished observations), and have revealed an expansion of the Intermediate monocyte subset. In some studies, in vitro stimulation of Intermediate monocytes with the TLR4 ligand LPS resulted in a strong pro-inflammatory cytokine profile. In the highly cited study of Cros et al., Intermediate monocytes produced the highest amounts of TNF-α and IL-1β, while additionally producing IL-6 and CCL3 at high levels similar to Classical monocytes (Cros et al., 2010). In another in vitro study, Intermediate and Classical monocytes produced similar high levels of TNF-α while Classical monocytes producing highest levels to IL-1β, and Non-Classical monocytes produced little of either cytokine (Thiesen et al., 2014). However, the pro-

inflammatory profile of Intermediate monocytes in response to TLR ligands has not been consistently observed. For example, in a 2011 study, Wong et al., reported that Intermediate monocytes were the lowest producers of TNF-α, and IL-1β (highest production by Non-Classical monocytes) (Wong et al., 2011).

In the study of Cros et al., hierarchical clustering of gene expression profiles of the monocyte subsets indicated that Intermediate monocytes clustered more closely with Classical than Non-Classical monocytes suggesting that the Intermediate subset may be directly derived from Classical monocytes (Cros et al., 2010). However, two other studies which also pursued a gene profiling approach with hierarchical clustering reported the opposite, and interpreted their results as indicating that Intermediate and Non-Classical subsets are more closely related (Wong et al., 2011, Zawada et al., 2011).

A number of the studies summarised in this section on Intermediate monocytes indicate that they represent a highly phagocytic cell type associated with pro-inflammatory cytokine production. Nonetheless, other published studies have reported some contradictory results. There are several potential explanations for such inconsistent results. In the first place, the methods by which monocytes are isolated from blood before experimentation may significantly influence the results of down-stream functional assays. Some studies have utilized Ficoll® density gradient centrifugation to achieve a PBMC mixture followed by bead-based extraction systems to remove the majority of lymphocytes and granulocytes, leaving an enriched monocyte population that may then be subjected to fluorescence-activated cell sorting (FACS) to generate highly-purified monocyte subset preparations (Wong et al., 2011, Thiesen et al., 2014). Another study used sequential employment of CD14 and CD16 microbeads to isolate monocytes into their subsets, negating the use of FACS. Cros et al used red blood cell lysis to achieve a PBMC suspension prior to FACS (Cros et al., 2010). Additionally, different anti-coagulants have been used during blood collection for individual studies. These have included heparin (Cros et al., 2010), ethylenediaminetetraacetic acid (EDTA) (Zawada et al., 2011) and sodium citrate (Thiesen et al., 2014). Differences in the placement of

gates during FACS cell sorting are also likely to have played a part in the discrepancies between individual studies. When dealing with a continuum of cell surface expression of a given marker, (e.g. CD16 in the case of monocytes) the use of flow minus-one (FMO) controls to define the cut-off point between two subsets may be poorly reproducible from one study to the next. Thus, the Intermediate monocyte sorting gate may be placed closer to the Classical or the Non-Classical subsets and this variability may be reflected in the gene profiles or functional responses of the resulting purified cell populations.

Heterogeneity of the Intermediate monocyte subset may also be an alternate explanation for conflicting results between studies. However, to date there have been no published studies which definitively prove the existence of one or more distinct subpopulations within the currently-defined Intermediate monocyte subset.

The lack of an apparent mouse equivalent of the human Intermediate monocyte subset has also played a part in the current ''identity crisis'' of Intermediate monocytes. More robust functional studies on Intermediate monocytes using better-standardised purification methods will be required in order to shed more light on the relative importance of their defined biological functions as currently understood (see **Table 1**).

The primary aim described in this thesis was to identify and investigate the functional properties of Intermediate monocytes. Specifically, we sought to further investigate heterogeneity within the Intermediate subset. Previous results generated by our group indicated Intermediate monocyte heterogeneity based HLA-DR expression, producing two Intermediate sub-populations, HLA-DR^{mid} and HLA-DR^{hi} (MC Dennedy, EP Connaughton and M Griffin, unpublished observations). Based on this observation, the goal of the project was to more precisely define the phenotypic and functional characteristics of the HLA-DR^{mid} and HLA-DR^{hi} Intermediate monocyte sub-populations in the healthy state.

Table 1- 1Properties of human monocyte subsets

Monocyte Subset	Classical	Intermediate	Non-Classical
Proportions	85%	5%	10%
Defining Surface Markers	$CD14^{hi}$, $CD62^{hi}$, $CCR2^{hi}$, CX3CR1-, CD16-, CD115-, $HLA.DR^{mid}$	$HLA.DR^{hi}$, $CX3CR1^{mid}$, $CCR2^{mid}$, $CD16^{mid}$, $CD14^{hi}$,	$CD16^{hi}$, $CD11a^{hi}$, $CX3CR1^{hi}$, $HLA.DR^{mid}$, CD14-, CCR2-
Migration Characteristics	CCL2, CCL7, CCL8 SDF-1α	~	CX3CL1
Associated Functions	High phagocytosis of beads and subsequent production of ROS, mRNA for lysozyme and myeloperoxidase. Contribute to macrophage populations in the gut and skin in the steady state. Exhibit a tissue specific surveillance in steady state for antigen with subsequent draining to lymph nodes with minimal differentiation.	Highly phagocytic and associated production of inflammatory cytokines; Lipid scavenging with decreased cholesterol efflux. Phagocytosis of parasite infected RBCs. High basal levels of ROS.	Patrolling of endothelium dependent on CX3CR1, LFA-1 and MAC-1. Disposal of damaged endothelial cells via TLR7 and recruitment of neutrophils. First responder to tissue inflammation in peritoneal infection, producing chemokines to recruit Classical monocytes and other effector cells.
Response to LPS	high amounts of IL-10, IL-8, IL-6, RANTES, CCL2, CCL3, Moderate TNF-α	High amounts of TNF-α and IL-1β. Moderate amounts of IL-6 and CCL3	Poor response to LPS, Low amounts of CCL3, IL-6, IL-8.
Response to TLR7/8 Ligands	CD14+ Monocytes Only (Classical and intermediate grouped together)		Production of TNF-α, CCL3 and IL-1, dependant on p42 MEK MAP kinase pathway
	Production of IL-6 and IL-8, dependant on p38 MAPK activation alongside classical NF-κB pathway		
Gene Profiles	Pro-inflammatory mediators, wound healing, plastic response to stimuli, carbohydrate metabolism (anaerobic energy production)	MHC II antigen processing and presentation; pro-angiogenic	Cytoskeletal mobility, complement components, phagocytosis, negative regulation of transcription, oxidative pathway components

Clinical Relevance of the Intermediate Monocyte Subset 1.3

Since human monocyte subset classification some in vitro functional studies point toward a pro-inflammatory role for Intermediate monocytes (Cros et al., 2010, Thiesen et al., 2014), a substantial number of clinical studies have investigated the associations of monocyte subset repertoire with various disease states known to be linked with abnormal inflammation. In subjects with human immunodeficiency virus (HIV) infection not receiving highly active antiretroviral therapy (HAART), Intermediate and Non-Classical monocyte subsets were expanded and the Intermediate population expansion correlated positively with viral load and negatively with $CD4^+$ T cell count (Han et al., 2009). Interestingly, Intermediate monocyte numbers returned to normal levels after initiation of HAART treatment (Han et al., 2009). Of interest, the Intermediate subset has been reported to display higher levels than other monocyte subsets of CCR5, a co-receptor for HIV infection of the cell (Cros et al., 2010). In hepatitis B-infected people with active disease, the Intermediate subset was expanded in comparison to uninfected controls (8.02% vs. 4.74% respectively) (Zhang et al., 2011). Intermediate subset expansion was positively correlated with liver damage, as determined by measurement of serum alanine aminotransferase (ALT) (Zhang et al., 2011).

Studies in chronic liver injury and inflammation revealed that $CD16^+$ monocytes, specifically proportions of the Intermediate and, to a lesser extent, Non-Classical monocytes, are increased in the circulation and the liver (Liaskou et al., 2013, Zimmermann et al., 2010). Intermediate and Non-Classical monocytes contribute to liver fibrosis, with intrahepatic accumulation of Intermediate monocytes secreting pro-inflammatory cytokines (TNF-α, IL-1β, IL-6, IL-8), pro-fibrogenic cytokines (IL-13) and chemokines (CCL2 and CCL3) (Liaskou et al., 2013).

People with chronic kidney disease (CKD) are at higher risk for developing atherosclerosis and expansion of Intermediate monocytes has been observed in the setting of CKD in a number of recent studies. Furthermore, higher

numbers of Intermediate monocytes are reported to independently predict cardiovascular events in CKD cohorts (Rogacev et al., 2014, Heine et al., 2008). Intermediate monocytes obtained from subjects with CKD avidly scavenged modified lipids and displayed reduced cholesterol efflux and lipid-induced IL-1β and TNF-α cytokine production, indicating a dysfunctional phenotype similar to that of foam cells found in atherosclerotic lesions (Rogacev et al., 2014). In another study, it was found that, in individuals with CKD, the combination of increased intermediate monocyte number and angiotensin converting enzyme (ACE, CD143) expression represented a strong predictor of mortality (Ulrich et al., 2010). Similarly, in a patient population with high cardiovascular risk referred for elective coronary angiography, the Intermediate monocyte subset was also found to independently predict severe cardiovascular events (Rogacev et al., 2012).

These studies point toward an expansion of Intermediate monocytes in a wide range of inflammatory settings, and, in some cases this expansion correlates with adverse health outcomes and/or their prognostic markers (Rogacev et al., 2012, Heine et al., 2008, Ulrich et al., 2010, Rogacev et al., 2014). However, despite the numerous studies profiling the expansion of Intermediate monocytes in a range of diseases, the specific biological processes underlying this phenomenon remain poorly understood. For instance, it is not clear if Intermediate monocytes have the same functional profile in the different disease states in which they are expanded. Also, it is unclear whether Intermediate monocyte expansion is a direct result of specific pathogenic processes in individual disease states or represents a non-specific response to general systemic inflammation. Finally, the extent to which Intermediate monocyte expansion may contribute functionally to the progression and complications of diverse disease states as opposed to being simply a marker of disease is not yet well elucidated. To achieve better understanding of Intermediate monocyte contributions to inflammatory diseases, we believe that it is essential to build a clearer picture of their variability, heterogeneity and functional potential in healthy individuals. Indeed many inflammatory diseases appear to be driven by chronic stimulation of the natural protective

functions of specific immune cell subtypes - for example the uncontrolled accumulation of monocytes and T cells in atherosclerotic plaques (Weber et al., 2008, Hansson and Libby, 2006). With this in mind, the core aim of this study was to better understand the phenotypic heterogeneity and potential biological functions of Intermediate monocytes during health in order to better inform investigations of monocyte dysfunction in inflammatory diseases.

Monocyte Development and Life Cycle 1.4

Monocytes develop in the BM and spleen and are released into the circulation. From there, they may extravasate to tissues to fulfil a variety of functional roles during infection, injury or disease (Hettinger et al., 2013, Leuschner et al., 2012). A number of studies have investigated monocyte surface expression of specific receptors using a sequential gating strategy across the recognised subsets with a view to better understanding the developmental relationships among the individual subsets. This has revealed that many characteristic monocyte cell surface markers appear to display a 'maturation of phenotype' from Classical to Intermediate and then to Non-Classical, suggesting (though not proving) that the Intermediate monocytes represent a transitional stage between Classical and Non-Classical monocytes (Wong et al., 2011, Hijdra et al., 2013) **Figure 1.4** provides a representative example of data from one such study.

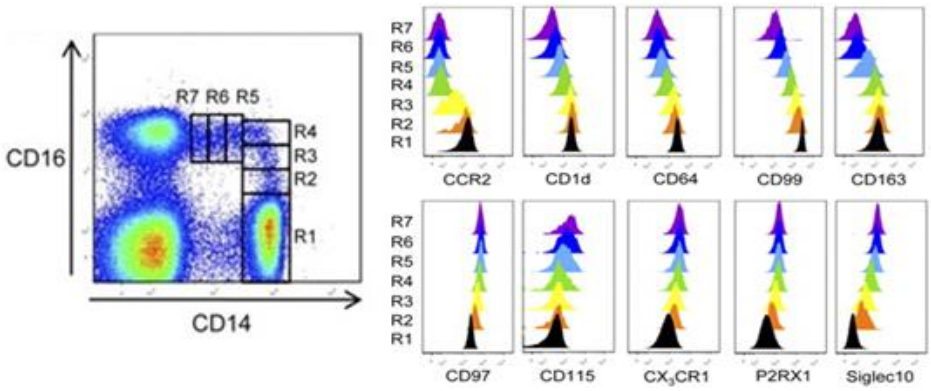

Figure 1. 4 Intermediate human monocytes display "intermediate" surface levels of multiple distinguishing surface markers

Based on sequential gating (gate R1-R7) from Classical to Intermediate to Non-Classical, Intermediate monocytes display intermediate levels of cell surface receptors which are either more highly expressed on Classical (CCR2, CD1d, CD64, CD99, CD163) or on Non-Classical (CD97, CD115, CX3CR1, P2RX1, Siglec 10) monocytes. Adapted from Hijdra et al. *Front Immunol*, 4,339, 2013.

Human monocytes originate in the bone marrow from a common hematopoietic stem cell (HSC). In monocyte development, myeloid progenitor cells (termed granulocyte/monocyte colony forming units) give rise sequentially to monoblasts, pro-monocytes and lastly monocytes which are released into the bloodstream from the bone marrow (**Figure 1.5**) (Mosser and Edwards, 2008, Doulatov et al., 2012). However, the majority of knowledge on monocyte development has been obtained by the use of sophisticated lineage tracing studies in mouse models.

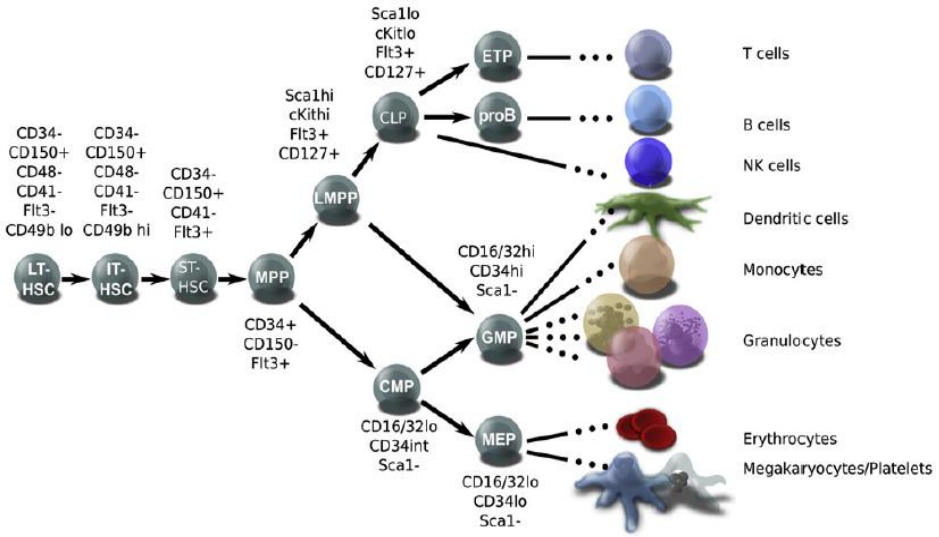

Figure 1. 5 Current model of lineage determination in the human haematopoietic hierarchy

Overview of proposed haematopoietic hierarchy in humans. In particular, human monocytes are derived from CD16/CD32/CD34^{hi} Sca1- granulocyte/monocyte progenitors. Adapted from Doulatov et al. *Cell Stem Cell*. 3;10(2):120-36., 2012.

In the mouse, monocytes originate in the BM from a recently-identified common monocyte progenitor (cMoP) defined as lineage-negative (Lin$^-$), CD117$^+$ (c-Kit$^+$), CD115$^+$ (M-CSFR$^+$), CD135$^-$ (Flt3$^-$), Ly6C$^+$ and CD11b$^-$(Hettinger et al., 2013). When isolated and cultured in vitro with stem-cell factor (SCF), leukaemia-inhibitory factor (LIF), IL-3 and IL-6, the cMoP gave rise to Ly6C^{hi} monocytes within 16 hours (Hettinger et al., 2013). Adoptive transfer of sorted CD45.2 cMoP to a CD45.1 animal reflected the in vitro results as the cMoP did not to give rise to DCs but potently produced Ly6C^{hi} monocytes. It was noted

that detection of Ly6C^{lo} monocytes peaked at four days after adoptive transfer of the cMoP, in contrast to the peak of Ly6C^{hi} monocytes after one to two days, suggesting a potential developmental relationship between the mouse equivalents of Classical and Non-Classical monocytes. Gene expression analysis of specific transcription factors (*Klf4*, *Irf8*, *PU.1*, *Cebpb*) also indicated a tighter relationship between the cMoP and Ly6C^{hi} compared to Ly6C^{lo} monocyte progeny. This also suggested Ly6C^{hi} conversion to Ly6C^{lo} monocytes or, potentially, the presence of a separate Ly6C^{lo} progenitor (Hettinger et al., 2013). This evidence in mouse for conversion from Ly6C^{hi} conversion to Ly6C^{lo} monocytes supports the theory of human monocyte conversion or 'maturation' from Classical, to Intermediate to Non-Classical subsets. The gradual shift in cell surface expression of CD16 and CD14 on human monocytes may represent the maturation pathway in humans, similar to shift in Ly6C expression on maturation of mouse monocytes.

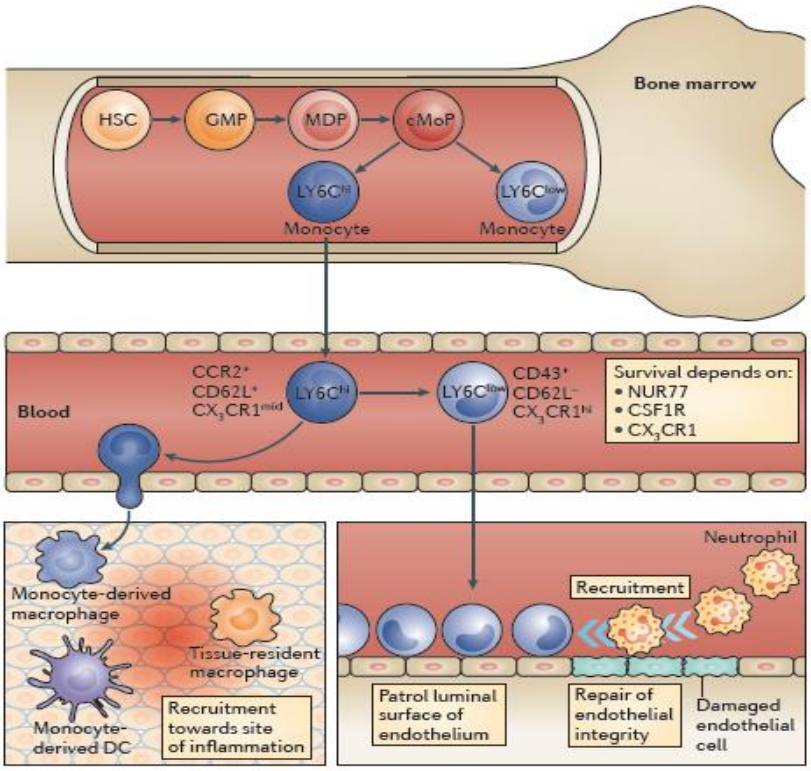

Figure 1. 6 Mouse monocyte progenitors and subset developmental relationships

Ly6C^{hi} monocytes arise in the bone marrow from the Common Monocyte Progenitor (cMoP) and Ly6C^{hi} (Classical) monocytes in turn differentiate into Ly6C^{lo} (Non-Classical) monocytes. Ly6C^{lo} monocytes depend on NUR77, CSF1R and CX3CR1 signals for survival. Adapted from Ginhoux et al. *Nat Rev Immunol*. 14(6):392-404, 2014.

The theory of Ly6C^{hi} to Ly6C^{lo}conversion was further supported by another study (Yona et al., 2013) which was carried out in murine models of constitutive and conditionally-induced (tamoxifen) expression of yellow fluorescent protein (YFP)-tagged Cre-recombinase driven by the CX3CR1 promoter. In these models, a gradual phenotypic shift was observed from Ly6C^{hi}YFP^{-} to Ly6C^{lo}YFP^{-} to Ly6C^{lo}YFP^{+} monocytes. The gradual acquisition of YFP (indicative of CX3CR1 expression) alongside the shift from Ly6C^{hi} to Ly6C^{lo} provides evidence for direct Ly6C^{hi} conversion to Ly6C^{lo} monocytes in the circulation (Yona et al., 2013). Furthermore, adoptively transferred CX3CR1$^{GFP/+}$Ly6C^{hi} splenic monocytes (taken from spleen to avoid any inclusion of BM progenitor lineages) into congenic WT mice revealed a differentiation of

grafted cells to Ly6C^{lo} CX3CR1/GFP^{hi} cells within the circulation after 3 days (Yona et al., 2013).

It has been shown that Ly6C^{hi} monocytes rely on CCR2 to exit the bone marrow into the circulation (Serbina and Pamer, 2006), where they differentiate into Ly6C^{lo} monocytes. In a mixed chimera using BM isolated from wild-type (CD45.1) and CCR2-deficient (CD45.2) *Cx3cr1*$^{gfp/+}$mice, analysis of monocyte populations in the blood revealed, as expected, that Ly6C^{hi}CCR2$^{+/+}$ monocytes outnumbered Ly6C^{hi}CCR2$^{-/-}$ monocytes. However, Ly6C^{lo} CCR2$^{-/-}$ monocytes were also outnumbered by Ly6C^{lo}CCR2$^{+/+}$ cells, consistent with Ly6C^{hi} conversion to Ly6C^{lo} monocytes in the circulation (Yona et al., 2013). Interestingly, Ly6C^{hi} monocytes were also shown to negatively control the life span of Ly6C^{lo} monocytes by acting as a CSF-1 'sink'. Ablation of Ly6C^{hi}/CCR2$^{+/+}$ monocytes using MC21 treatment (an anti-CCR2 blocking antibody) resulted in an increase in the half-life of Ly6C^{lo} monocytes from 2.2 to 11 days, with the half-life returning to baseline after withdrawal of MC21 treatment. Administration of blocking antibody to CD115 (CSF-1 receptor) along with MC21 partially corrected the increased half-life of Ly6C^{lo} monocytes from 11 to 5.33 days (Yona et al., 2013). This increase in Ly6C^{lo} Non-Classical monocyte half-life may represent an evolved pathway to compensate for conditions in which Ly6C^{hi} monocytes are depleted in the circulation due to extravasation to inflamed tissue, potentially leading to a lower generation rate of Ly6C^{lo} monocytes. Sphingosine 1 phosphate receptor 5 (S1PR5), a G-protein coupled receptor (GPCR) for sphingosine-1 phosphate was found to mediate Ly6C^{lo} monocyte egress from the bone marrow. *S1pr5*$^{-/-}$ mice displayed increased numbers of Ly6C^{-} monocytes in the BM and a consequent reduction in the periphery (Debien et al., 2013).

The differentiation and survival of Ly6C^{lo} monocytes is critically dependant on the expression of the nuclear receptor Nur77 (*Nr4a1*), as evidenced by death of Ly6C^{lo} monocytes in the bone marrow of *Nr4a1*$^{-/-}$ knockout mice (Hanna et al., 2011).

Similarly, mouse Ly6C^{lo} monocyte survival is also dependent on the CX3CR1-CX3CL1 axis. Deletion of the genes encoding CX3CR1 or its ligand CX3CL1 results in a significant reduction of Ly6C^{lo} monocytes in the circulation in the steady state and during inflammation (Landsman et al., 2009). In fact, addition of human recombinant CX3CL1 to human CD16^{+} monocytes in vitro exhibited an anti-apoptotic effect, suggesting a critical role for CX3CR1 in the survival of human Non-Classical monocytes (Landsman et al., 2009).

Since the beginning of this study in 2011, there have been significant advances in knowledge pertaining to monocyte subset lineage and developmental relationships. When our experimental work began, cell surface phenotyping of human monocyte subsets suggested a developmental dynamic, progressing from Classical to Intermediate to Non-Classical monocytes (Wong et al., 2011). This phenotypic data was supported, to a certain extent, by gene profiling studies of monocyte subsets (Wong et al., 2011, Cros et al., 2010, Zawada et al., 2011). However such evidence could be best viewed as suggestive rather than definitive and alternative relationships, including reverse progression or separate progenitors for Classical and Non-Classical monocytes remained possible. Subsequently, as described above, the study by Hettinger et al., in which the mouse cMoP was identified provided more direct evidence for conversion of Ly6C^{hi} (Classical) to Ly6C^{lo} (Non-Classical) monocytes. Moreover, these findings were consistent with the earlier study by Serbina et al. (Hettinger et al., 2013, Serbina and Pamer, 2006), as well as the results of Yona et al. (Yona et al., 2013).

Taking the information generated in mouse models and relating it to human monocyte subsets, it is tempting to conclude that human Intermediate monocytes reflect an 'intermediate' stage in a dynamic maturational transition from Classical to Non-Classical monocytes. This may explain their expansion in a range of inflammatory diseases (see **Section 1.3**), in which there may be an increased stimulation of monocyte maturation as well as increased turn-over of Non-Classical monocytes. If such a model is valid in humans, then the Intermediate subset may consist of a spectrum of monocytes undergoing

phenotypic, functional and molecular changes. This could potentially explain the persistent difficulty in defining a specific biological role or function of these cells. For instance, as concluded in **Section 1.2.3,** differences in gating strategy and gate placement during monocyte subset purification could result in down-stream read-outs of the functional, molecular and phenotypic properties of purified monocytes resembling to a greater or lesser extent those of Classical or Non-Classical monocytes. This may well explain some of the reported inconsistencies in Intermediate monocyte cytokine production (Cros et al., 2010, Wong et al., 2011, Thiesen et al., 2014) and genetic signature (Wong et al., 2011, Zawada et al., 2011, Cros et al., 2010). Overall, it remains to be seen whether the elegant data generated from mouse models are directly translatable to human monocyte subset development.

Monocyte migration 1.5

Monocytes are highly migratory cells, initially leaving the BM and entering the circulation. From the bloodstream, they may transmigrate through endothelium to enter the tissue and exert tissue-specific functions. In certain scenarios they may also traffic to the lymph nodes or return to circulation and the BM. Thus, regulation of monocyte migration is required to be a complex and highly regulated process. The two best-studied chemokine receptors expressed on monocyte subsets are CCR2 and CX3CR1. CCR2 serves as a receptor for chemokine ligands CCL2 (CCL2) and MCP-3 (CCL7), both of which act as powerful chemoattractants for CCR2-expressing monocytes. A large body of evidence indicates that CCR2 is critical for monocyte exit from the BM. In *CCR2*$^{-/-}$ mice, CCR2^{+}/Ly6C^{hi} monocytes accumulate in BM and are present in significantly reduced numbers in the blood stream in the steady state (Tsou et al., 2007). The mechanism proposed for CCR2-mediated monocyte egress from BM is outlined in **Figure 1.6**. Mesenchymal stem cells (MSCs) or CXCL12-abundant reticular (CAR) cells in the BM niche produce CCL2 gradients and are thought to be primed by circulating TLR ligands (Shi et al., 2011). This stromal cell-secreted CCL2 may promote monocyte contact with the BM blood vessels in soluble form or via binding to glycosaminoglycans (GAGs) located near

vascular sinuses to create a gradient for monocyte transmigration into circulation (**Figure1.6**).

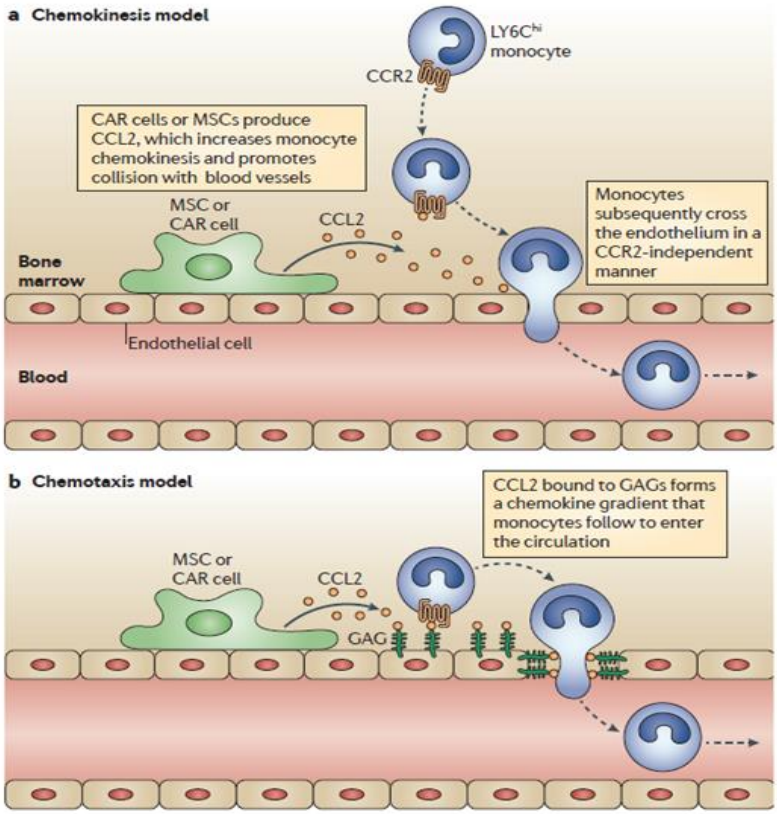

Figure 1. 7 CCL2-mediated monocyte egress from bone marrow
Mesenchymal Stem Cells (MSCs) or CXCL12 Abundant Reticular cells (CARs) release CCL2, a chemotactic for $CCR2^{+}$ monocytes. Free or glycosaminoglycans (GAG)-bound CCL2 gradients induce monocyte egress from the BM. CCL2 production by MSCs and CARs is increased by TLR signals leading to further monocyte egress under inflammatory conditions. Adapted from Shi et al. *Immunity*. 34(4):590-601, 2011.

Once present in the circulation, monocytes are thought to migrate to areas of inflammation using multiple chemokine receptors including CCR2, CCR5 and CX3CR1. Under some circumstances, chemokine receptor-mediated monocyte transmigration my represent a key step in the pathogenesis of diseases associated with dysfunctional inflammation. For example, inhibition of CCL2, CCR5 and CX3CR1 resulted in a 90% reduction in atherosclerosis in hypocholesterolemic apolipoprotein E-deficient ($apoE^{-/-}$) mice (Combadiere et al., 2008). Furthermore, $Ly6C^{hi}/CCR2^{+}/CX3CR1^{lo}$ monocytes were found to require CX3CR1 and CCR5, as well as CCR2 in order to accumulate within

atherosclerotic lesions. Conversely, Ly6C^{lo}/CCR2^{-}/CX3CR1^{hi} monocytes relied partially on CCR5, which was upregulated in the setting of atherosclerosis, to enter lesions in *apoE*$^{-/-}$ mice (Tacke et al., 2007).

In vitro studies of human monocyte subsets have revealed similar migration characteristics. Classical monocytes have been shown to transmigrate robustly through an endothelial layer in response to CCL2 while Non-Classical monocytes transmigrate more effectively toward CX3CL1 (Ancuta et al., 2004, Ancuta et al., 2003). In an earlier study, both CD16^{-} and CD16^{+} monocytes migrated strongly to stromal derived factor-1 (SDF-1), although not in the presence of an endothelial layer (Ancuta et al., 2003). More recent in vitro transmigration studies indicated a poor trans-migratory response to CCL2 displayed by Intermediate monocytes, which were reported to have CCR2^{int} phenotype, with migration values slightly higher than CCR2^{lo} Non-Classical monocytes (Thiesen et al., 2014, Krankel et al., 2011).

Before monocytes enter tissues, they must first pass through an endothelial layer. This process consists of several distinct steps which are outlined in **Figure 1.7**. Activation of endothelial cells by inflammatory cytokines such as TNF-α and IL-1β induces up-regulation of a host of adhesion molecules including ICAM-1, VCAM-1, E- and P-Selectin, as well as GAG- or transmembrane heparan sulphate proteoglycan-tethered chemokines present on the luminal side of the endothelium (Imhof and Aurrand-Lions, 2004, Ley et al., 2007). P-selectin protein ligand-1 (PSGL-1) is expressed by all monocytes and interacts with endothelial selectins (E- and P-selectin) and L-selection expressed on leukocytes (Ley et al., 2007). Selectin-ligand binding appears to have been adapted for monocyte tethering under sheer flow, such as experienced in the circulation, because selectin-ligand binding constitutes a 'catch bond', that is stronger in the presence of a pulling force (Marshall et al., 2003).

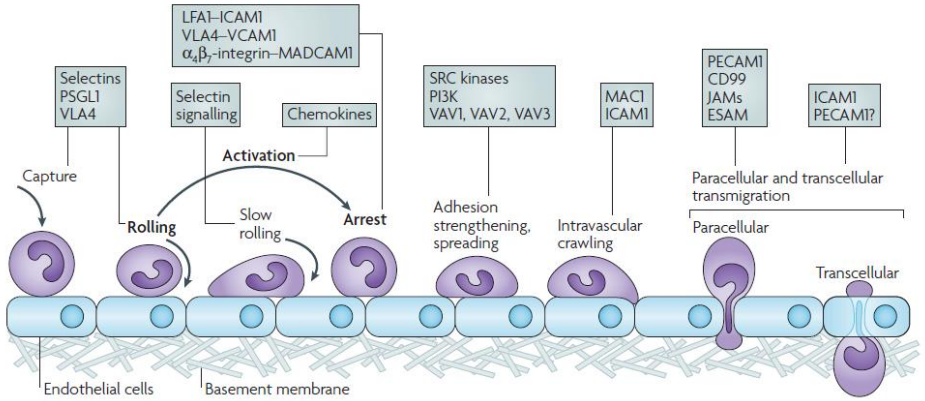

Figure 1. 8 The leukocyte adhesion cascade
Leukocytes initially tether and roll via selectin engagement and activation. Integrins mediate slow rolling and crawling which may permit cells to sample endothelial bound chemokines that initiate inside-out signalling, producing activation of integrins and subsequent tighter adhesion and spreading. Chemokine engagement of GPCRs eventually leads to leukocyte paracellular or transcellular migration. Adapted from Ley et al, 2007. *Nat Rev Immunol*. 7(9):678-89, 2007.

Integrins mediate initial leukocyte rolling, crawling and subsequent firm adhesion to endothelium. The main monocyte integrins involved in crawling and adhesion are very late antigen-4 (VLA-4, $\alpha_4\beta_1$ integrin, CD49d/CD29) which binds to VCAM-1, and LFA-1 ($\alpha_L\beta_2$ integrin, CD11a/CD18) which binds to ICAM-1. As previously described, isolated human monocyte subsets were observed to display different crawling and adhesion characteristics when perfused over micro- or macrovascular endothelium (Collison et al., 2015). Classical monocytes adhered more strongly to macrovascular endothelium and long-range crawling was dependant on ICAM-1. Non-Classical monocytes adhered preferably to microvascular endothelium and crawling was dependant on CX3CR1, ICAM-1 and VCAM-1. In contrast, Intermediate monocytes adhered to microvascular endothelium and remained static, exhibiting no crawling behaviour (Collison et al., 2015).

Chemokine activation of monocytes, likely encountered after initial selectin mediate tethering to the endothelium, can produce conformational changes to integrin receptors, termed ‘inside-out signalling’, resulting in increased receptor affinity and valency and subsequent tighter monocyte adhesion

(Laudanna et al., 2002). Chemokine signalling through GPCRs also produces a wide range of intracellular downstream signals which initiates active, cytoskeleton-driven changes conducive to transmigration (see **Section 1.6**). Adherent monocytes adhere to 'transmigratory cups' induced on endothelial cells, which are areas high in ICAM-1, VCAM-1 and cytoskeletal components (α-actinin, talin-1) (Ley et al., 2007). Endothelial cells actively re-distribute molecules that do not support transmigration, such as VE-cadherin, away from junctional regions. Conversely, molecules that support strong leukocyte adhesion like junctional adhesion molecule A (JAM-A) and platelet/endothelial-cell adhesion molecule-1 (PECAM-1) are mobilised to the luminal surface at endothelial junctions creating a haptotactic gradient facilitating leukocyte paracellular transmigration (Muller, 2003). Leukocytes may use transcellular migration, passing through the endothelial cell rather than passing through endothelial cell junctions in a process that is mediated by vesiculo-vacular organelles (VVOs). These are small continuous membrane associated pathways found at sites of leukocytes adhesion to endothelial cells (Dvorak and Feng, 2001). However, paracellular migration is thought to account for a majority of transmigrating leukocytes (**Figure1.8**) (Carman and Springer, 2004).

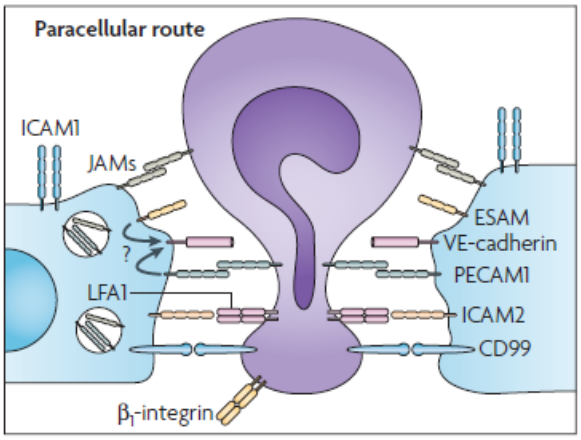

Figure 1. 9 Paracellular transmigration
Paracellular migration involves re-positioning of molecules inhibitory to migration (e.g. VE-cadherin) away from cellular junctions while recruiting intracellular membrane compartment s rich in PECAM-1, JAM-A, CD99, ICAM-2, and endothelial-cell selective adhesion molecule (ESAM) which provides a haptotactic gradient for leukocyte transmigration. Adapted from Ley et al. *Nat Rev Immunol*. 7(9):678-89, 2007.

G-protein Coupled Receptors and Monocyte Transmigration 1.6

As described above, monocyte migration from the BM into the circulation and then to tissues is coordinated under steady-state and disease conditions by sequential engagement of selectin and integrin ligands as well as G protein coupled chemokine. But when one considers the array of chemokine receptors on immune cells and the complex mix of chemokine signals in different tissues, it would appear vital to have tight regulation of signals produced by GPCR-type chemokine receptors to provide direction and purpose.

Chemokine Engagement of GPCRs 1.6.1

G-Protein Coupled Receptors (GPCRs) are a family of seven transmembrane domain spanning receptors linked to intracellular heterotrimeric guanine nucleotide binding proteins (G-proteins) which facilitate intracellular signalling. At around one thousand individual members encoded within the mammalian genome, the GPCR family represents one of the largest groups of cell surface receptors. GPCRs are activated by a wide range of ligands, including hormones, neurotransmitters, light, calcium ions, and chemokines (Ritter and Hall, 2009). As a consequence, GPCR-generated signals are responsible for the control of many physiological mechanisms involved in leukocyte chemotaxis, proliferation, cell survival and sensory perception. For this reason, GPCRs are very common molecular targets for pharmacological therapies (Bridges and Lindsley, 2008). Heterotrimeric G-proteins are coupled to GPCRs and consist of three subunits named α, β, and ϒ. However, the β and ϒ subunits form a functional complex that is not dissociable without full denaturation. When a GPCR is not occupied by its ligand, the G-protein Gα and Gβϒ subunits are co-associated. When a GPCR binds its ligand, extracellular domains of the receptor undergo conformational changes in the transmembrane spanning domains. The activated GPCR acts as a guanine nucleotide exchange factor (GEF) for the Gα subunit, resulting in the release of bound guanosine diphosphate (GDP) and the binding of guanosine triphosphate (GTP) and in G-protein activation. This results in the dissociation of the heterotrimeric G-protein into the Gα subunit and the Gβϒ complex, freeing them to associate

with other downstream effectors and to mediate cell signalling events (**Figure 1.9**). However, the Gα subunit has intrinsic GTPase activity, resulting in exchange of Gα bound GTP for GDP. This results in the re-association of the heterotrimeric G-protein Gα subunit and GβϒY sub complex, culminating in cessation of the GPCR signal. Thus, in a sense, ligand-induced GPCR-mediated intracellular signalling represents a self-regulated process.

There are approximately 23α, 6β and 11ϒ mammalian G-protein subunits. G-proteins are divided into 4 broad subfamilies: Gαi, which inhibits adenylyl cyclase; Gαs, which stimulates adenylyl cyclase; Gαq, which activates phospholipase C and Gα12/13, which is thought to activate RHOGEF/RhoA (**Figure 1.9**) (Bridges and Lindsley, 2008). The majority of chemokine receptors couple to Gαi and Gαq subunits, although chemotaxis is not exclusively initiated by receptors coupled to these subunits (Arai et al., 1997).

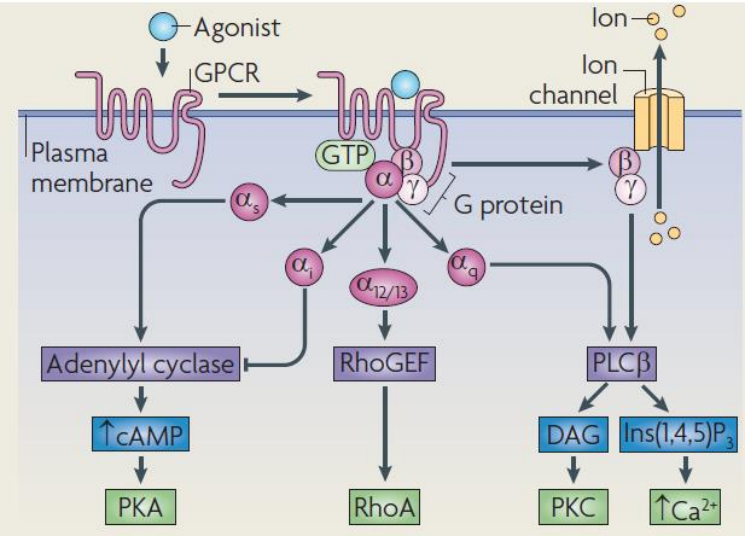

Figure 1. 10 Overview of GPCR signalling

Agonist (ligand) binding to GPCR results in the exchange of GDP for GTP on the Gα subunit causing dissociation of the Gα and GβΥ subunits from each other and the GPCR. Gα subunits, (Gαi, Gαs, Gαq, Gα12/13 shown here), when activated, bind downstream regulators such as adenylyl cyclase, RhoGEF and phospholipase Cβ (PLCβ). The dissociated GβΥ sub-complex also triggers functional pathways including ion channel activation and PLCβ signalling. These primary actions modulate further activation of downstream events including activation of Protein Kinase C, calmodulin and calcium flux. Adapted from Ritter et al. *Nat Rev Mol Cell Biol.* 10(12):819-30, 2009.

In monocytes, chemokine-stimulated GPCRs generate signals that are key to transmigration such as actin polymerization, integrin activation and directed cell movement. As described above, chemokine ligand binding to its receptor triggers dissociation of the heterotrimeric G-protein complex. Subsequently, the Gα subunit or Gβγ complex, or both, activate phospholipase C (PLC). Phosphoinositol 4,5 diphosphate ($PI(4,5)P_2$; PIP2) is hydrolyzed by activated PLC producing diaglycerol (DAG) and inositol 1,4,5-trisphosphate (IP3) (Alberts, 2008). The latter binds to IP3-gated Ca^{2+} in the endoplasmic reticulum (ER) membrane resulting in the release of Ca^{2+} into the cytosol. The released Ca^{2+}, in conjunction with DAG and phophatidylserine, can activate Protein Kinase C (PKC). Released Ca^{2+} may also bind to Calmodulin. Both Ca^{2+}-bound Calmodulin and activated PKC can then phosphorylate target proteins that promote actin polymerisation at the leading edge of the cell resulting in polarisation and cell movement toward the chemokine gradient (Alberts, 2008, Arai et al., 1997).

Regulation of Chemokine Receptor Signalling 1.5.2

GPCR Receptor Internalization 1.5.1.1

An obvious mechanism of regulation of G-protein signalling is the down regulation of the amount of GPCR present on the cell surface. When a GPCR is ligand bound, the intracellular domains of the receptor may become phosphorylated by kinases, in particular G-protein receptor kinases (GRKs). The phosphorylation of GPCRs has a desensitizing effect, resulting in binding of other effector proteins (e.g. arrestins, see **Section 1.5.1.3**) which can directly link receptors to clathrin-coated pits to facilitate receptor endocytosis. The receptor is then trafficked to the lysosome for degradation (Ferguson, 2001). Alternatively, in certain instances, internalized receptors may be dephosphorylated by endosomal-associated phosphorylases and returned to the cell membrane in a functional state (Sorkin and Von Zastrow, 2002). This results in GPCR ligands having the ability to affect receptor sensitization and endocytosis. Some GPCRs will recognize multiple ligands each of which produces different response. For example, CCR7 binds CCL19 and CCL21, but is phosphorylated to a greater extent by CCL19 resulting in effective receptor internalization (Byers et al., 2008). Differential rates of receptor recycling and degradation after ligand-induced endocytosis can also control GPCR signalling. Binding of CCL5 to CCR1, CCR3 and CCR5 produces receptor endocytosis. However CCR5 is recycled in its entirety while CCR3 is partially degraded and recycled, resulting in differential receptor expression on the cell surface and altered CCL5 signalling (Zimmermann et al., 1999, Borroni et al., 2010).

G-Protein Receptor Kinases 1.5.1.2

As mentioned above, G-protein Receptor Kinases (GRKs) phosphorylate ligand-bound GPCRs. This phosphorylation increases the affinity of the receptor for arrestin binding (see **Section 1.5.1.3**), which results in G-protein uncoupling from the receptor and receptor internalization (Moore et al., 2007). High concentrations of ligand are a prerequisite for GRK phosphorylation of G-proteins (Kelly et al., 2008). G-protein Receptor Kinases are a family of seven related kinases (GRK 1-7) which are differentially expressed across tissues and

have selectivity for specific receptors (Reiter and Lefkowitz, 2006, Premont and Gainetdinov, 2007). G-protein Receptor Kinases 2, 3, 5 and 6 are highly expressed in immune cells and are decreased during inflammation (Lattin et al., 2007, Pitcher et al., 1998). In humans, PBMCs isolated from patients with multiple sclerosis or rheumatoid arthritis displayed markedly decreased expression of GRK2 and GRK6 (Lombardi et al., 1999, Giorelli et al., 2004). A similar trend of GRK2 and GRK6 down-regulation was observed in rat models of chronic relapsing experimental autoimmune encephalomyelitis and experimental adjuvant arthritis (Vroon et al., 2005). Stimulation of polymorphonuclear neutrophils (PMNs) in vitro with LPS also results in down regulation of GRK2 and GRK6 (Fan and Malik, 2003). The latter regulates the responsiveness of CXCR4 to SDF-1 in neutrophils and absence of GRK6 is associated with increased calcium signalling and chemotaxis. The SDF-1/CXCR4 axis in the BM is a vital retention signal for hematopoietic cells and neutrophils, with administration of G-CSF inducing cell mobilisation. In GRK6$^{-/-}$ mice, neutrophils are retained in the bone marrow after the administration of G-CSF, most likely as a result of increased CXCR4 signalling (Vroon et al., 2004).

Similarly, GRK5 has been shown to negatively regulate monocyte CCL2-induced chemotaxis. In an in vitro assay using murine *GRK5*$^{-/-}$ monocytes, chemotaxis towards CCL2 was increased compared to wild type monocytes (Wu et al., 2012). Overexpression studies of GRK2 have resulted in increased receptor phosphorylation and subsequent internalisation and degradation of CCR2b and CCR5 (Oppermann et al., 1999, Aragay et al., 1998). In summary, the expression and activation of GRKs serve to regulate GPCR signalling and down regulation of GRKs may be an important mechanism underlying increased immune cell migration during inflammation.

Arrestins 1.5.1.3

The arrestins are also a family of proteins which regulate G-protein signal transduction. Activation of GPCRs and subsequent phosphorylation by GRKs enhance the affinity for arrestin binding. Arrestin binding mediates de-sensitization by sterically blocking GPCR and G-protein interaction.

Additionally, arrestin binding targets the GPCR for internalization via clathrin coated pits on the cell surface resulting in receptor degradation or de-phosphorylation and recycling to the cell membrane. The internalised GPCR-arrestin complex may also form a signalosome which activates signalling proteins including ERK1/2, p36 MAPK, and JNK (Luttrell and Lefkowitz, 2002). There are four known mammalian arrestin subtypes: Arrestin-1, β-arrestin-1, β-arrestin-2 and Arrestin-4. β-arrestin-1 and β-arrestin-2 are expressed ubiquitously in all tissues, whereas Arrestin-1 and Arrestin-4 are restricted to photoreceptors in the eye (Ferguson, 2001). Arrestins are known to be multifunctional adapter proteins with other roles in signal transduction. For example, they have been implicated in LPS-induced cytokine release in a model of endotoxin shock (Porter et al., 2010). β-arrestins are critical for embryonic development in animals. Generation of a β-arrestin-1 and β-arrestin-2 double knockout in mouse was associated with embryonic lethality (Li et al., 2010). β-arrestin-2 has also been implicated in development of Alzheimer's disease. In two patient cohorts, Thathiah et al found that expression of β-arrestin-2 was elevated. In vitro knock down of *Arrb2* (β-Arrestin-2) in HEK293-APP_{695} cells resulted in attenuated amyloid-β peptides, while in *Arrb2*$^{-/-}$ mice similar attenuation was observed (Thathiah et al., 2013). However, despite β-arrestin-2 involvement in receptor internalisation, it appears to function as both a positive and negative regulator of transmigration depending on immune cell type. In β-arrestin-2 deficient neutrophils, increased calcium signalling and chemotaxis is displayed, likely due to decreased β-arrestin-2 mediated CXCR2 receptor internalisation in response to CXCL1 (Su et al., 2005). In vitro it has been shown that β-arrestin-2 deficient lymphocytes exhibited increased G-protein signalling, however, despite this lymphocyte chemotaxis in response to CXCL12 was impaired (Fong et al., 2002). In an in vivo model of ova-induced allergic asthma, β-arrestin-2 deficient mice exhibited significantly reduced infiltration of T cells into the lung after ova administration compared to wild type mice, suggesting a vital role for β-arrestin-2 in T cell chemotaxis (Walker et al., 2003). In a monocyte cell line, desensitization of the CCR2b receptor by CCL2 stimulation is orchestrated by β-arrestin-1 after initial GPCR

phosphorylation by GRK2, resulting in impaired CCL2-induced transmigration (Aragay et al., 1998).

In a study using human monocytes isolated by adherence, CCR5 receptor internalisation was mediated by TLR2 stimulation with lipoteichoic acid (LTA). CCR5 receptor internalisation was associated with initial phosphorylation of the G-protein by GRKs and subsequent binding of β-arrestin-1 and 2 (Fox et al., 2011). This may suggest a role for TLR2 sensing of microbial compounds by monocytes in vivo triggering chemokine receptor internalisation mediated by β-arrestin-1 and 2 and resulting in monocyte retention in the area. Conversely, in another study, migration of mouse BM-derived monocytes towards CCL2 was enhanced by LPS, in a TLR4 dependant mechanism. The enhanced transmigration was a result of LPS induced p38 MAPK signalling, producing phosphorylation of GRK2 at serine 670, inhibiting its translocation to the membrane and, thereby, preventing CCR2 internalisation (Liu et al., 2013). Thus, TLR-mediated signals have the potential to both promote and inhibit monocyte migration through complex effects on chemokine receptor internalisation mechanisms.

Finally, β-arrestins can also serve as a scaffold for proteins such as the actin filament severing protein Cofilin. This can mediate actin cytoskeletal re-arrangements and induce chemotaxis in the absence of G-protein signalling (Zoudilova et al., 2010). Overall, while arrestins can modulate GPCR signalling by promoting receptor internalisation, they are also involved in broader cell signalling and fulfil multifunctional roles in immune and non-immune cells.

Regulators of G-Protein Signalling 1.5.1.4

Regulator of G-Protein Signalling (RGS) proteins are a family of highly conserved proteins which bind directly to activated Gα subunits to modulate G-protein signalling. As previously described, when a GPCR is engaged by its ligand, the G-protein dissociates into GβϒY sub complex and GTP-bound Gα subunit. RGS proteins bind to the active Gα subunit, greatly accelerating its

intrinsic GTPase activity (almost > 2000 fold in vitro (Ross and Wilkie, 2000)) and catalysing the conversion of GTP to GDP. This leads to re-association of the G-protein complex and subsequent termination of any downstream signalling. More than 30 RGS and RGS-like proteins of varying sizes and structures have been identified (Hollinger and Hepler, 2002, De Vries et al., 2000). To date, the genomic structure of only five RGS proteins has been described, namely RGS2, RGS3, RGS9, RGS16 and Axin (De Vries et al., 2000). Gene sizes vary from small (RGS16, 4kb) to large (Axin, 56kb). The RGS domain itself RGS2, RGS3, RGS9 and RGS16 is encoded by three exons, and the sites of the two introns in the RGS domain are conserved in RGS2, RGS3 and RGS16, suggesting a similar ancestor gene (De Vries et al., 2000).

Individual RGS proteins are reported to bind different Gα subunits (**Figure 1.9**). Most RGS proteins accelerate the GTPase activity of Gai and Gaq but not Ga12/13 and Gas (Watson et al., 1996). RGS proteins have been shown to have a high degree of evolutionary conservation. For example, Sst2p (SuperSensiTivity to pheromone) functions as an inhibitor of yeast pheromone responses and this function can be replicated by expression of mammalian RGS4 in yeast, (Weiner et al., 1993, Dohlman et al., 1995).

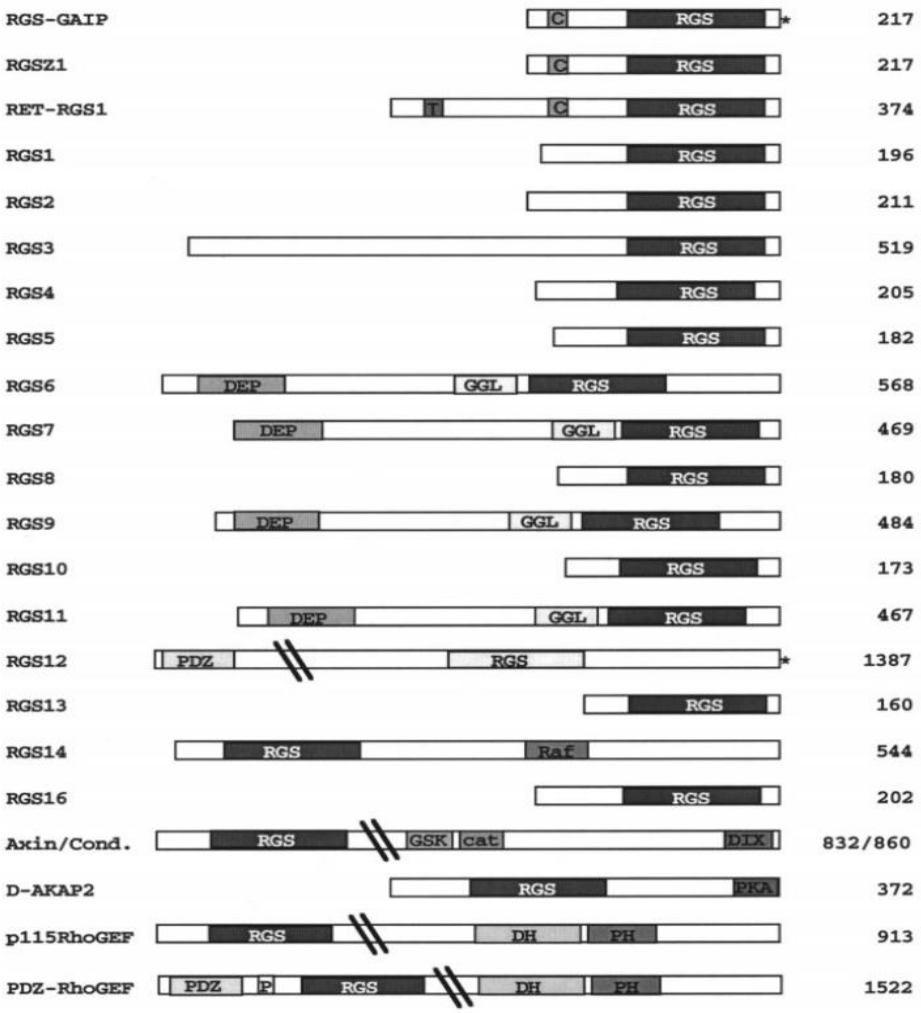

Figure 1. 11 Schematic representation of mammalian RGS proteins.
Total number of amino acids for each family member indicated on right hand side. Abbreviations: RasGAP,RasGAP-like domain; C, cysteine string domain; Cat, b-catenin binding domain; DEP, DEP domain (Dishevelled/EGL-10/pleckstrin homology); DH, double homology domain; DIX, dishevelled homology domain; GGL, GGL (G protein gamma-like) domain (homology to Gc); GSK, glycogen synthase kinase 3b binding domain; *, PDZ-binding motif; PDZ, PDZ domain (PSD95/Dlg/ZO1 homology); PH, pleckstrin homology domain; PID, PID domain (phosphotyrosine interacting domain); PKA, PKA-anchoring domain; Raf, Braf homology domain; T, transmembrane domain. Adapted from De Vries et al., *Annu Rev Pharmacol Toxicol.*;40:235-71, 2000.

In mammalian cells, RGS proteins are generally located in the cytosol or are tightly bound to the plasma membrane. The expression level of RGS proteins in different cell types may depend on the half-life of the particular protein with some RGS proteins, RGS7 in particular, having a short half-life. In the case of

RGS7, endotoxin exposure increases its half-life in HEK 293 cells via TNF-α mediated phosphorylation of the RGS7 p38-kinase recognition motif (Benzing et al., 1999). However, transcriptional control of RGS proteins may be the primary mechanism of regulation (Hollinger and Hepler, 2002). Expression of RGS proteins appears to be strongly influenced by various inflammatory stimuli. In a study by Shi et al, in vitro LPS stimulation of murine BM-derived DCs produced strong up-regulation of RGS1 and RGS16 in comparison to unstimulated DCs, while RGS14, RGS18 and RGS20 were almost completely down-regulated (Shi et al., 2004). Elevated expression of RGS1, 13 and 16 in regulatory T cells compared to naïve conventional T cells in vivo was found to positively correlate with reduced transmigration in a murine parabiosis model (Agenes et al., 2005). In a transgenic mouse model of RGS16 over-expression in $CD4^+$ and $CD8^+$ lymphocytes, intra-peritoneal injection of CXCL12- but not CCL12-induced T-cell migration, implying that RGS16 inhibits CXCR4 but not CCR2 mediated signalling in T-cells (Lippert et al., 2003). Using the same transgenic model subjected to ova-induced allergic response, RGS16-overexpressing T-cells produced significantly more Th2 cytokines in comparison to those of wild type mice (Lippert et al., 2003). RGS12 is an essential regulator for osteoclast differentiation as evidenced by the finding that $RGS12^{-/-}$ mice exhibit impaired osteoclast development and Ca^{2+} oscillations resulting in increased bone mass and decreased osteoclast numbers (Yuan et al., 2015). Conversely, in experimental models of bone loss, $RGS12^{-/-}$ deletion significantly inhibited osteoclast induced bone resorption (Yuan et al., 2015).

RGS1 is heavily involved in antigen-stimulated B-cell retention in germinal centres. In $RGS1^{-/-}$ mice, B-cells exhibited strong migration to CXCL12 and CXCL13 and impaired desensitisation, resulting in excessive and aberrant germinal centre formation following immunization (Moratz et al., 2004). Little is known about the role of RGS proteins in disease although it has been recently studied in atherosclerosis. Patel et al. observed that vascular inflammation was associated with increased RGS1 expression in thoracic aortas of atherosclerotic $ApoE^{-/-}$ mice along with the macrophage marker CD68 (Patel

et al., 2015). Using a ApoE$^{-/-}$/RGS1$^{-/-}$ model, RGS1$^{-/-}$ myeloid cell migration toward to CCL2 and CCL5 was found to be increased in vitro, while in vivo this resulted in decreased vascular inflammation and increased protection against aneurysm rupture mediated by reduced myeloid cell retention in site of vascular inflammation (Patel et al., 2015). This associates RGS1 expression with decreased chemokine signalling and subsequent cell retention in inflamed vasculature tissues. There is also evidence of a role for RGS1 expression in human vascular inflammation. Increased RGS1 mRNA expression has been reported in calcified aortic stenosis (Anger et al., 2008) and in the left ventricles of patients with ischemic cardiomyopathy (Mittmann et al., 2002). Additionally, CD14^{+} monocytes isolated from the blood of patients with early onset coronary artery disease revealed a down regulation of RGS1 mRNA levels compared to healthy controls, which may suggest increased chemokine signalling of blood monocytes in this disease setting (Sivapalaratnam et al., 2012).

Figure 1.11 below provides an illustration of the mechanisms of GPCR signalling regulation described in the preceding sections.

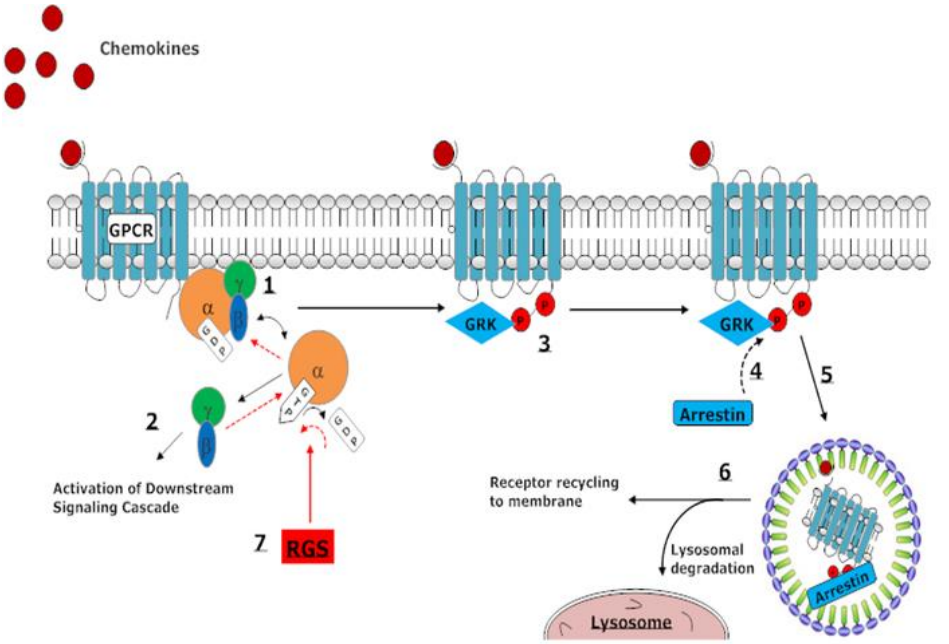

Figure 1. 12 Overview of mechanisms regulating G-protein coupled receptor signalling

1. GPCR Engagement: Binding of chemokine ligand to GPCR results in binding of GTP to the Gα subunit producing dissociation of the Gα and GβϒY complex.
2. G-Protein Signal Transduction: The free G-protein subunits then initiate other downstream signalling cascades.
3. Phosphorylation by GRKs: Phosphorylation of GPCR cytoplasmic tail by GRKs results in increased affinity for arrestin binding.
4. Arrestin Binding: Arrestin binding results in receptor desensitization by sterically blocking GPCR and G-protein interaction.
5. Receptor Internalization: GRK-induced phosphorylation and arrestin binding may promote receptor internalisation into lipid bilayer-enclosed vesicles.
6. Receptor Degradation or Re-cycling: Internalised GPCR may be directed to the lysosomal compartment for degradation or de-phosphorylated and re-cycled to the cell membrane.
7. RGS Proteins: After initial GPCR engagement and subsequent Gα activation, RGS proteins bind to and accelerate the intrinsic GTPase activity of the Gα subunit, replacing bound GTP for GDP, causing re-association of the Gα and GβϒY subunits and terminating the G-protein signal.

Regulation of GPCR-mediated Monocyte Migration 1.5.1.5

In relation to monocyte migration, there appear to be two main mechanisms for regulating chemokine-induced GPCR signalling: 1. GPCR desensitisation and/or GPCR internalisation mediated initially by G-protein phosphorylation by GRKs and subsequent arrestin binding (Fox et al., 2011, Liu et al., 2013, Aragay et al., 1998). 2. Inhibition or termination of G-protein signalling by RGS proteins (Denecke et al., 1999, Patel et al., 2015). Interestingly, few (if any) studies have directly investigated how these mechanisms may differ among the newly-classified human monocyte subsets. We believe to a large extent this reflects the difficulty of conducting such studies with primary human immune cells, and, in fact, many of the studies which have focused on the regulation of GPCR signalling in myeloid cells have employed cell lines such as THP-1 (Denecke et al., 1999) or genetically-modified mouse lines (Patel et al., 2015) which may or may not accurately reflect the biological properties of primary human monocytes

Nevertheless, results from a number of relevant studies indicate that monocyte chemokine receptor desensitisation and internalisation may be influenced by specific signals encountered. For example, as described above, TLR2 and TLR4 stimulation can result in specific alterations to the expression or function of GRK, β-arrestins and RGS proteins resulting in potent modulatory effects on monocytes migratory responses (Liu et al., 2013, Fox et al., 2011)

In the final results Chapter of this thesis, we have examined expression of members of the RGS protein family in purified monocyte subsets from healthy human subjects. Our interest in this family of regulatory proteins was stimulated, in part, by the fact that RGS proteins appear to regulate GPCR signalling on a receptor-specific basis. For example, as previously described, RGS16 inhibits CXCR4- but not CCR2-mediated migration in T cells (Lippert et al., 2003). Similarly, RGS1 has been shown to have a distinct regulatory effect on monocyte migration to and accumulation within atherosclerotic lesions of vessels in mouse (Patel et al., 2015) with consistent expression characteristics in human samples (Anger et al., 2008, Mittmann et al., 2002). Such evidence

would suggest that inflammatory activation effects RGS protein regulation in immune cells – a concept that may be of specific relevance to the transition of monocytes from one functional state (or subset) to another. Notably, in a study by Shi et al., stimulation of murine DCs with LPS resulted in a strong upregulation of RGS1 and RGS16 (Shi et al., 2004). However, no study to date has specifically investigated the effects of differentiation and maturation events on the regulation of RGS protein in human monocyte subsets.

It is interesting to note that Intermediate human monocytes, despite expressing CCR2, migrated poorly to CCL2 in two separate studies (Krankel et al., 2011, Thiesen et al., 2014) and exhibited no transmigration when perfused over inflamed endothelium in vitro (Collison et al., 2015). As discussed above, Intermediate monocytes are expanded in a range of inflammatory diseases and there is evidence for the modulation of key GPCR signalling regulatory mechanisms by inflammatory signals. It is possible, therefore, to consider a model for Intermediate monocyte expansion whereby diverse inflammatory stimuli drive the transition from Classical to Intermediate monocytes and, concurrently, modulate chemokine-associated GPCR signalling to blunt the migration of Intermediate monocytes from the circulation

Study Rationale 1.7

The rationale for focussing this project on the heterogeneity of human Intermediate monocytes derived from previous data generated by our group during the time that the Candidate was completing a Master's degree at NUI Galway (MC Dennedy, EP Connaughton and M Griffin, unpublished observations). This work revealed that there may be heterogeneity within the Intermediate monocyte subset as currently defined. Specifically, by initially applying subset gates according to the recognised convention based on CD14 and CD16 expression then examining the expression levels of additional candidate markers, we identified two discreet sub-populations within the Intermediate subset that demonstrated respectively, mid-level and high-level surface expression of the MHC Class II protein, HLA-DR. We termed these HLA-DR^{mid} ($CD14^{+}/CD16^{+}/DR^{+}$) and HLA-DR^{hi} ($CD14^{+}/CD16^{+}/DR^{++}$) Intermediate sub-populations. Subsequently, a cohort study of these novel sub-populations revealed that there was consistent expansion of HLA-DR^{mid} but not HLA-DR^{hi} Intermediate monocytes in blood of obese compared to healthy adults. Additionally, in vitro studies demonstrated that the most avid scavenging of modified lipoprotein particles by human monocytes occurred within the HLA-DR^{mid} subset of Intermediate monocytes.

As summarised in the Introduction, multiple studies have reported an expansion of Intermediate monocytes in various disease states but the causes and the functional and pathogenic significance of this phenomenon remain poorly understood. Our observation that, in one clinical setting at least (obesity), Intermediate monocyte expansion was confined to an as-yet unrecognised subpopulation, led us to pursue a more extensive and basic characterisation of Intermediate monocytes in healthy adults. In doing so, we posited that some of the inconsistencies present in the current literature in regard to Intermediate monocyte phenotype and function could be explained by the presence of two or more distinct subpopulations which may have been variously represented among studies based on the current human monocyte nomenclature.

Overall Goal 1.7.1

To determine whether HLA-DR^{mid} and HLA-DR^{hi} human Intermediate monocyte subpopulations, defined according to a novel gating strategy, are phenotypically and functionally distinct immunological cell types.

Specific Aims and Hypotheses 1.7.2

Specific Aim 1A: To confirm that HLA-DR^{mid} and HLA-DR^{hi} subpopulations in peripheral blood of healthy adults represent bona fide monocytes based on morphological characteristics and surface marker expression profiles.

Specific Aim 1B: To compare expression of cell surface receptors linked to adhesion, transmigration and chemotaxis among Classical, Non-Classical, HLA-DR^{mid} Intermediate and HLA-DR^{hi} Intermediate monocyte subpopulations of healthy adults.

Hypothesis 1: In healthy adults, peripheral blood cells defined by a novel gating strategy as HLA-DR^{mid} and HLA-DR^{hi} Intermediate subpopulations represent true monocytes that are distinguishable from each other and from Classical and Non-classical monocytes by their expression of multiple, functionally-relevant surface markers.

Specific Aim 2: To compare endothelial adhesion and transmigration and their associated signalling mechanisms among Classical, Non-Classical, HLA-DR^{mid} Intermediate and HLA-DR^{hi} Intermediate monocytes of healthy adults.

Hypothesis 2: In healthy adults, HLA-DR^{mid} and HLA-DR^{hi} Intermediate monocytes exhibit specialised functionality with regard to endothelial adherence and transmigration.

Chapter 2

Materials and Methodology 2.0

Preparation of peripheral blood mononuclear cells and phenotyping by multi-colour flow cytometry 2.1

Blood was drawn from healthy volunteers following informed consent (see **Appendix** for relevant forms) into EDTA Vacutainer® tubes (Becton Dickinson (BD) Biosciences, San Jose, CA, USA). A total of 3 ml of anticoagulated blood were layered over 3 ml of Ficoll Paque® density gradient medium (GE Healthcare, Little Chalfont, UK) in a 15 ml falcon tube (Sarstedt, North Rhine-Westphalia, Nümbrecht, Germany) and the tubes were centrifuged at 400 RCF for 22 minutes at 4°C with full acceleration and no braking. Afterwards, a thin cloudy layer containing PBMCs ("buffy coat") was carefully removed using a plastic Pasteur pipette (Sarstedt). This was transferred to a 15 ml Falcon® tube and the volume was made up to 10 ml with FACs buffer [2% foetal calf serum (FCS) (Lonza, Basel, Switzerland) PBS, 0.05% NaN_3 (Sigma-Aldrich, , St. Louis, MO, USA)]. The cell suspensions were pelleted by centrifugation at 400 RCF for 5 minutes at 4°C with full brake and acceleration. Supernatants were discarded and cell pellets were re-suspended in 5 ml of FACs buffer and washed again using the same procedure. The final cell pellets were re-suspended in 1 ml of FACs buffer and counted using a haemocytometer. Aliquots of 500,000 cells each were transferred to 3 ml polystyrene FACs tubes (Sarstedt) and the final volumes were made up to 100µl with FACs buffer. Cells were stained with combinations of fluorochrome-conjugated antibodies directed against various cell surface markers and expression levels were subsequently expressed as mean or median fluorescent intensity (MFI) as appropriate. Flow cytometric analyses were carried out in the NUI Galway Flow Cytometry Core Facility using a FACSCanto A or FACSCanto II cytometer (BD Biosciences). Compensation and gate settings were generated using compensation beads (Life Technologies, Carlsbad, CA, USA) and Flow Minus One (FMO) controls. Data files were analysed using FlowJo v.7 software (Tree Star Inc. Ashland, OR, USA).

May-Grunwald and Giemsa staining of monocyte subsets 2.2

Individual monocytes subsets were isolated using fluorescence activated cell sorting (FACS) (see **Section 2.4**). Between 10,000 and 20,000 cells were re-suspended in 200 µl of FACs buffer and spun onto glass microscope slides (VWR, Radnor, PA, USA) at 200 rpm for 5 minutes using a Shandan Cytospin 3, (Thermo Fisher Scientific, Waltham, MA, USA). The slides were air dried for 10 minutes at room temperature before being fixed for 5 minutes in 100% methanol (Sigma-Aldrich). The slides were air dried for 2 minutes at room temperature then were stained for 5 minutes in undiluted May-Grunwald stain (Sigma-Aldrich). Next, the slides were washed three times for 2 minutes each in phosphate buffered saline (PBS), pH 7.2, then stained in Giemsa stain (Sigma-Aldrich) (diluted 1:20 with deionized water) for 10 minutes. Finally, the slides were washed 3 times in deionized water for 20 seconds per wash and were air dried for 10 minutes with excess stain wiped from the back of the slide using tissues soaked in industrial methylated spirits (Sigma-Aldrich). Bright field images were immediately captured on an Olympus BX43 microscope (Olympus Corporation, Shinjuku, Tokyo, Japan).

In vitro transmigration assay 2.3

An in vitro transmigration assay was used to assess monocyte subset transmigration towards chemokine gradients. Transwells with 3.0 µm pore size (Corning, New York, USA) were used in 24-well tissue culture plate format for individual experiments. Migration medium was first added to the apical (100 µl) and basal chambers (600 µl) and left for 2 hours to equilibrate. Freshly isolated PBMCs were re-suspended in 1 ml of migration medium and were kept at 4°C for 40-60 minutes prior to initiating the transmigration assays. Aliquots of 500,000 serum-starved cells were added to the apical chamber and migration medium containing optimised concentration of chemokines, namely CCL2 (Immnotools, Friesoythe, Germany) CCL8 (MCP-2) (Immunotools) or CCL7 (MCP-3) (Immunotools), or without chemokine were added to the basal

chamber. The plates were then placed in a humidified tissue culture incubator at 37°C, 5% CO_2 for 60 minutes. Additional cells were cultured in a separate 24 well plate under the same conditions to serve as controls. After incubation, the Transwells were carefully removed from the wells and the undersides were gently washed with FACs buffer to rinse off transmigrated cells into the basal well. The cells from the basal well were then removed with a hand-held pipettor and were washed twice with FACs buffer before being transferred to FACs tubes. The suspended cells were centrifuged at 400 RCF for 5 minutes, the supernatants were discarded and the pellets were re-suspended in 50 µl of FACs buffer. The appropriate tubes were then stained with anti-human CD16-FITC (BD Biosciences), anti-human CD14-PerCP (Miltenyi Biotech, Cologne, Germany), anti-human CD45-APC (BD Bioscience) and anti-HLA-DR-APC.H7 (BD Biosciences) at 4°C for 20 minutes, protected from light. The stained cells were washed in FACS buffer as before and re-suspended in 100 µl of FACs buffer. To facilitate quantitation of cell transmigration, 20 µl of FACs compatible counting beads (Life Technologies) were added to each tube. Samples were then analysed on a BD FACSCanto II cytometer. To quantify transmigration and account for inter-individual variability, transmigration was represented as an 'index of migration'. This index was calculated by dividing the number of transmigrated cells in experimental wells (chemokine-containing) by the number of transmigrated cells in the no-chemokine control well. Data files were analysed using FlowJo v.7. Transmigration indices of individual monocyte subsets were analysed by gating on each subset based on surface staining for CD45, CD14, CD16 and HLA-DR.

In vitro monocyte transendothelial migration assay 2.4

To assess monocyte transmigration through an endothelial cell layer, human aortic endothelial cells (HAEC) (Promocell, Heidelberg, Germany) were seeded onto fibronectin-coated 3 µm pore size Transwell membranes (Corning), in a 12-well tissue culture plate format.

Transwell membranes were coated by adding a sterile solution of bovine fibronectin (2µg/cm2) (Sigma-Aldrich) and incubating overnight at 4°C. The next day, the fibronectin solution was removed and the membranes were washed twice using D-PBS (Life Technologies). The coated Transwells were used immediately or stored for up 2 weeks. Fibronectin-coated Transwell inserts were then seeded with HAECs at Passage (P)8 or P9 at 100,000 cells/cm^2. Endothelial cell growth medium (Promocell, Cat No. C22020) was added to the apical and basal chambers and the plates were placed in a tissue culture incubator overnight in order to allow the HAECs to attach. The following day, a single Transwell was removed from the plate and stained with crystal violet dye (Sigma-Aldrich) to document HAEC coverage of the membrane. Confluent layers of HAECs from individual Transwells were either left unstimulated or were stimulated by addition of human TNF-α (Immunotools) at a final concentration of 2.5 ng/ml for 6 hours at 37°C. After this, the medium was removed from apical and basal wells and replaced with pre-warmed migration medium followed by 1 hour incubation at 37°C. During this time, PBMCs were isolated and prepared for the transmigration assay as described in the previous section. Briefly, 500,000 PBMCs were added to the apical side of each well containing either un-activated endothelium or TNF-α-activated endothelium. The basal wells were either filled with migration medium as a control or with medium containing optimised concentration of human CCL2, CCL8 or CCL7 (all from Immunotools). The cells were allowed to transmigrate for 60 minutes in a tissue culture incubator at 37°C, 5% CO_2. After the end of this period, cells from the floating and transmigrated fraction were separately collected as described in **Section 2.2**. Adherent cells were removed from the inner surface of the transmembrane by incubation with trypsin solution (Life Technologies) for 30 seconds, followed by trypsin quenching with RPMI containing 10% FCS. Cells were gently flushed using a hand pipettor to remove any remaining adherent cells. Cells were prepared for flow cytometric analysis as described in **Section 2.2**. Results were calculated as the percentages of each monocyte subset within the total monocytes present in the Floating, Adherent and Transmigrated fractions. In the same flow cytometric analysis,

HAECs were distinguished from monocytes based on expression of CD45 (see **Figure 2.1** below).

Activation of HAECs by human TNF-α was determined by increased cell surface expression of VCAM-1 and ICAM-1. Briefly, HAECs were seeded on forty eight-well tissue culture plates coated with fibronectin, seeded with HAECs and treated with TNF-α as described above. After six hours of TNF-α stimulation, the HAECs were removed by 30 second incubation with trypsin solution at 37°C followed by neutralization with RPMI containing 10% FCS. Cells were gently flushed using a hand pipettor to remove any remaining adherent cells. The HAECs were then stained with anti-human VCAM-1 (eBioscience, San Diego, CA, USA) and anti-human ICAM-1 (Immunotools), and prepared for flow cytometric analysis in the same way as outlined as in **Section 2.2**.

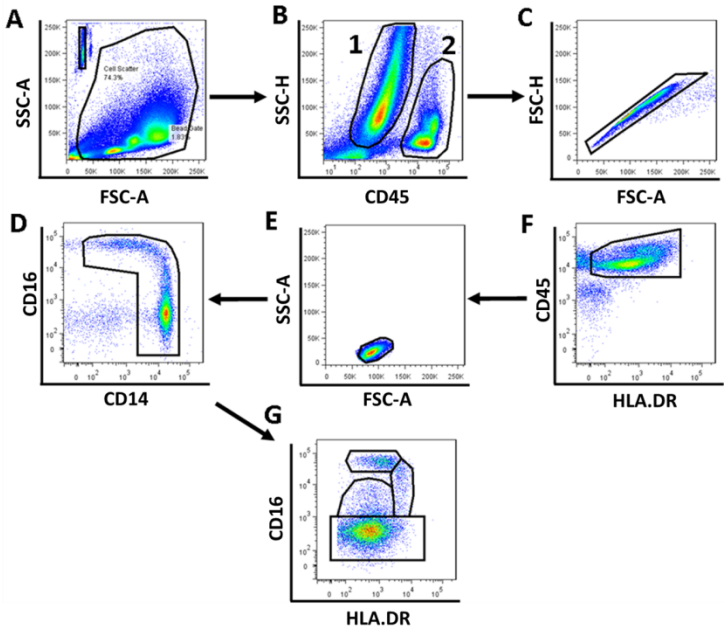

Figure 2. 1 Gating strategy for separating HAECs from monocytes.
(**A**). A mixture of viable monocytes and HAECs retrieved from Transwell experiments are initially gated together using forward and side scatter characteristics with counting beads (low FSA, high SSC) gated separately. (**B**). HAECs (**1**) and PBMCs (**2**) are separated from each other based on cell surface expression of CD45. (**C-G**). This gate excludes any endothelial cells from subsequent stepwise analysis of monocyte subsets.

Blockade of monocyte adherence to inflamed endothelium using neutralizing antibodies 2.5

Monocyte subsets express different levels of cell surface receptors involved in adhesion to endothelium (Schenkel et al., 2004, Imhof and Aurrand-Lions, 2004). Neutralizing antibodies against specific receptors involved in monocyte –endothelial adhesion were used to assess whether monocyte subsets employed different adhesion receptors to adhere to activated (TNF-α treated) HAEC monolayers.

Forty eight-well tissue culture plates were coated with fibronectin, seeded with HAECs and treated with TNF-α as described in the preceding section. Six hours after addition of TNF-α, the medium was removed and replaced with pre-warmed migration medium. Freshly isolated PBMCs were are added to each well at 300,000 cells/well along with optimised concentrations of specific neutralizing antibodies or respective isotype controls (see **Tables 2-1 and 2-2**) and were made up to final volumes of 250 µl with migration medium. The plates were then placed in a tissue culture incubator at 37°C, 5% CO^2 for 60 minutes. After this, floating and non-adherent cells were retrieved by washing with D-PBS (Life Technologies). Next, adherent cells were removed by 30 second incubation with trypsin solution at 37°C followed by neutralization with RPMI containing 10% FCS. Cells from the floating and adherent fractions were prepared for flow cytometric analysis by surface staining and addition of counting beads as described in **Section 2.2**. Results were calculated as the proportions of the total numbers of each monocyte subset present in the adherent fraction.

Table 2- 1 Blocking Antibody Information.

Blocking Antibody	Antibody Source	Isotype	Clone	Blocking Concentration
CD18	eBiosciene Cat. No. BMS103	Mouse IgG1	R3.3	8µg/ml
CD11a	ImmumoTools, Cat. No. 21270110	Mouse IgG1	MEM-25	8µg/ml
CD11b	ImmunoTools, Cat. No. 21279110	Mouse IgG2a	MEM-174	8µg/ml
CD11c	eBioscience, Cat. No. BMS112	Mouse IgG2a	CBR-p150/4G1	8µg/ml
CD29	R&D Systems, Cat. No. MAB17781	Mouse IgG1	P5D1	8µg/ml
CD49	ImmunoTools, Cat. No. 21858490	Rat IgG2b	PS/2	8µg/ml

Table 2- 2 Isotype Control Blocking Antibody Information.

Isotype Control	Isotype Source	Clone	Blocking Concentration
Mouse IgG1	ImmunoTools, Cat. No. 21275510	PPV-06	8µg/ml
Mouse IgG2a	ImmunoTools, Cat. No. 21275520	PPV-04	8µg/ml
Rat IgG2b	ImmunoTools, Cat. No. 22225031	TBE 15	8µg/ml

Monocyte calcium flux assay 2.6

Fluo-4 AM cell permeant (Life Technologies) is a labelled calcium indicator that has been extensively used for measuring intracellular dynamics of Ca^{2+} by flow cytometry (Desmeules et al., 2009, Hu et al., 2008) and confocal microscopy (Wei et al., 2009). Fluo-4 molecules bind Ca^{2+} resulting in increased fluorescence excitation at 488nm with a typical fluorescence increase > 100 fold (Harkins et al., 1993).

Monocyte intracellular Ca^{2+} release was measured by detecting Fluo-4 AM fluorescence changes by flow cytometry. Fresh PBMCs were isolated as

described in **Section 2.1** and aliquots of $1x10^6$ cells were transferred to FACs tubes and re-suspended to a final volume of 1 ml with Ca^{2+} free Dulbecco's PBS (D-PBS) (Life Technologies). Next, 5 µl of stock 1 mM Fluo-4 were diluted to 25-µl (0.2mM) in D-PBS and 1.5 µl of this diluted stock were added to each tube (final concentration 0.3 µM) and the tubes were vortexed. The FACs tubes were sealed with Parafilm® (Sigma-Aldrich) and a small hole was made in the film with a pipette tip. The cell suspensions were placed in an incubator at 37°C, 5% CO_2 (away from light) for 30 minutes then were pelleted by centrifugation at 400 RCF for 5 minutes at 20°C. The supernatants were removed and 100 µl of Ca^{2+} free D-PBS were added to each tube. The cells were then stained with the following fluorochrome-conjugated monoclonal antibodies: anti-human CD16-BV450 (eBioscience), anti-human CD14-PerCP, anti-human CD45-APC and anti-human HLA-DR-APC.H7 for 20 minutes at room temperature protected from light. After staining, 1 ml of Ca^{2+} free D-PBS was added to each tube and the tubes were centrifuged at 400 RCF for 5 minutes at 20°C. The supernatants were removed completely and the cells were re-suspended in 150 µl of Ca^{2+} free D-PBS. The stained cell suspensions were immediately analysed on a BD FACSCanto II at medium acquisition speed. Events were acquired for 30 seconds in each tube before addition of a stimulus (either 50ng/ml human CCL2 in 0.1% bovine serum albumin (BSA) (Sigma-Aldrich) in Ca^{2+} free D-PBS, 10ng/ml Ionomycin (Life Technologies) (positive control), or 0.1%BSA in Ca^{2+} free D-PBS alone (negative control). The stimulus solutions were injected into the FACs tube using a modified 500 µl syringe (BD Biosciences). Changes in intracellular calcium over time were measured by plotting mean fluorescence in the FITC channel against time of acquisition. The data was transformed to kinetic data using the kinetics platform in FlowJo v.7. Calcium flux within individual monocyte subsets was analysed by gating on each subset based on surface staining for CD45, CD14, CD16 and HLA-DR. The results were displayed as an index of Ca^{2+} flux, which was calculated for each sample by dividing the peak fluorescence reached by the average baseline fluorescence during the 30 seconds prior to injection of stimulus.

F-Actin polymerization assay 2.7

FITC-conjugated Phalloidin (Sigma-Aldrich) is a toxin which binds polymeric filamentous actin (F-actin), stabilizing it and interfering with the function of actin-rich structures. Consequently, FITC conjugated phallodin can be utilized to detect F-actin polymerization by quantifying FITC fluorescence at the single cell level using a method such a flow cytometry or immunofluorescence microscopy (Hu et al., 2008).

Monocyte subset F-actin polymerization in response to CCL2 stimulation was assessed by flow cytometry. Freshly isolated PBMCs were added in $0.5x10^6$ aliquots to FACs tubes and the volume made up to 100 µl with FACs buffer. The cells were then stained with anti-human CD16-BV450, anti-human CD14-PerCP, anti-human CD45-APC and anti-HLA-DR-APC.H7 at 4°C for 20 minutes, protected from light. After staining, 1 ml of FACs buffer was added to each tube and the tubes were centrifuged at 400 RCF for 5 minutes. The supernatants were completely aspirated and the cells were re-suspended in 190 µl of migration medium [RPMI (Life Technologies) supplemented with 0.5% FCS (Lonza), L-glutamine (Life Technologies) and penicillin/streptomycin (Life Technologies)]. The tubes were then placed in a water bath at 37°C for 10 minutes to equilibrate. Next, 10 µl of human CCL2 1 µg/ml stock were added to the appropriate tubes to give final concentration of 50 ng/ml. The cells were fixed by adding 200 µl of 4% paraformaldehyde (PFA) in PBS at 0 , 10, 30, 60, and 120 seconds after addition of CCL2. As controls, three tubes were incubated without addition of CCL2 and were fixed at the appropriate time-points. After addition of PFA, FACS tubes were removed from the water bath and incubated at 4°C for 12 minutes, protected from light. Then, 1ml of 1% BSA in PBS was added to each tube and the tubes were centrifuged at 400 RCF for 5 minutes. The supernatants were discarded and the cells were re-suspended in 100 µl of 0.1% saponin (Sigma-Aldrich) containing Phalloidin-FITC at a final concentration of 0.2 µM. The tubes were vortexed gently and incubated for 10 minutes at 4°C, protected from light. After this, 1ml of 1% BSA in PBS was added to each tube and the tubes were centrifuged at 400 RCF for 5 minutes.

The supernatants were discarded and the cells re-suspended in 100 µl 1% BSA in PBS and analysed immediately on a BD FACSCanto II. Data files were analysed using FlowJo v.7. Phalloidin-FITC fluorescence within individual monocyte subsets was analysed by gating on each subset based on surface staining for CD45, CD14, CD16 and HLA-DR. Results were displayed as a percentage increase in F-actin polymerisation in stimulated samples compared to un-stimulated samples.

Counter current centrifugal elutriation 2.8

Introduction 2.5.1

Buffy-coat derived PBMCs contain monocytes as well as a mixture of platelets, lymphocytes and granulocytes. Monocytes represent approximately 10% of buffy coat derived PBMCs, the other 90% largely accounted for by lymphocytes (T cells, B cells, NK cells and other less frequent innate lymphocytes) with a less frequent population of blood DCs. When using flow cytometry to gate on monocyte subsets, it is not possible to fully separate lymphocytes and monocytes without the use of multiple monocyte-specific antibody stains. While labelling PBMC preparations with monocyte subset-specific antibodies can facilitate the use of fluorescence-activated cell sorting (FACS) to generate highly-purified populations of individual monocyte subsets, the numerical predominance of lymphocytes over monocytes can greatly increase sorting time and potentially adversely affect the purity, number, viability and functional state of the final sorted cells. In particular, the relative rarity of the Intermediate and Non-Classical monocytes or of sub-populations within these subsets make it highly challenging to purify meaningful numbers from unfractionated PBMC preparations. In addition, Non-Classical monocytes are reported to shed antibody-bound CD16 during sorts of three hours or longer. Therefore, an enrichment step to achieve a purer total monocyte population without depleting one or more of the individual subsets prior to FACS would be of distinct value for investigating the functional properties of human monocyte sub-populations.

Counter current centrifugal elutriation (CCE) is a method of cell separation that is achieved using a centrifuge with a special chamber through which a stream of fluid moves at a constant rate in "counter-current" fashion to the centrifugal forces resulting in separation of cells/particles of differing sizes (Figdor et al., 1982, Coulais et al., 2012) (see **Figures 2.1A and 2.1B** below)

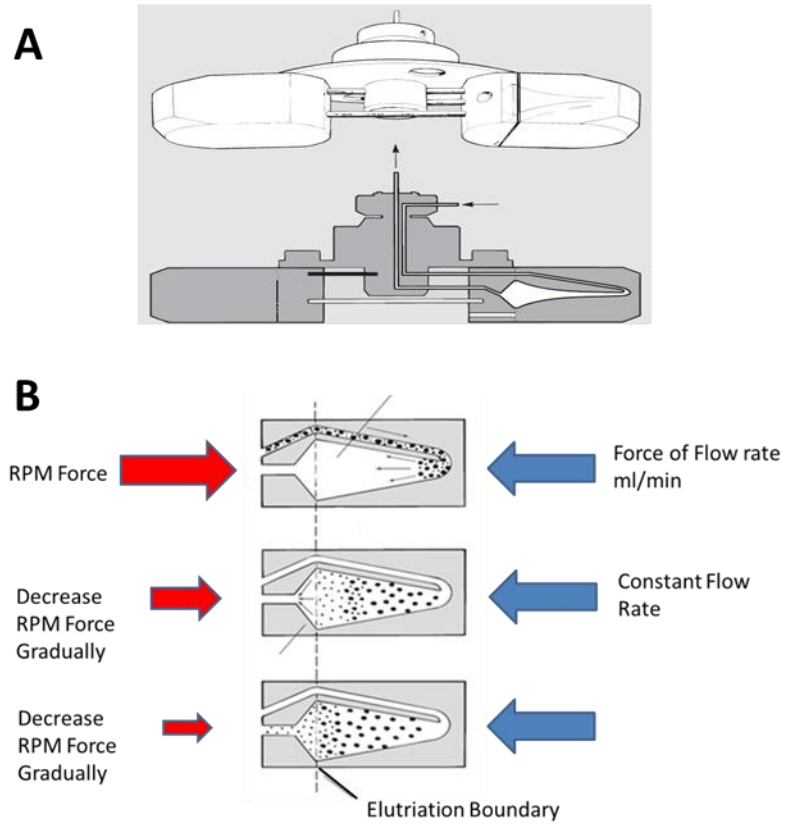

Figure 2. 2 Overview of elutriation process.
A. Illustration of an elutriator centrifuge chamber. **B.** Separation of cell based on size by elutriation. Cells are loaded into the elutriation chamber under the force of constant flow rate. The force generated from the centrifuge acts as a counter force, resulting in separation of cells based on size throughout the chamber. Decreasing the force of the centrifuge (by reducing the RPM) results in smaller cells being elutriated in early fractions and bigger cells elutriated in later fractions.

As shown in **Figure 2B,** the cells are loaded into the chamber and carried by the force of the flow rate. In the chamber the force generated by the centrifuge (g-force) is also exerted on the cells, countering the force of the flow rate. By keeping the flow rate constant and decreasing the g-force of the

centrifuge it is possible to produce a gradual separation of cells of different sizes. Larger cells will have more g-force exerted on them than smaller cells resulting in larger cells being retained toward the back of the chamber while the smaller cells flow more freely to the front. With further decrease in the centrifugal force, smaller cells at the front of the chamber pass the elutriation boundary, are carried off by the force of the constant flow rate and can be collected into tubes placed at the exit portal of the device. On-going reduction of the centrifugal force eventually allows for collection of fractions of ever increasing size.

Elutriation method 2.8.2

Eight 6 ml EDTA Vacutainer® tubes of blood are drawn from a healthy volunteer and PBMCs were prepared by Ficoll gradient centrifugation as described in **Section 2.1** with the blood split into multiple 3 ml aliquots. Buffy coats were transferred to sterile 15 ml Falcon® tubes (two buffy coats per tube) with the volumes made up to 10 ml with 2% FCS in PBS. These were pelleted by centrifugation at 400 RCF for 5 minutes at 4 °C. The supernatants were discarded and the pellets were washed and re-suspended in 5ml each 2% FCS in PBS. Finally, the washed PBMCs were filtered through 30 µm nylon mesh into two 50 ml tubes which were then filled with 2% FCS in PBS. For a detailed protocol on operation of the elutriator (Avanti JE, Beckman Coulter, Pasadena, CA, USA), see Appendix. Briefly, the elutriator was accelerated to 2600 rpm with the flow rate set at 25 ml/min using 2% FCS in PBS. The PBMC suspensions were added to the loading syringe 20 ml at a time, followed by 20ml of 2% FCS in PBS. When all cells were loaded, 2 x 50ml fractions were collected in sterile Falcon® tubes. The elutriator was then stopped and 2 further 50 ml 'stop' fractions were collected which contained elutriation-enriched monocytes. The stop fractions were then centrifuged at 400 RCF for 7 minutes, the supernatants were discarded and the cells from each tube were re-suspended in 500 µl of 2% FCS in PBS then were pooled together and counted to determine the final cell numbers.

For determining the elutriation profiles of monocyte subsets, the same protocol was used as mentioned above with certain differences. After loading cells (at 2600 rpm) and collecting 2 x 50ml fractions, the centrifugal force was reduced in 200 rpm increments (from 2600 to 0 rpm) with 2 x 50ml fractions collected after each reduction in centrifugal force. Fractions collected were centrifuged at 400 RCF for 7 minutes, the supernatants were discarded and the cells from each tube were suspended in 100 µl of FACs buffer and were then stained with anti-human CD16-FITC, anti-human CD14-PerCP, anti-human CD45-APC and anti-HLA-DR-APC.H7 at 4°C for 20 minutes, protected from light. Samples were then analysed on a BD FACSCanto II cytometer.

Magnetic activated cell sorting of human monocytes 2.9

Magnetic activated cell sorting (MACs) was used, where indicated, to isolate human monocytes from a PBMC mixture. Two different MACS systems were used: 1. a positive selection for $CD14^+$ monocytes using CD14 magnetic microbeads and 2. the no-touch pan-monocyte isolation kit (Miltenyi Biotech), which contains magnetic microbeads to positively select the major lymphocyte, granulocyte and DC populations, leaving an enriched monocyte population which includes Classical, Intermediate and Non-Classical subsets.

The isolation of $CD14^+$ monocytes was carried out using human CD14 microbeads (Miltenyi Biotech) as per the manufacturer's instructions. Briefly, Ficoll gradient-derived PBMCs were incubated with 20 µl of microbeads per 10^7 cells at 4°C for 15 minutes. Cells were then washed in 2 ml of MACS buffer (0.5% BSA in PBS with 0.2 mM EDTA) at 400 RCF for 5 minutes. Next, supernatant was discarded and the cells were suspended in 500 µl MACS buffer for every 10^8 cells. The cell suspension was then passed through a magnetic column where cells labelled with CD14 microbeads bound to the column while unlabelled cells passed though. After all the cells had passed through the column, it was rinsed with 3 x 500 µl MACs buffer. Finally, the column was removed from the magnet and 1 ml of MACs buffer was added to the column and flushed. This effluent contained $CD14^+$ cells.

The isolation was of monocytes using the human pan-monocyte isolation kit (Miltenyi Biotech) was carried out according to manufacturer's instructions. Briefly, Ficoll gradient-derived PBMCs were labelled with 10 µl of FcR blocking reagent and biotin-antibody cocktail per 10^7 cells for 5 minutes at 4°C. Next, 20 µl of anti-biotin microbeads were added per 10^7 cells and the mixtures were incubated for 10 minutes at 4°C. Following this, the labelled cells were passed through a magnetic column as described above. Unlabelled cells which passed through the column were collected and constituted the unlabelled monocytes while the labelled cells bound to the column consisted of lymphocytes, granulocytes and DCs.

After isolation of monocytes using the $CD14^+$ microbeads and the pan-monocyte isolation kit, the purity of the respective isolated monocytes was determined. An aliquot of isolated monocytes were taken, suspended in 100 µl of FACs buffer and were then stained with anti-human CD16-FITC, anti-human CD14-PerCP, anti-human CD45-APC and anti-HLA-DR-APC.H7 at 4°C for 20 minutes, protected from light. Samples were then analysed on a BD FACSCanto II cytometer.

Fluorescent activated cell sorting of human monocyte subsets 2.10

Monocytes were enriched by elutriation (see **Methods 2.5**) and then sorted into Classical, HLA-DR^{mid} Intermediate, HLA-DR^{hi} Intermediate and Non-Classical monocyte subsets (**Figure 2.3**). Between 3 and 10 x 10^6 elutriation-enriched monocytes were stained in 2% FCS in PBS with anti-human CD16-BV450 (1µl/10^6 cells) and anti-human HLA-DR-PE (BD Biosciences, UK) (2.5µl/10^6 cells) with Flow Minus One (FMO) controls prepared at the same time. Antibody incubations were carried out for 20 minutes at 4°C. Sorting was performed on a FACSAria II flow cytometer (BD Biosciences) using an 85 µm nozzle with a high flow rate, dead cells exclusion using Sytox Red® viability dye (Invitrogen) and doublets excluded using a singlet gate. Cells were sorted into polystyrene FACs collection tubes (BD Biosciences) that were pre-coated with

FCS and contained 1 ml each of RPMI supplemented with 10% FCS, L-glutamine and penicillin/streptomycin.

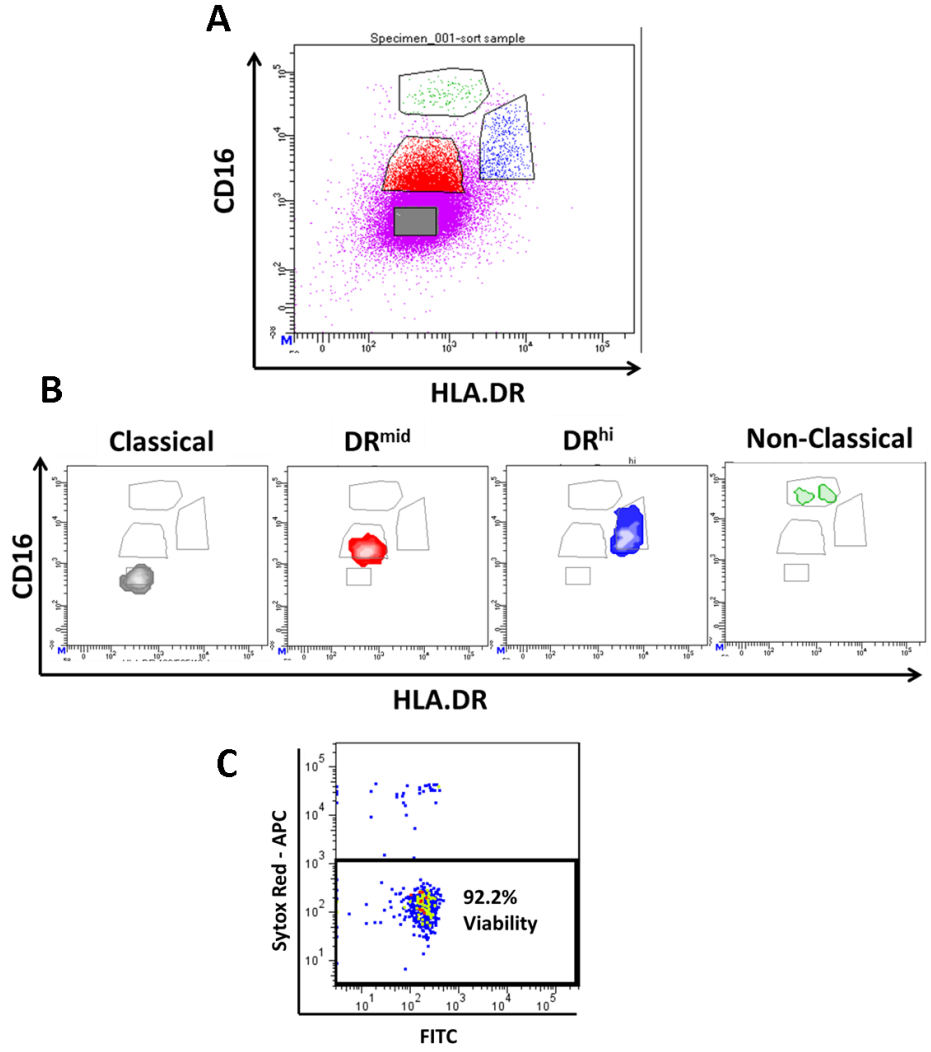

Figure 2. 3 Illustration of fluorescent activated cell sorting of human monocyte subsets.

(**A**) Illustration of typical gate placement for FACS-based purification of individual monocyte subsets. (**B**) Representative example of the post-sort purity dot-plots of monocyte subsets after FACS. **(C)** Representative example of sorted monocyte viability, post sort.

The collection chamber temperature was set at 4°C. Immediately after sorting, the collected cells were pelleted by centrifugation at 400 RCF for 5 minutes. The supernatants were removed, D-PBS was added and the cells were re-pelleted and re-suspended in RLT cell lysis buffer (Qiagen, Venlo, Netherlands).

Total RNA was isolated from the sorted monocyte subsets using an RNeasy Micro Kit (Qiagen) by the manufacturer's suggested protocol for isolation of RNA from PBMCs.

RT-PCR of human monocytes 2.11

Expression of mRNA for RGS proteins was analysed by RT-PCR in $CD14^+$ monocytes that were enriched from freshly isolated PBMCs by magnetic activated cell sorting (MACs) using anti-CD14-coated microbeads (Miltenyi Biotech) according to the manufacturer's protocol (see **Methods 2.9**). The isolated monocytes were placed in 1.5 ml Eppendorf® tubes (Sarstedt) and were washed in PBS to remove any remaining medium before the addition of 1 ml of Tri-Reagent® solution (Sigma-Aldrich). The mixture was pipetted thoroughly to ensure efficient lysis and 200 µl of chloroform (Sigma-Aldrich) were added. The tubes were shaken vigorously for 15 seconds and then left to stand for 15 minutes at room temperature. Next, the tubes were centrifuged at 12,000 x g for 15 minutes at 4°C. The aqueous phase was collected, added to a fresh tube along with 500 µl isopropanol (Sigma-Aldrich), allowed stand for 10 minutes at room temperature and then placed at -20°C overnight. The next day, the preparations were centrifuged at 12,000 x g for 10 minutes at 4°C. The supernatants were removed carefully and the RNA pellets were washed in 75% ethanol in de-ionized water (Sigma Aldrich). The tubes were briefly vortexed and then centrifuged at 7,500 x g for 5 minutes at 4°C. The supernatants were removed carefully and the RNA pellets were air dried for 8 minutes in a fume hood at room temperature. The RNA pellets were then re-suspended in 50 µl of diethylpyrocarbonate (DEPC)-treated water and were mixed well using a pipette. The quality and quantity of RNA were then assessed using a NanoDrop® 2000 spectrophotometer (Thermo Fisher Scientific).

First strand cDNA synthesis was carried out using a RevertAid H Minus First Strand cDNA Synthesis Kit (Thermo Fisher Scientific) with an oligo (dT)18 primer mix according to manufacturer's instructions. Briefly, cDNA synthesis was performed in a Veriti Gradient Thermal Cycler (Thermo Fisher Scientific) for 60 minutes at 42°C and reactions were terminated at 70°C for 5 minutes. The cDNA samples were then stored at -80°C until required. A no template control (NTC) and a no reverse transcriptase control (-RT) were carried out with each cDNA synthesis.

For each PCR reaction, 75 ng of cDNA were used. The sequences of the forward and reverse primers used for individual amplifications are listed in **Table 2.3**:

Table 2- 3 Primer sequences for RT-PCR of sorted monocyte subsets.

Primer	Sequence : (5' to 3')	Length	Tm
RGS1 Fwd	ACCTGAGATCTATGATCCCACATCTGG	27	69.8
RGS1 Rev	GGCTATTAGCCTGCAGGTCAT	21	64.2
RGS2 Fwd	CAGACCCATGGACAAGAGCGC	21	71.3
RGS2 Rev	TAGCATGAGGCTCTGTGGTGA	21	66
RGS3 Fwd	TTGGCTGTCAGGGCAGCTGTACAATAGTGG	30	77
RGS3 Rev	CACTGAACTCAGTGCGAAGGAAGGCTTGGA	30	78.3
RGS4 Fwd	GCCGGCTTCTTGCTTGAGGAG	21	71.3
RGS4 Rev	CACTGAGGGACCAGGGAAGCA	21	70.9
RGS12 Fwd	ACCAGGAGCACCGGGAGGTCC	21	74.7
RGS12 Rev	CTCTCCCGTAGCCGAGTGGTT	21	68.6
RGS16 Fwd	CACCTGCCTGGAGAGAGCCAA	21	71.1
RGS16 Rev	TGGCAGAGGCGGCTGAGGCTT	21	76.3
RGS18 Fwd	ATGGAAACAACATTGCTTTTCT	22	61.3
RGS18 Rev	TTATAACCAAATGGCAACATCTGA	24	63.9
Actin Fwd	GTTTGAGACCTTCAACACCC	20	61
Actin Rev	ATACTCCTGCTTGCTGATCC	20	60.9
HPRT Fwd	CCTGGCGTCGTGATTAGTGA	20	66.2
HPRT Rev	AACAATCCGCCCAAAGGGAA	20	69.4
GADPH Fwd	CACTAGGCGCTCACTGTTCT	20	62.2
GADPH Rev	GCCAAATTCGTTGTCATACCAGG	23	68.1

Polymerase chain reactions were carried in 0.2 ml RNase-free Eppendorf® tubes (Sarstedt) at final reaction volumes of 25 µl using the reagents listed in **Table 2.4**:

Table 2- 4 Composition of PCR reactions.

Reagent	Volume	Final Concentration
10x Standard *Taq* reaction buffer	2.5 µl	1X
10mM dNTPs	0.5 µl	200 µM
10µM Forward Primer	0.5 µl	0.2 µM
10µM Reverse Primer	0.5 µl	0.2 µM
Taq DNA polymerase	0.125 µl	1.25 units/50ul PCR
Template DNA	Variable	75 ng per reaction
Nuclease-Free Water	Made up to 25 µl	

Abbreviations: Deoxynucleotide triphosphates (dNTPs)

The PCR reactions were carried on a Verity Gradient Thermal Cycler (Thermo Fisher Scientific) using the settings summarised in **Table 2.5**.

Table 2- 5 PCR reaction conditions.

Step	Temperature	Time
Initial Denaturation	95°C	30 seconds
35 Cycles	95°C 45-68°C (Annealing) 68°C	15-30 seconds 15-60 seconds 1 minute/kb
Final Extension	68°C	5 minutes
Hold	4-10°C	

For gel electrophoresis of PCR products, 5 µl aliquots of each reaction were mixed with 2 µl of gel loading dye (New England BioLabs, Ipswich, MA, USA) and loaded onto 1X SYBR® Safe (Invitrogen) 1% agarose (Sigma-Aldrich) gels along with an aliquot of Quick-Load® 100 base-pair DNA ladder (New England BioLabs) The gels were subjected to electrophoresis at 100 volts until the dye front had migrated to the lower third of the gel. Images of the gels were acquired on a Gel Doc® Imager (Bio-Rad Laboratories, Hercules, CA, USA). Expected PCR product sizes are listed in **Table 2.6**.

Table 2- 6 Expected PCR product sizes for RGS protein mRNA detection in sorted human monocyte subsets.

Primer	PCR Product Size
RGS1	460bp
RGS2	590bp
RGS3	1300bp
RGS4	590bp
RGS12	710bp
RGS16	540bp
RGS18	708bp
HPRT	867bp

For more detailed specifications on RT-PCR primers, see Appendix.

Quantitative RT-PCR of sorted monocyte subsets 2.12

Total RNA was isolated from freshly sorted monocyte subsets, quantified and reverse transcribed as described in the preceding section. Before use, cDNA samples were diluted to a concentration of 1 ng/μl, with 2 μl used per well. Quantitative PCR was carried out on a Step One Plus® Real Time PCR system (Thermo Fisher Scientific) using a SensiFAST SYBR Hi-ROX kit (Bioline, London, UK) and a two-step cycle. SYBR Green I RT-qPCR primers for GAPDH, HPRT, RGS1, RGS2, RGS12, RGS18, FCG3RB were purchased as pre-designed and validated KiCqStart™ primers from Sigma Aldrich. The primer sequences, predicted product lengths and melting temperatures (Tm) for the primers used are summarised in **Table 2.7**.

Table 2- 7 Primer characteristics for qPCR of mRNA of RGS proteins and housekeeping genes.

Primer	Primer Sequence	Length	Tm
GAPDH Fwd	ACAGTTGCCATGTAGACC	18	55.7
GAPDH Rev	TTTTTGGTTGAGCACAGG	18	59.9
HPRT1 Fwd	ATAAGCCAGACTTTGTTGG	19	56.8
HPRT1 Rev	ATAGGACTCCAGATGTTTCC	20	57
RGS1 Fwd	ACTGGTCAAAATGTCTTTGG	20	59.1
RGS1 Rev	CTTATAGTCTTCACAAGCCAG	21	55.8
RGS2 Fwd	AATATGGTCTTGCTGCATTC	20	59.2
RGS2 Rev	TTTTCCTTGCTTTTGAGGAC	20	60.8
RGS12 Fwd	TAAACTTTTCTCACACGCAC	20	58
RGS12 Rev	GACTGCTGGTCATTAGAAAC	20	56.3
RGS18 Fwd	AGATGGACTAGAGGCTTTTAC	21	55.8
RGS18 Rev	TTCTTGAAATCTTCACAGGC	20	59.4
FCGR3B Fwd	GAACATCACCATCACTCAA	20	58
FCGR3B Rev	AGAGAAATATAGTCCTGTGTCC	22	55.5

The reaction mix composition used for qPCR reactions is summarised in **Table 2.8** with final reaction volume of 10 µl. The reaction conditions are summarised in **Table 2.9**.

Table 2- 8 Quantitative PCR reaction composition.

Reagent	Volume	Final Concentration
2x SensiFAST	5µl	1x
10µm Forward Primer	0.4µl	400nM
10µm Reverse Primer	0.4µl	400nM
Template cDNA	2µl	2ng
H_2O	2.2µl	
10µl final volume		

Table 2- 9 Quantitative PCR conditions for analysis of RGS protein mRNA expression in sorted human monocyte subsets.

Cycles	Temperature	Time	Notes
1	95°C	2 minutes	Polymerase Activation
40	95°C 65°C	5 seconds 30 seconds	Denaturation Annealing/extension

Reactions were carried out in duplicate on a StepOnePlus™ real-time PCR system (Step One Plus® Real Time PCR system) and data were collected using StepOne software v2.3 (Step One Plus® Real Time PCR system). Analysis of relative mRNA expression levels was performed using the relative 2^ΔCT method. GAPDH was used as housekeeping gene for normalisation and Classical monocytes were set as the reference sample for each individual subset analysis. RNA quality was determined by the A260/A280 ratio using using a NanoDrop® 2000 spectrophotometer. All sample used had a A260/A280 ratio >1.6.

For more detailed specifications on qRT-PCR primers, see **Appendix 2**.

Data analysis and statistics 2.13

All statistical comparisons were performed with GraphPad® Prism V 5.0 (GraphPad Software, San Diego, CA, USA) and Microsoft® Excel 2010 (Microsoft Corporation, Redmond, Washington, USA).

Multiple-group comparisons were made using a single factor analysis of variance (ANOVA). Paired sample analysis was performed using a two-sided paired Student's t-test. The paired t-test was considered to be appropriate to test for differences between the monocyte subsets, as observations were matched between donors. Statistical significance was assigned for values <0.05.

In general, a minimum of 3 biological replicates were performed for each experiment. However, for many experiments more than 3 biological replicates were performed (numbers indicated in the relevant figure legends).

Chapter 3

Phenotypic Characterisation of Two Newly-Identified Human Intermediate Monocyte Sub-populations 3.0

Introduction 3.1

At the beginning of this study, human monocyte subsets had recently been classified into three distinct subsets: Classical, Intermediate and Non-Classical (Ziegler-Heitbrock et al., 2010). A number of high impact studies followed shortly afterwards (Cros et al., 2010, Zawada et al., 2011, Wong et al., 2011) to shed light on the functional characteristics and genetic profiles of the newly-described Intermediate subset. However, some of the results of these studies were apparently contradictory. For example, Cros et al, found Intermediate monocytes to be the highest producers of TNF-α in response to LPS in vitro, while Wong et al. reported Non-classical monocytes to be the dominant secretors of TNF-α (Wong et al., 2011, Cros et al., 2010). Genetic profiling of Intermediate monocytes produced a gene signature that suggested roles in antigen processing and presentation and angiogenesis. However, in some functional studies, Intermediate monocytes were reported to be poor stimulators of T-cell proliferation and failed to produce cord-like structures in Matrigel assays (Zawada et al., 2011). Possibly the most consistently reported functional characteristic of Intermediate monocytes is their phagocytic capacity, with high phagocytosis of latex beads (Cros et al., 2010), modified lipids (Rogacev et al., 2014) and malarial infected red blood cells (Zhou et al., 2015) all reported. Furthermore, in some studies, phagocytosis was accompanied by intracellular production of pro-inflammatory cytokines such as TNF-α and IL-1β (Zhou et al., 2015, Rogacev et al., 2014).

The conflicting data to date may indicate heterogeneity within in the Intermediate monocyte subset. Previous work from our laboratory revealed phenotypic heterogeneity amongst the Intermediate subset and raised the possibility that this subset could be further divided into two distinct populations based on surface expression of HLA-DR (MC Dennedy, EP Connaughton and MD Griffin, unpublished observations). *These sub-populations were initially termed HLA-DR^{mid} and HLA-DR^{hi} Intermediate monocytes and, for the purposes of this thesis, are abbreviated to DR^{mid} and DR^{hi} Intermediate monocytes.*

Subsequent experimental work by Dennedy et al. compared blood-derived DR^{mid} and DR^{hi} Intermediate monocyte populations between healthy controls and an obese patient cohort, revealing that DR^{mid} Intermediate monocytes are significantly expanded in obesity in comparison to healthy controls. In contrast, there was no significant difference in absolute numbers or proportions of the DR^{hi} Intermediate monocytes between the obese cohort and healthy controls.

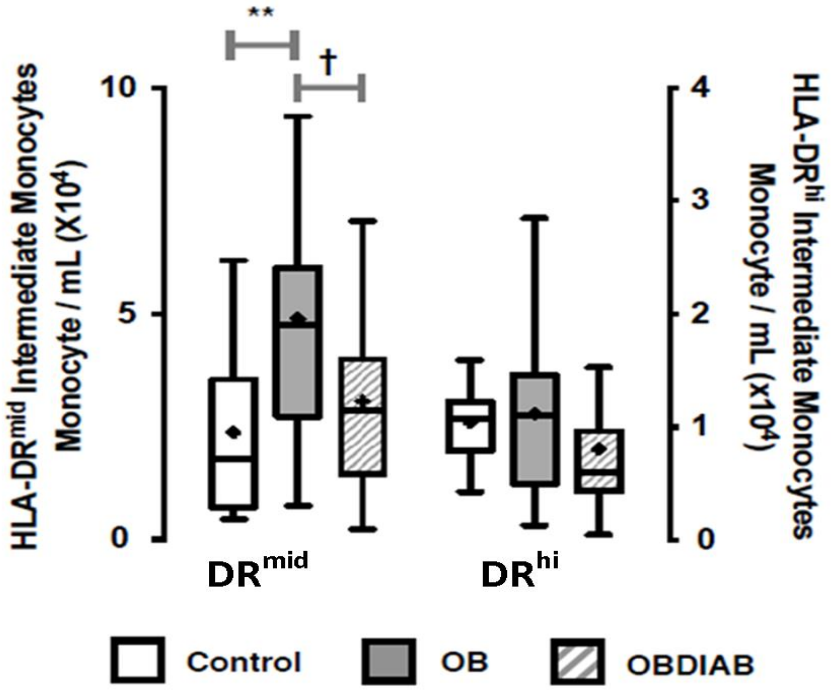

Figure 3. 1 DR^{mid} and DR^{hi} Intermediate Monocyte Subsets in Obesity and Type 2 Diabetes

Comparisons of numbers of DR^{mid} and DR^{hi} Intermediate monocytes in blood samples of Non-obese Controls (Clear; n=33) Non-diabetic Obese (OB, Shaded; n=42) and Diabetic Obese (OBDIAB, Patterned; n=53) groups. Boxplots compare proportional changes of the DR^{mid} and DR^{hi} Intermediate subsets across groups and demonstrate a significant increase in DR^{mid} but not the DR^{hi} monocytes in OB and OBDIAB compared to Control. Statistical Analysis: Multivariate Analysis of Variance (MANOVA) with Tukey's posthoc. * $p<0.05$; ** $p<0.01$ vs. Control. † $p<0.05$; ‡ $p<0.01$ vs. OB.

This study further functionally characterised DR^{mid} Intermediate monocytes as avid scavengers of the modified lipoproteins, acetylated low density lipoprotein (ac-LDL) and oxidised LDL (ox-LDL), with scavenging dependant on CD36 and SRA-1 receptors (MC Dennedy, EP Connaughton and M Griffin,

unpublished observations). *These results suggested both phenotypic and functional heterogeneity within the Intermediate subset. They also suggested that increased numbers of DR^{mid} monocytes in the circulation may account for the noted expansion of Intermediate monocytes observed in studies of various clinical cohorts* (Rogacev et al., 2012, Rogacev et al., 2014, Heine et al., 2008, Ulrich et al., 2010).

Therefore, as a starting point for the project reported in this thesis, we sought to characterise the phenotypes of the proposed DR^{mid} and DR^{hi} Intermediate monocyte sub-populations in healthy adults and to confirm that these subsets, as identified by multi-colour flow cytometry, were free from non-monocytic immune cells such as dendritic cells, lymphocytes and granulocytes. .

Hypothesis and Objectives 3.2

Hypothesis 3.2.1

Intermediate monocytes with mid- and high-level surface expression of HLA-DR represent phenotypically distinct human monocyte sub-populations which differ in their expression of multiple functionally-relevant surface markers.

Objectives 3.2.2

1. To use a stringent flow cytometry gating strategy to determine whether the proposed DR^{mid} and DR^{hi} Intermediate monocyte sub-populations are free from contaminating non-monocytic immune cells.
2. To further phenotypically characterise human DR^{mid} and DR^{hi} Intermediate monocytes for their relative expression of cell surface receptors involved in chemotaxis, adhesion, and transmigration.
3. To morphologically characterise human Classical, DR^{mid} Intermediate, DR^{hi} Intermediate and Non-Classical monocytes.

Results 3.3

Monocyte subset identification 3.3.1

An 8-colour flow cytometric gating strategy was developed to achieve more accurate definition of the monocyte subsets than had previously been achieved in freshly-isolated PBMC samples from healthy adult volunteers. Sytox Blue® viability dye and anti-CD56 were combined in a dump channel, excluding in an initial step both non-viable cells and $CD56^{+}$ natural killer cells **(Figure 3.2A)**.

Viable monocytes were then defined based on size and granularity (FSC-A vs SSC-A), with cell doublets next eliminated using a singlet gate (FSC-A vs FSC-H) **(Figure 3.2A)**. Monocytes were then sequentially gated on using anti-HLA-DR vs anti-CD45, anti-CX3CR1 vs anti-CD45, anti-CX3CR1 vs anti-CD33 and, finally, anti-CD14 vs anti-CD16 with the intention of fully eliminating non-monocytic cells from the final population of interest **(Figure 3.2A)**.

The three conventional human monocyte subsets were then gated on according to the internationally agreed nomenclature (Ziegler-Heitbrock et al., 2010), producing the Classical '$CD14^{++}CD16^{-}$', Intermediate '$CD14^{++}CD16^{+}$' and Non-Classical '$CD14^{+}CD16^{++}$' monocytes **(Figure 3.2B)**.

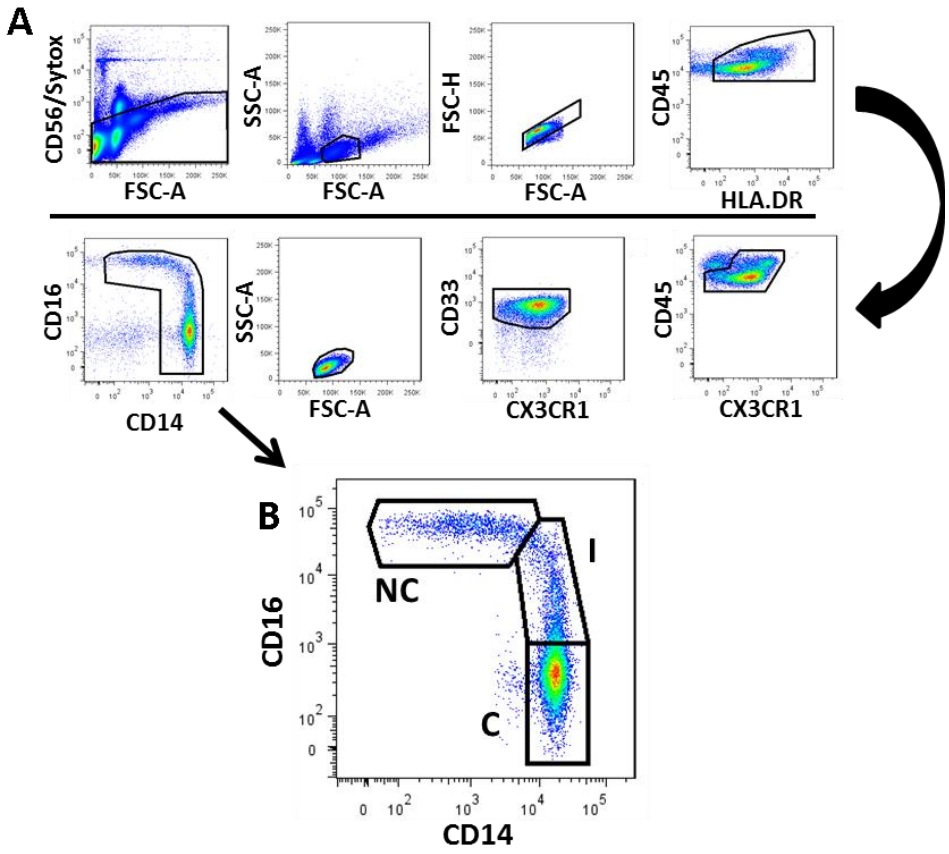

Figure 3. 2 Stringent gating strategy for identification of human monocyte subsets in blood isolated from healthy individuals.

(A) $CD56^{+}$ and non-viable cells are initially eliminated and a crude monocyte population is gated on based on FSC vs SSC. Sequential gating using antibodies against CD45, HLA-DR, CD33 and CX3CR1 generates a pure monocyte population which can be subdivided into three subpopulations based on CD14 vs CD16 (**B**), producing Classical **(C)**, Intermediate **(I)** and Non-Classical **(NC)** subsets**.** Figure representative of 1 donor.

Based on previous work from our group described in the Introduction to this Chapter, we then further subdivided the Intermediate monocyte subset into two further sub-populations using cell surface expression of HLA-DR and CD16**.** By this approach, monocytes can be separated into four distinct sub-populations, namely (**i**) Classical ($CD16^{-}CD14^{+}DR^{+}$), (**ii**) DR^{mid} Intermediate ($CD16^{+}CD14^{+}DR^{+}$) (**iii**) DR^{hi} Intermediate ($CD16^{+}CD14^{+}DR^{++}$) and (**iv**) Non-Classical ($CD16^{++}CD14^{dim}DR^{+}$) **(Figure 3.3A)**.

Back-gating these four monocyte subsets onto CD14 vs CD16 plots with gates set for the currently recognized three monocyte subsets revealed that Classical and Non-classical monocytes fall within the expected gates **(Figure3.3B i and iv)** while the two newly-proposed DR^{mid} and DR^{hi} Intermediate sub-populations both fall within the conventional Intermediate gate **(Figure3.3B ii and iii)**.

A colour-coded overlay of all four proposed monocyte sub-populations within a CD16 vs CD14 plot further highlights the substantial phenotypic overlap between the DR^{mid} and DR^{hi} Intermediate sub-populations **(Figure3.3C)**.

In addition to differential expression of HLA-DR by DR^{mid} and DR^{hi} sub-populations **(Figure3.3D)**, the DR^{hi} subpopulation also exhibits higher cell surface expression of CD45 than the DR^{mid} subpopulation **(Figure3.3E)**.

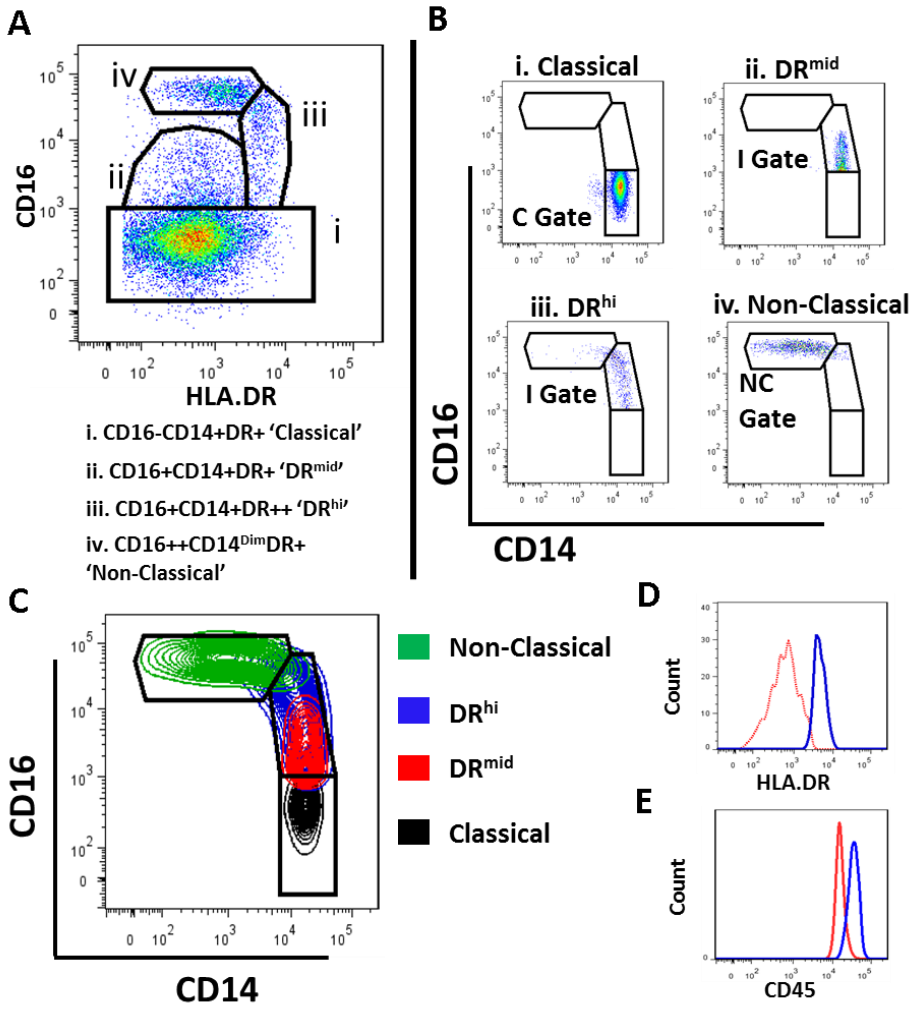

Figure 3. 3 Cell surface expression HLA-DR reveals heterogeneity of the intermediate monocyte subset.

Flow cytometric analysis of PBMCs from a healthy adult. Using the same gating strategy as in **Figure 3.2**, the final monocyte population is plotted using HLA-DR vs CD16. **(A)** Separation of the Intermediate monocytes into two separate populations based on HLA-DR expression, termed DR^{mid} **(i)** and DR^{hi} **(ii)** monocytes, along with Classical **(i)** and Non-Classical **(iv)** monocytes. **(B)** Back-gating of each of the newly-described monocyte subpopulations onto CD14 vs CD16 plot reveals that both DR^{mid} and DR^{hi} Intermediate monocytes fall within the $CD16^{+}CD14^{+}$ "Intermediate" gate. **(C)** Colour-coded back-gating of all four proposed monocyte sub-populations within a single CD14 vs. CD16 contour plot. **(D)** Histograms illustrating relative surface expression of HLA-DR and CD45 on DR^{mid} and DR^{hi} Intermediate monocytes. Figure representative of 1 donor.

Having established from the 8-colour gating strategy outlined above that both of the newly-proposed Intermediate sub-populations consisted of bona fide monocytes we then tested whether a less complex, 4-colour gating strategy (using antibodies against CD16, CD14, HLA-DR and CD45 only) could be used to identify and enumerate the same monocyte sub-populations with a similar degree of accuracy **(Figure 3.4)**.

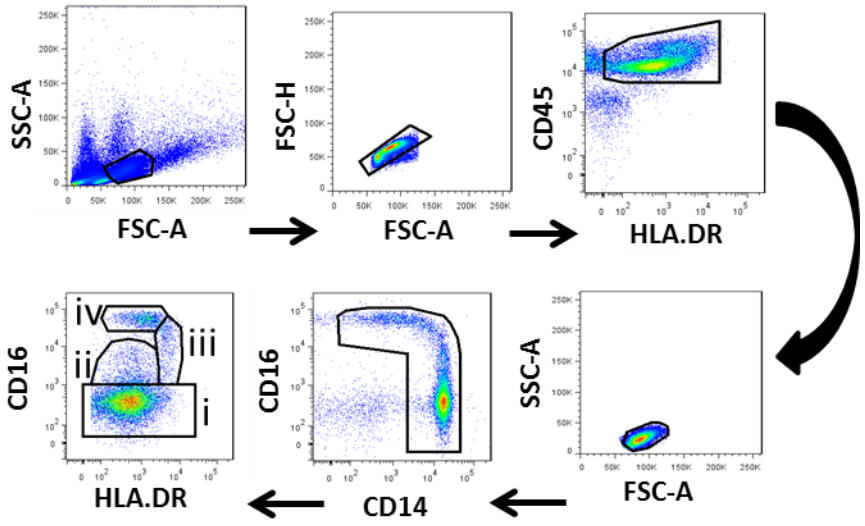

Figure 3. 4 Simplified, 4-colour gating strategy for identification of monocyte sub-populations.
Monocytes were identified using a minimal 4-marker staining combination, producing Classical (**i**), DR^{mid} Intermediate (**ii**), DR^{hi} Intermediate (**iii**) and (**iv**) Non-Classical sub-populations as shown. Figure representative of 1 donor.

The 8-colour and 4-colour gating strategies were, therefore, concurrently used to analyse monocyte subset proportions from a series of 7 adult volunteers and the results were compared. As shown in **Table 3-1** below, the monocyte sub-population proportions generated from the 8-colour and 4-colour gating strategies were not significantly different. Monocyte subset proportions are expressed as a percentage of the CD14 vs CD16 monocyte gate (8^{th} gate**, Figure 3.2** and 5^{th} gate, **Figure 3.4**)

Based on these results, the typical proportions of each monocyte subpopulation in the circulation of healthy adults were concluded to be

approximately: Classical 69%, DR^{mid} Intermediate 14%, DR^{hi} Intermediate 6% and Non-Classical 9%.

Table 3- 1 Healthy adult PBMC monocyte sub-population proportions based on 8-colour and 4-colour gating strategies. (n=7)

	Average Monocyte Subset Proportions +/- SD		
Monocyte Subset	**8 Colour Staining and Viability Dye**	**Minimal 4 Colour Staining**	**P value (paired t test)**
Classical	69.53 ± 10.5%	69.41 ± 11.44%	ns
DR^{mid}	14.04 ± 9.132%	13.96 ± 8.858%	ns
DR^{hi}	5.620 ± 2.130%	5.605 ± 2.108%	ns
Non-Classical	9.313 ± 6.246%	9.173 ± 6.170%	ns

Following this initial series of experiments it was concluded that: (**a**) $CD16^{+}CD14^{+}$ monocytes can be further divided into two separate sub-populations based on cell surface expression of HLA-DR, producing DR^{mid} and DR^{hi} Intermediate subsets, (**b**) The newly proposed Intermediate sub-populations are viable cells which are not cross-contaminated by other cell types such as NK cells, (**c**) The DR^{mid} and DR^{hi} sub-populations represent approximately 14% and 6% of the total blood monocytes of healthy adults, and (**d**) A 4-colour gating strategy can reliably identify the Intermediate sub-populations, with similar efficiency to the 8-colour gating strategy.

Phenotypic characterisation of monocyte sub-populations. 3.3.2

Phenotypic characterisation of a range of cell surface receptors by flow cytometry using the simplified 4-colour staining panel was next carried out on PBMC samples from healthy adults to determine whether there were further demonstrable differences between the DR^{mid} and DR^{hi} Intermediate monocyte sub-populations as well as between the Classical and Non-classical subsets.

By this approach, surface expression of chemokine receptors revealed significant differences between DR^{mid} and DR^{hi} subsets for CCR2 ($p<0.0001$) and

CX3CR1 ($p<0.0001$), while no significant differences between the two sub-populations were detected for CCR5, CCR6 and CXCR4 **(Figure 3.5)**.

Receptors involved in monocyte adhesion to endothelium and trans-endothelial migration were also detected at differential levels on DR^{mid} and DR^{hi} Intermediate monocytes. The integrin chains, CD11a ($p=0.0008$), CD11b ($p=0.003$), CD11c ($p=0.0001$) and CD49d ($p=0.02$) were all expressed at higher levels on the DR^{hi} compared to the DR^{mid} Sub-population **(Figure 3.6)**. In contrast, L-selectin ($p=0.007$) and P-selectin glycoprotein ligand-1 (PSGL-1) ($p=0.002$) were most highly expressed on the DR^{mid} Intermediate sub-population **(Figure 3.6)**. No significant difference was found for expression of CD31.

Receptors for granulocyte colony-stimulating factor (GCSF-R) and colony stimulating factor-1 (CSF-1R) were also expressed at similar levels on both DR^{mid} and DR^{hi} monocyte subsets **(Figure 3.7)**.

Comparing receptor expression of Classical to DR^{mid} Intermediate monocytes, there was no significant difference for CCR2, CCR5, CXCR4, CD31, CD62L and CSF1-R. However, significant differences in cell surface receptor expression were detected for chemokine receptors CX3CR1 ($p=0.0001$) and CCR6 ($p=0.03$), integrins CD11a ($p=0.0045$), CD11b ($p=0.03$), CD11c ($p=0.002$) and CD49d ($p=0.03$), PSGL-1 ($p=0.02$) and for GCSF-R ($p=0.002$) (**Figures 3.5-3.7**).

Comparing Non-Classical with DR^{hi} Intermediate monocytes, there were significant differences in surface expression of CX3CR1 ($p=0.0001$), CCR2 ($p=0.0001$), CCR5 ($p=0.0006$), CXCR4 ($p=0.0020$), CD11a ($p=0.0003$), CD11b ($p=0.0005$), CD11c ($p=0.015$), PSGL-1 ($p=0.0005$), CD62L ($p=0.02$), CD31 ($p=0.012$), GCSF-R ($p=0.03$) and CSF-1R ($p=0.04$) (**Figures 3.5-3.7**).

As expected, there were also multiple significant differences between Classical and Non-classical monocytes subsets as regards surface expression of the panel of functional markers (**Figures 3.5-3.7**)

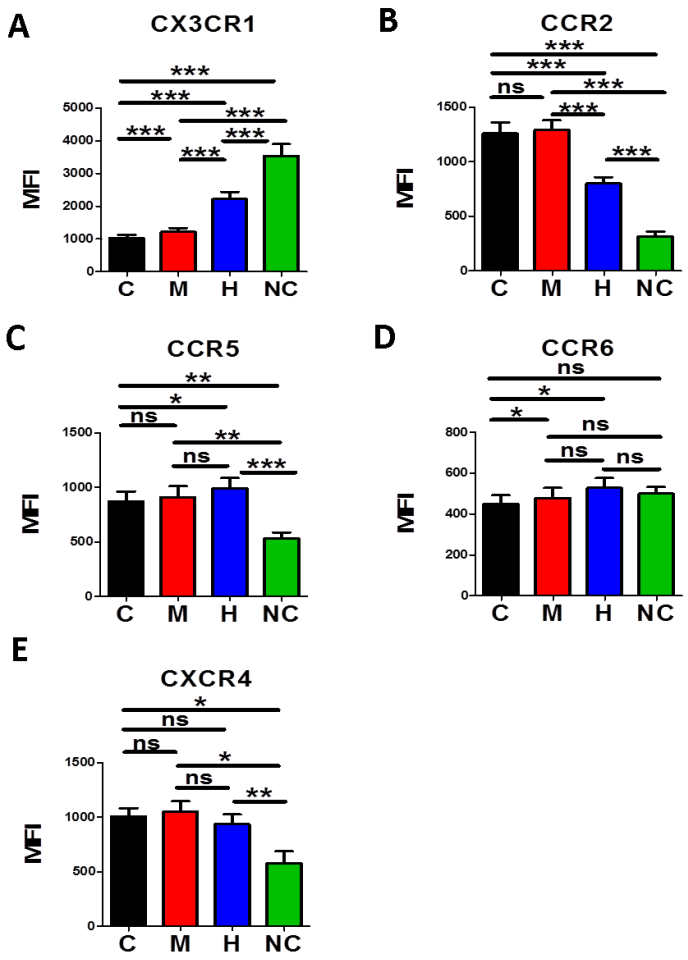

Figure 3. 5 Chemokine receptor phenotyping of monocyte sub-populations

Monocyte subsets were analysed by flow cytometry using the simplified 4-colour staining panel combined with antibodies against specific chemokine receptors as shown (**A-E**). Legend: **(C)** Classical, **(M)** DR^{mid} Intermediate, **(H)** DR^{hi} Intermediate, **(NC)** Non-Classical monocytes. Data derived from n= (CX3CR1 n=9, CCR2 n=12, CCR5 n=5, CCR6 n=5, CXCR4 n=4) healthy adult PBMC samples. Data presented as mean ± standard deviation. Statistical comparisons performed using two-sided paired t test. ns = $p>0.05$, * = $p<0.05$; ** = $p<0.01$; *** = $p<0.001$.

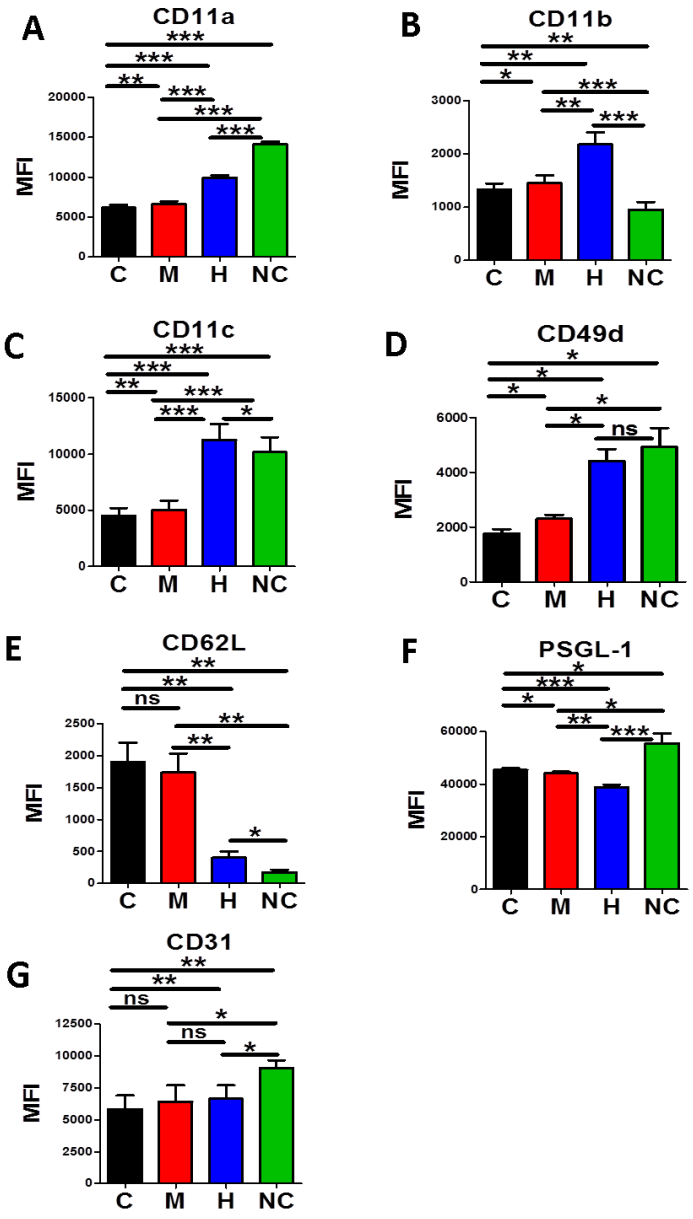

Figure 3. 6 Adhesion receptor phenotyping of monocyte sub-populations.
Monocyte subsets were analysed by flow cytometry using the simplified 4-colour staining panel combined with antibodies against specific adhesion receptors as shown (**A-G**). Legend: (**C**) Classical, (**M**) DR^{mid}, (**H**) DR^{hi}, (**NC**) Non-Classical monocytes. Data derived from n= (CD11a n=5, CD11b n=5, CD11c n=9, CD49d n=3, CD62L n=5, PSGL-1 n=9, CD31 n=5) healthy adult PBMC samples. Data presented as mean ± standard deviation. Statistical comparisons performed using two-sided paired t test. ns = $p>0.05$, * = $p<0.05$; ** = $p<0.01$; *** = $p<0.001$.

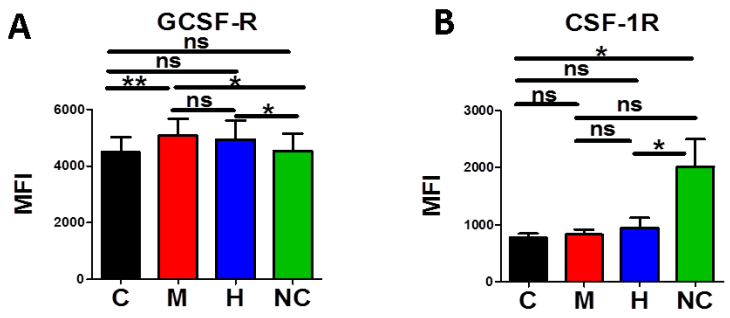

Figure 3. 7 Growth factor receptor phenotyping of monocyte sub-populations.

Monocyte subsets were analysed by flow cytometry using the simplified 4-colour staining panel combined with antibodies against growth factor receptors as shown (**A, B**).Legend: (**C**) Classical, (**M**) DR^{mid}, (**H**) DR^{hi}, (**NC**) Non-Classical monocytes. Data derived from n= (GCSF-R n=8, CSF-1R n=7) healthy adult PBMC samples. Data presented as mean ± standard deviation. Statistical comparisons performed using two-sided paired t test. ns = $p>0.05$, * = $p<0.05$; ** = $p<0.01$; *** = $p<0.001$.

It was concluded, from the phenotyping studies above, that human monocyte sub-populations differentially express a range of cell surface receptors. In particular, the newly-described DR^{mid} and DR^{hi} Intermediate monocytes display significant differences in their cell surface expression of the chemokine receptors CCR2, CX3CR1, the integrin receptors CD11a, CD11b, CD11c, CD49d and selectins CD62L and PSGL-1. These differences further enhance the evidence that the DR^{mid} and DR^{hi} subsets represent distinct monocyte populations.

Morphological properties of monocyte subpopulations 3.3.3

As cells are passed through a flow cytometer, their granularity and size can be determined by detection of light scattering. In regard to the passage of a cell or particle through a laser beam, it has been stated that: 'light scattered in the forward direction at low angles (0.5-10°) from the axis is proportional to the square of the radius of a sphere, and so to the size of the cell' (Macey, 2007). Thus "forward scatter" may be interpreted as an indicator of cell size. Light may also enter a cell and become refracted trough reflection off cell contents such as the nucleus, cytoplasmic granules and other cell contents. In the case of such "side scatter" it has been stated that ' the 90° light (right angled, side) scatter may be considered proportional to the granularity' (Macey, 2007).

In our flow cytometric analysis of freshly isolated PBMCs from healthy adult volunteers, Non-Classical monocytes were the smallest and least granular of the subsets, with average forward scatter (FSC) of 89700±2757 fluorescence units and average side scatter (SSC) of 15100±1190 fluorescence units. In comparison, all other monocyte subsets had significantly higher FSC (Classical: 95300±5083, $p<0.04$; DR^{mid}: 98100±5172, $p<0.01$; DR^{hi}: 99300±435, $p<0.004$) and higher SSC (Classical: 18600±1988, $p<.0.016$; DR^{mid}: 19200±1840, $p<0.0075$; DR^{hi}: 17700±1706 MFI, $p<0.02$) (see **Figure 3.8**). Overall, DR^{mid} Intermediate monocytes were the most granular based on SSC, being also significantly more granular than Classical ($p<0.004$) and DR^{hi} Intermediate monocytes ($p<0.009$).

In addition, based on FSC, the DR^{mid} and DR^{hi} Intermediate monocyte sub-populations represent larger cells than both Classical ($p<0.0015$ and $p<0.0004$ respectively) and Non-Classical ($p<0.04$ and $p<0.004$ respectively) subsets (**Figure 3.8 A and C**). Overall, DR^{hi} Intermediate monocytes appeared to be the largest of the monocyte sub-populations having significantly higher FSC than all other sub-populations (**Figure 3.8 A and C**).

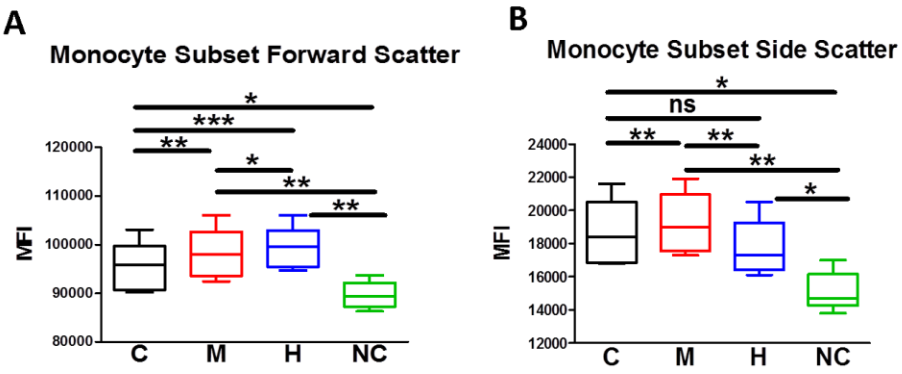

C

Monocyte Subset Forward Scatter		
Test	p Value	Summary
C vs M	0.0015	**
C vs H	0.0004	***
C vs NC	0.0397	*
M vs H	0.0421	*
M vs NC	0.0099	**
H vs NC	0.0038	**

D

Monocyte Subset Side Scatter		
Test	p Value	Summary
C vs M	0.0039	**
C vs H	0.0554	ns
C vs NC	0.0164	*
M vs H	0.0090	**
M vs NC	0.0075	**
H vs NC	0.0200	*

Figure 3. 8 Light scatter properties of human monocytes sub-populations

Flow cytometric analysis of freshly-isolated PBMCs from healthy adult volunteers. **(A) and (C)**: Graphical representation monocyte sub-population Forward Scatter measurements and table of statistical comparisons among the individual monocyte sub-populations. **(B) and (D)**: Graphical representation monocyte sub-population Forward Scatter measurements and table of statistical comparisons among the individual monocyte sub-populations. **C**=Classical, **M**= DR^{mid}, **H**= DR^{hi}, **NC**= Non-Classical. Data derived from n = 7 healthy adult PBMC samples. Data presented as box plots: Box limits = upper and lower interquartile range, median line = median, whiskers represent smallest and largest values that are not outliers. Statistical comparisons performed using two-sided paired t test. ns = $p>0.05$, * = $p<0.05$; ** = $p<0.01$; *** = $p<0.001$.

Classical, DR^{mid} Intermediate, DR^{hi} Intermediate and Non-Classical monocytes were also morphologically compared by light microscopy by purification into individual populations using FACS followed by cyto-spin transfer onto glass slides and staining with May-Grunwald and Giemsa stains. By this staining protocol, nuclei are stained deep purple, with the cytoplasm stained a lighter blue/purple.

All of the imaged cells exhibited typical 'kidney bean' or 'horseshoe' shaped nuclei confirming their monocytic nature (**Figure 3.9 A-D**). In agreement with the FSC data from the flow cytometric analyses, Non-Classical monocytes appeared smaller in size than each of the other sub-populations when assessed by light microscopy (**Figure 3.9 A-D**). Consistent with their SSC characteristics, both of the Intermediate sub-populations appeared to have a more granular cytoplasm and greater amount of vacuole-like spaces compared to Classical and Non-Classical monocytes (**Figure 3.9 A-D**).

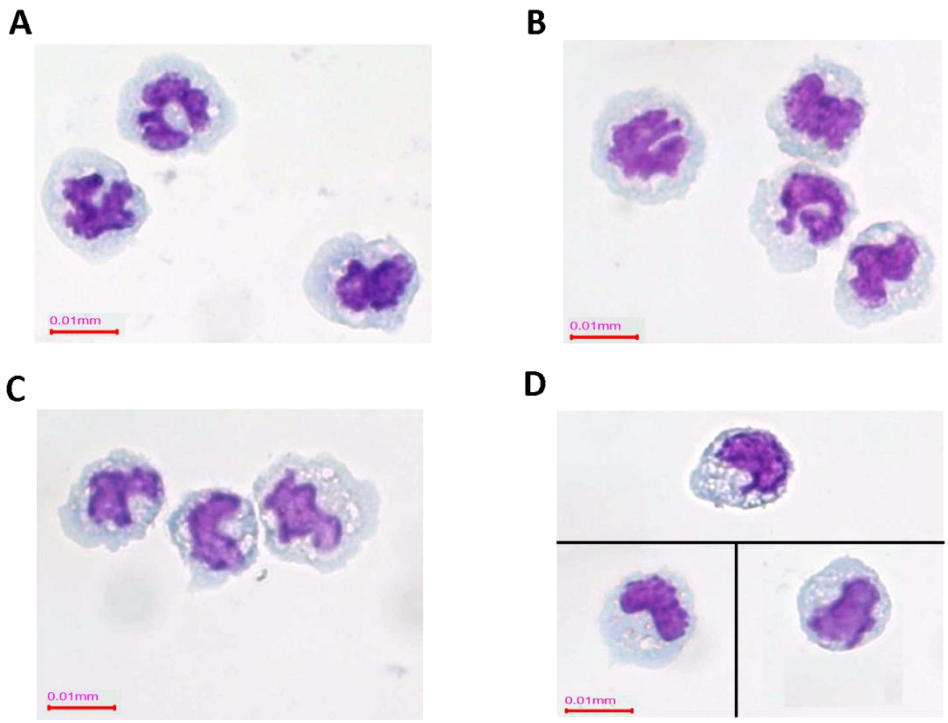

Figure 3. 9 May-Grunwald and Giemsa staining of purified monocyte subsets
Representative examples of FACS-purified: **(A)** Classical. **(B)** DR^{mid} Intermediate. **(C)** DR^{hi} Intermediate. **(D)** Non-Classical monocytes. Images taken a 60X. Scale bar represents 0.01mm. Figure representative of 1 donor.

In agreement with the FSC values obtained for Non-Classical monocytes in **Figure 3.7 B**, Non-Classical monocytes appear to be the smallest of the monocyte subsets when assessed by light microscopy (**Figure 3.8 D**). The Intermediate subsets, DR^{mid} (**Figure 3.8 B**) and DR^{hi} (**Figure3.8 C**) appear to have the most granular cytoplasm and greater amount of vacuole-like spaces within the cytoplasm when compared to Classical (**Figure 3.8 A**) and Non-Classical (**Figure 3.8 D**). All monocyte subsets displayed 'kidney bean' or 'horseshoe' shaped nuclei (**Figure 3.8**).

In conclusion, the monocyte sub-populations appear to be quite heterogeneous in terms of size and granularity as determined by light scatter characteristics detected by flow cytometry. Microscopic analysis confirmed the presence of typical 'kidney bean' or 'horseshoe' shaped nuclei suggesting the sub-populations, and importantly the DR^{mid} and DR^{hi} Intermediate subsets identified by multi-colour flow cytometry, are of monocytic origin.

Discussion 3.4

In Chapter 3, we began to further characterise the proposed DR^{mid} and DR^{hi} Intermediate monocyte sub-populations that were previously defined in both healthy and obese subjects. Morphological analysis was carried out to confirm the presence of a typical monocyte-like nucleus, and a stringent flow cytometry gating strategy was applied to rule out the possibility that the Intermediate monocyte gates we developed contained a substantial number of non-monocytic cells. Additionally, extensive surface phenotyping was carried out to further characterise all of the monocyte sub-populations under the current classification, and also to determine whether other markers apart from CD16 and HLA-DR could also clearly distinguish the monocyte populations.

A primary aim at the start of the study was confirm the newly described DR^{mid} and DR^{hi} Intermediate gates (MC Dennedy, EP Connaughton and M Griffin, unpublished observations) as containing genuine monocytes. This would appear essential due to a number of different immune cell types, such as blood DCs, NK cells and other lymphocytes, displaying similar cell surface receptors to monocytes. Even in the highly-cited study by Cros et al, the authors found it necessary to establish that Non-Classical monocytes were indeed bona-fide monocytes (Cros et al., 2010) despite the fact that Non-Classical monocytes (or $CD16^{+}$ monocytes) were well established in the literature before that study. Additionally, most of the major studies involving monocyte subsets use a series of monocyte specific cell surface receptors to establish a pure monocyte population (Cros et al., 2010, Wong et al., 2011).

Thus, in order for the newly-proposed DR^{mid} and DR^{hi} Intermediate subsets to be accepted, we considered it to be vital that the criteria used for defining them meet or exceed those of other studies. In **Figure 3.1**, we have illustrated that the newly described DR^{mid} and DR^{hi} subsets represent a viable population of monocytes, and are free from any contaminating lymphocytes, such as $CD56^{+}$ NK cells.

Additionally, one of the strongest defining characteristics of monocytic cells is their size and 'horseshoe'- or 'kidney bean'-shaped nucleus. This characteristic has been used to identify monocytes from other immune cell types. In our microscopic examination of highly purified monocyte sub-populations, all sorted cells displayed such a nucleus, and closely resembled monocyte morphological images from other studies (Zawada et al., 2011, Cros et al., 2010). Of note, in these studies, the Intermediate populations appeared to contain more vacuoles in the cytoplasm than the others. This correlates with our own observation that Intermediate DR^{mid} and DR^{hi} sub-populations appeared to contain a greater number of vacuoles than their Classical and Non-Classical counterparts.

It was also important to clearly demonstrate that, under the currently recognised monocyte subsets (Classical, Intermediate and Non-Classical monocytes), the newly proposed DR^{mid} and DR^{hi} monocytes are contained within the Intermediate gate and that either or both do not simply represent "over-spill" from the Classical or Non-Classical subsets. Using back gating approaches we believe that this point is well addressed in our detailed flow cytometry characterisations using PBMCs from multiple healthy adults.

Having shown, using a stringent gating strategy, that our Intermediate sub-populations were free from any contaminating cell type, we additionally illustrated that using a minimal 4 colour staining combination can achieve the same purity of monocyte subsets. The establishment of this 4-colour gating strategy represented a key step toward later experiments in which additional fluorescence channels were required for further phenotypic and functional characterisations as well as for FACS-based purification.

Monocyte chemotaxis and endothelial interactions are a key function of monocyte biology. Indeed, Classical (high CCL2-induced chemotaxis and tissue migration) and Non-Classical (patrolling of endothelial vasculature) monocytes are functionally distinguished by these properties. Hence, we assessed DR^{mid} and DR^{hi} Intermediate monocytes cell surface expression of chemokine receptors, integrins and colony stimulating factor receptors.

While phenotypic characterisation of the DR^{mid} and DR^{hi} Intermediate monocyte sub-populations indicated significant differences between the subsets for CX3CR1, CCR2, CD11a, CD11b, CD11c, CD49d, CD62L, PSGL-1, no cell surface receptor analysed during this process provided a clearer separation of the Intermediate monocyte sub-populations than did HLA-DR. This lack of a true defining cell surface receptor signature indicated by our results is also borne out in the literature, as there has been no unique cell surface receptor discovered for the Intermediate monocyte population, despite extensive screening of Intermediate monocytes in several studies (Wong et al., 2011, Zawada et al., 2011, Cros et al., 2010). The cell surface and gene expression of HLA-DR has been reported to be most highly expressed on Intermediate monocytes in a number of published studies (Thiesen et al., 2014, Wong et al., 2011, Zawada et al., 2011) and, in one of these, HLA-DR microbeads were used to remove a HLA-DR^{+} monocyte population from the $CD16^{+}CD14^{+}$ Intermediate monocyte population (Zawada et al., 2011). This consistent evidence for high expression of HLA-DR on Intermediate monocytes is important to consider in regard to our proposed definition of Intermediate monocyte sub-populations. Our results indicate that heterogeneity of HLA-DR (MHC II) expression within the Intermediate monocyte subset has not been fully appreciated by other groups studying this part of the human monocyte repertoire.

In our phenotypic analysis of the DR^{mid} and DR^{hi} monocyte sub-populations, there was some evidence for a progression from Classical to DR^{mid} to DR^{hi} to Non-Classical monocytes. For example, expression of certain markers (e.g. CX3CR1, CD11a, CD49d, CD31) started off lowest in Classical and sequentially progressed to higher levels in DR^{mid}, DR^{hi} and Non-Classical sub-populations. In the case of others (e.g. CCR2 and CD62L) the opposite trend was observed. This 'intermediate' expression of cell surface receptors at levels between Classical and Non-Classical monocytes is also reflected the literature (Hijdra et al., 2013, Wong et al., 2011). Importantly, however, we demonstrated that Classical and DR^{mid} monocytes display similar cell surface expression of a range of receptors and the DR^{mid} Intermediate sub-populations could be considered to be a direct phenotypic (and perhaps functional) progression of Classical

monocytes most clearly manifest by the initiation of CD16 up-regulation in the absence of increased HLA-DR. Additionally DR^{hi} and Non-Classical monocytes display similar surface levels of multiple surface receptors which are expressed at levels either above or below those of Classical and DR^{mid} Intermediates. This may suggest that DR^{hi} Intermediate and Non-Classical monocytes also represent contiguous stages of a process of intravascular development or maturation. Indeed, the respective size and granularity characteristics of the four defined sub-populations are also in keeping with such relationships. Nonetheless, as discussed in detail elsewhere in this thesis, formal proof of a sequential transition of human blood monocytes through four or more functionally distinct stages (beginning with the bone marrow-derived Classical subset) will require highly sophisticated in vivo experimental systems. Furthermore, other models (e.g. separate "Intermediate" populations derived from both Classical and Non-classical monocytes) also remain possible to explain human Intermediate monocyte heterogeneity.

Monocyte subset proportions varied between donors (**Table 3-1**). Of the Intermediate subsets, the DR^{hi} subset was proportionately the most consistent with the lowest deviation between donors. This may suggest that the DR^{hi} subset may be tightly regulated in terms of presence and numbers in the circulation. In contrast, the DR^{mid} subset was highly variable between donors, with a high deviation. This may indicate that the DR^{mid} subset proportions may be influenced by different factors between donors. This reflects previous work shown by our lab, albeit in an obese patient cohort, that the DR^{mid} subset was expanded in an obese patient cohort, while the DR^{hi} subset remained consistent (MC Dennedy, EP Connaughton and M Griffin, unpublished observations). Even though our monocyte proportions were determined form the blood of healthy adults, it may be possible that other factors may be influencing DR^{mid} subset proportions, such as diet. Phenotyping results indicated that cell surface receptor expression for a broad range of receptors were consistently expressed on the monocyte subsets, indicating that while there may be other factors influencing the monocyte subset proportions, such factors do not appear to affect monocyte phenotype drastically.

In summary, results from this Chapter indicate that DR^{mid} and DR^{hi} Intermediate sub-populations are bona fide monocytes with significant differences in expression of chemokine and integrin receptors. However it was unclear whether different expression levels of these receptors reflects functional differences and this clearly required further experimental elucidation. Morphological features and expression levels of certain receptors suggest the DR^{mid} Intermediate subset is more closely related to the Classical subset, while DR^{hi} Intermediates appear to be more similar to Non-Classical monocytes. Despite phenotyping for a range of cell surface receptors, we did not identify a marker that was superior to HLA-DR for separation of the DR^{mid} and DR^{hi} sub-populations or could substitute for CD16 as a defining marker for all four sub-populations. This reinforces a model whereby the Intermediate monocyte represents a cell in transition, rather than being a fully developed cell type in its own right.

Chapter 4

In Vitro Transmigration of Monocyte Subsets 4.0

Introduction 4.1

Transmigration is a critical process in monocyte biology and is co-ordinated by sequential engagement of chemokine receptors, integrins and selectins. Monocytes initially exit the bone marrow in a CCR2-dependant manner into the circulation. From there, they may use a variety of chemokine receptors such as CXCR4, CCR2, CCR5, CX3CR1 along with sequential engagement of inflammation-induced endothelial ligands for selectins and integrins to engage in transendothelial migration from the circulation to extravascular tissues. Once in the tissue, depending on signals encountered, monocytes may differentiate to a macrophage-like phenotype in inflammatory settings or, in some healthy tissues to replenish the resident population of mononuclear phagocytes. In certain settings, tissue infiltrating monocytes or monocyte-derived macrophages and dendritic cells may subsequently migrate to the draining lymph nodes.

The transmigratory properties of human $CD16^{+}$ (Intermediate and Non-Classical) and $CD16^{-}$ (Classical) monocytes have been characterised in vitro. Such studies have revealed strong migration of $CCR2^{+}/CX3CR1^{-}/CD16^{-}$ monocytes toward CCL2 (MCP-1), while $CCR2^{lo}/CX3CR1^{+}/CD16^{+}$ monocytes migrated towards CX3CL1 (fractalkine) in Transwell assays (Ancuta et al., 2003, Ancuta et al., 2004). A more recent study using endothelium-covered Transwell systems revealed that Classical $CCR2^{+}$ monocytes migrated strongly to CCL2, in contrast to the Intermediate ($CCR2^{mid}$) and Non-Classical ($CCR2^{-}$) monocytes which migrated poorly to this chemokine (Krankel et al., 2011). Similar results were reported in another study (Thiesen et al., 2014). When human monocyte subsets were perfused over inflammatory cytokine-treated endothelium, both Classical and Non-Classical monocytes crawled in ICAM-1/ICAM-2- and VCAM-1/CX3CR1-dependant manners respectively (Collison et al., 2015). In this study, Intermediate monocytes did not exhibit crawling behaviour, instead adhering to the endothelium tightly (Collison et al., 2015).

Such studies, although relatively few in number, suggested a poor transmigratory response by Intermediate monocytes to traditional monocyte chemokines accompanied by a tendency to be highly adherent to activated endothelium without engaging in crawling-type behaviour. This evidence may indicate that the Intermediate monocyte subset is unresponsive to chemokines which typically act strongly upon Classical (and perhaps also Non-classical) monocytes. Alternatively, Intermediate monocytes may be restrained from transendothelial migration by other, as yet unidentified mechanisms. As we demonstrated in **Chapter 3**, the DR^{mid} and DR^{hi} Intermediate monocyte subsets have significant heterogeneity in their expression of certain chemokine receptors (CCR2, CX3CR1), selectins (CD62L) and integrins (CD11a, CD11b, CD11c, VLA-4). Thus, we questioned whether they exhibit differential chemotaxis, adhesion and transendothelial migration characteristics.

Hypothesis and Objectives 4.2

Hypothesis 4.2.1

Intermediate monocytes with mid- and high-level surface expression of HLA-DR differ from each other and from their Classical and Non-Classical counterparts in regard to their adhesion and transendothelial migration.

Objectives 4.2.2

1. To quantify the transmigration of the four individual human monocyte sub-populations toward relevant chemokines in an in vitro transmigration assay.
2. To quantify endothelial adherence and transmigration of the four individual human monocyte sub-populations in the absence and presence of relevant chemokines.

Results 4.3

Monocyte subset transmigration toward chemoattractants 4.2.1

A Transwell assay system was developed to assess human monocyte subset transmigration through a 3.0 µm pore size membrane toward selected chemokines. Freshly-isolated PBMCs from healthy adult volunteers were allowed to transmigrate for 60 minutes, after which the transmigrated cells in the basal chamber were retrieved, stained with monocyte-specific mAbs and analysed using flow cytometry as described in **Chapter 2**. Quantification of transmigrated monocytes was achieved using flow cytometry-compatible counting beads. Monocyte transmigration was calculated as an index of transmigration (see **Materials and Methods, Section 2.3**).

The assay system, examples of flow cytometric analysis of transmigrated monocytes and quantitative results of a series of such experiments carried out on a total of 6 individual PBMC preparations are shown in **Figure 4.1 A-E.**

Classical monocytes migrated robustly towards CCL2, -7 and -8, with the highest index of migration achieved in response to CCL7 (9.9±4.5) followed by CCL2 (5.2±1.1) and CCL8 (3.6±1.7). Classical monocyte migration toward each of the three chemokines was significantly higher than that of all other monocyte sub-populations (**Figure 4.1 C-E**).

The two Intermediate monocyte sub-populations, DR^{mid} and DR^{hi} monocytes migrated only weakly toward CCL2, -7 and -8 in comparison to Classical monocytes. The DR^{mid} and DR^{hi} sub-populations did not differ significantly from each other in these migration assays although DR^{mid} monocytes exhibited non-significant trends toward higher migration indices than DR^{hi} monocytes (**Figure 4.1 C-E**).

Consistent with previous reports and with the chemokine receptor profiling described in **Chapter 3**, the Non-Classical monocyte subset demonstrated minimal migration toward CCL2, -7 and -8 (**Figure 4.1 C-E**).

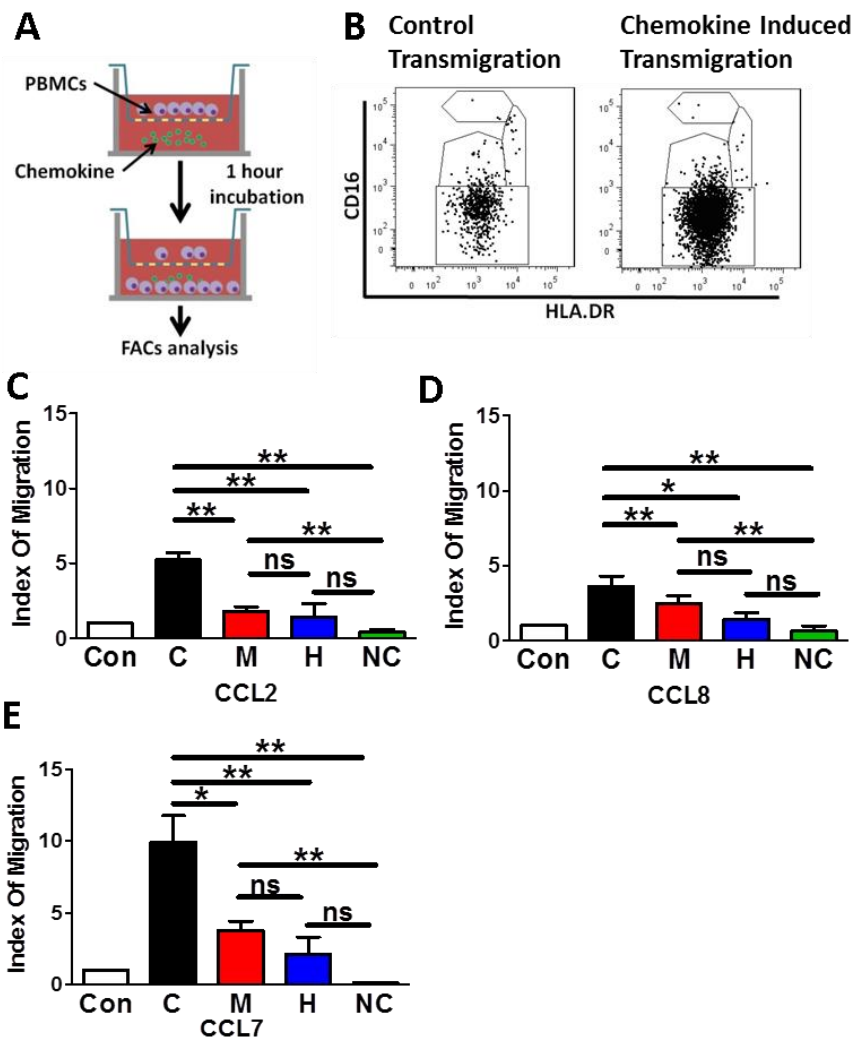

Figure 4. 1 Monocyte subset transmigration toward CCL chemokines

(A) Diagram of Transwell assay. PBMCs are added to the apical chamber with chemokine-containing medium or medium alone added to the basal well. Cells are left to transmigrate for 60 minutes before retrieving for flow cytometric analysis. (**B)** Representative examples of monocyte subset flow cytometry dot plots for anti-HLA-DR vs anti-CD16 showing both control and chemokine-induced transmigration. (**C-E).** Results of monocyte sub-population transmigration toward CCL2, CCL8 and CCL7. Legend: (**C**) Classical, (**M**) DR^{mid}, (**H**) DR^{hi}, (**NC**) Non-Classical monocytes. Data derived from n = 6 healthy adult PBMC samples. Data presented as mean ± standard deviation. Statistical comparisons performed using two-sided paired t test. ns = $p>0.05$, * = $p<0.05$; ** = $p<0.01$; *** = $p<0.001$.

Monocyte subset adherence to and transmigration through human primary endothelial layers 4.3.2

Physiologically, monocytes frequently pass through an endothelial monolayer (and subsequent layers) before entering extra-vascular tissues. To model this phenomenon in an in vitro setting, primary human aortic endothelial cells (HAECs) were seeded onto fibronectin-coated Transwell membranes (3.0µm pore size) and were allowed to form confluent endothelial monolayers as described in **Chapter 2**. To confirm that HAECs seeded onto the fibronectin-coated Transwells formed confluent monolayers, a single membrane from each experiment was stained with crystal violet dye which stains the cell nuclei a purple colour and is readily visible by light microscopy (**Figure 4.2 E**)

During tissue inflammation, the endothelium of local blood vessels becomes activated in response to inflammatory stimuli resulting in up-regulation of a range of adhesion receptors, such as ICAM-1 and VCAM-1. Monocytes express the co-receptors lymphocyte function-associated antigen-1 (LFA-1) and very late antigen-4 (VLA-4) which bind to ICAM-1 and VCAM-1 respectively (Imhof and Aurrand-Lions, 2004, Ley et al., 2007).

Mimicking this endothelial activation in our in vitro system, treatment of HAECs with TNF-α (2.5 ng/ml for 6 hours) resulted in strong increase in HAEC surface expression of VCAM-1 (**Figure 4.2 A and C**) and ICAM-1 (**Figure 4.2 B and D**).

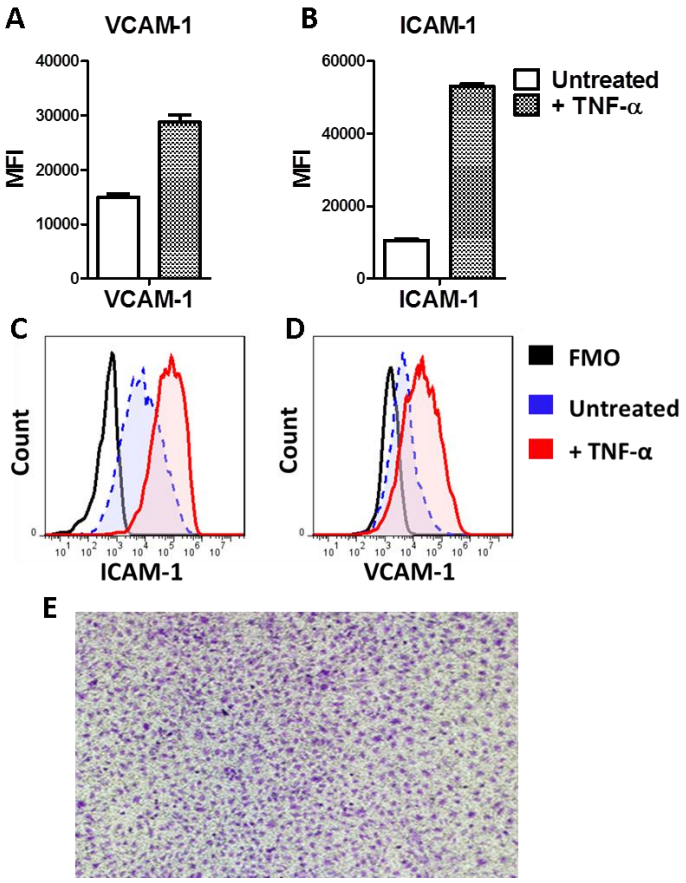

Figure 4. 2 Human aortic endothelial cell up-regulation of adhesion molecules following TNF-α stimulation

(**A**) and (**B**) Quantified surface expression of VCAM-1 and ICAM-1 by unstimulated and TNF-a-stimulated HAECs (analysed by flow cytometry, n=2). (**C**) **and** (**D**) Examples of flow cytometric histograms of anti-VCAM-1 and anti-ICAM-1 staining of unstimulated and TNF-a-stimulated HAECs (FMO = fluorescence minus one control). (**E**) Crystal violet staining of a confluent HAEC layer seeded onto a fibronectin-coated Transwells.

For human monocyte transendothelial migration assays, untreated and TNF-α-stimulated HAEC-covered Transwells were prepared. Freshly-isolated PBMCs from healthy adult volunteers were added to the top chamber and were cultured for 1 hour following which they were harvested as separate Floating, Adherent and Transmigrated fractions as described in **Chapter 2**. The fractions were stained with a 4-colour panel to distinguish the individual monocyte sub-populations which were quantified by addition of counting beads. Results for a series of such experiments carried out using freshly isolated PBMCs from 4 healthy adult volunteers are summarised in **Figure 4.3**.

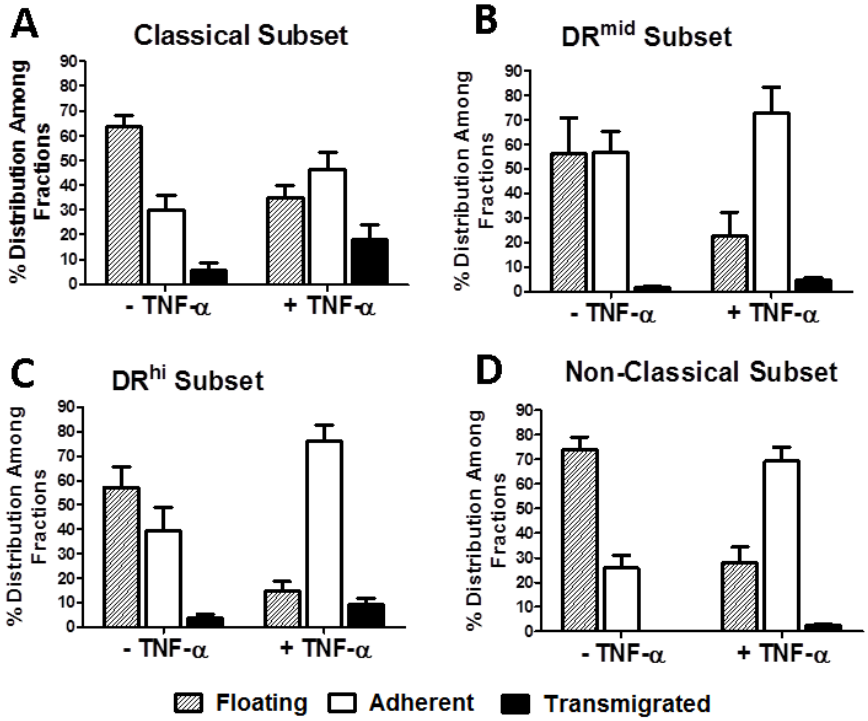

E

	Test	p-Value	Summary
Floating	C TNF– vs C TNF+	0.0399	*
	M TNF– vs TNF+	0.0296	*
	H TNF– vs M TNF+	0.0028	**
	NC TNF– vs NC TNF+	0.0049	*
Adherent	C TNF– vs C TNF+	0.0517	ns
	M TNF– vs TNF+	0.0324	*
	H TNF– vs M TNF+	0.0021	**
	NC TNF– vs NC TNF+	0.0062	**
Transmigrated	C TNF– vs C TNF+	0.094	ns
	M TNF– vs TNF+	0.0618	ns
	H TNF– vs M TNF+	0.1051	ns
	NC TNF– vs NC TNF+	0.0342	*

Figure 4. 3 Monocyte sub-population adhesion to and transmigration through primary human endothelial monolayers with and without TNF-α activation.
(**A-D**) Proportionate distributions of the four individual monocyte sub-populations into floating, adherent and transmigrated fractions in HAEC Transwells with and without TNF-α activation. (**E**) Summary of statistical comparisons. Data derived from n = 4 healthy adult PBMC samples. Data presented as mean ± standard deviation. Statistical comparisons performed using two-sided paired t test. ns = $p>0.05$, * = $p<0.05$; ** = $p<0.01$; *** = $p<0.001$.

As shown, TNF-α induced activation of the HAEC monolayer resulted in a significant decrease in the percentage of Classical, DR^{mid} Intermediate, DR^{hi} Intermediate and Non-Classical monocyte sub-populations present in the floating fraction in comparison to those of untreated endothelium (**Figure 4.3 A, B, C and D** respectively). This was accompanied by proportionate increases in the adherent fractions of all 4 monocyte sub-populations in the presence of TNF-α-activated HAECs. Thus, all of the sub-populations responded to endothelial activation by increased adherence.

Of note, the DR^{mid} Intermediate monocytes exhibited the highest proportionate adherence rate to resting endothelium, while DR^{mid} Intermediate, DR^{hi} Intermediate and Non-Classical all had similar, high rates of adherence to TNF-α activated endothelium.

As there was no specific chemokine stimulus present in the lower chambers, the proportionate transmigration of all monocyte sub-populations was predictably low. However, there were significant increases in the transmigrated fraction of each of the four defined sub-populations, this being notably greatest for the Classical subset in comparison to the other three populations.

Overall, the non-chemokine driven endothelial Transwell co-cultures revealed distinctly different adhesion/transmigration characteristics for Classical compared to DR^{mid} and DR^{hi} Intermediate and Non-classical sub-populations. **Figure 4.4** is an alternate representation of the same data presented in **Figure 4.3**, but re-configured to highlight the differences in the distribution of the individual monocyte subpopulations in the floating, adherent and transmigrated fractions in the presence of TNF-α-activated HAEC monolayers. Of particular note, the transmigration of DR^{mid} Intermediate monocytes through an activated primary human endothelial monolayer was significantly lower than that of Classical monocytes despite their broadly similar chemokine receptor expression patterns (as demonstrated in **Chapter 3**).

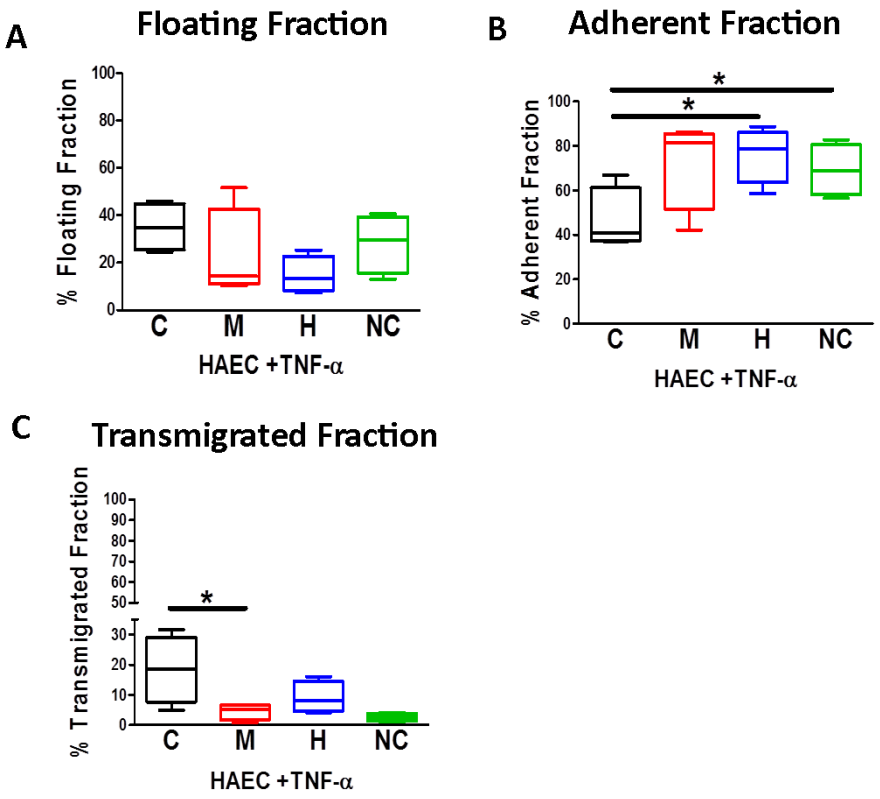

Figure 4. 4 Proportionate distributions of the four monocyte sub-populations across the floating, adherent and transmigrated fractions.

Using the same data set presented in Figure 4.3, the proportions of each monocyte subpopulations among the (**A**) floating, (**B**) adherent and (**C**) transmigrated fractions are shown for Transwell cultures involving TNF-α-activated HAEC monolayers. Legend: (**C**) Classical, (**M**) DR^{mid}, (**H**) DR^{hi}, (**NC**) Non-Classical monocytes. Data derived from n = 4 healthy adult PBMC samples. Data presented as box plots: Box limits = upper and lower interquartile range, median line = median, whiskers represent smallest and largest values that are not outliers. Statistical comparisons performed using two-sided paired t test. ns = $p>0.05$, * = $p<0.05$; ** = $p<0.01$; *** = $p<0.001$.

Chemokine-induced transmigration of monocyte sub-populations across resting and activated primary human endothelial monolayers 4.3.3

Having established a suitable assay system and defined the endothelial adhesion and transmigration characteristics of the four human monocyte sub-populations, we next sought to compare monocyte sub-population transmigratory response to CCL2 (MCP-1) through an endothelial monolayer under resting and "inflamed" conditions. Results of a series of such experiments performed using freshly-isolated PBMCs from three healthy adult donors are summarised in **Figure 4.5** below.

Similar to the non-chemokine-driven assays shown in the preceding section, Classical monocytes exhibited markedly higher transmigration toward CCL2 compared to the other monocyte sub-populations for all three PBMC samples under both resting and activated conditions. This contrasted with the relatively low levels of CCL2-induced transmigration exhibited by DR^{mid} and DR^{hi} Intermediate monocytes. Although we had established in **Chapter 3** that DR^{mid} Intermediate monocytes express significantly higher surface CCR2 compared to their DR^{hi} counterparts, the two sub-populations demonstrated equally low transendothelial migration toward CCL2.

Overall, the trends for monocyte subset transendothelial migration were consistent, whether "spontaneous" (**Figures 4.3 and 4.4**) or CCL2-induced (**Figure 4.5**) or under "resting" and "activated" endothelial conditions. Of specific interest in regard to the two proposed Intermediate monocyte sub-populations, these experiments indicated that they both exhibited a greater tendency to adhere to and a lesser propensity to transmigrate through a human endothelial monolayer.

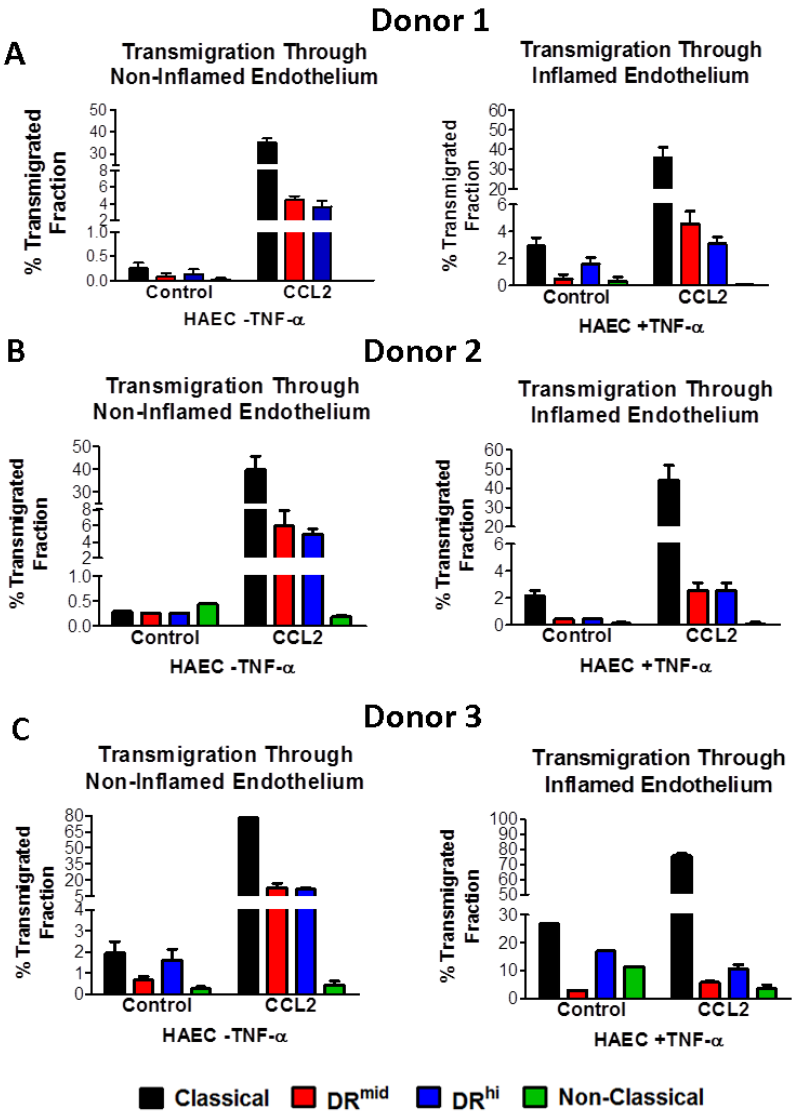

Figure 4. 5 Monocyte sub-population transmigration through resting and TNF-α-activated primary human endothelium in response to CCL2.

Transmigrated percentages of four monocyte subpopulations in Transwells containing resting (HAEC -TNFα) or activated (HAEC +TNFα) endothelial monolayers in the absence (Control) or presence of CCL2 (50ng/ml) in the lower chamber. (**A**), (**B**) and (**C**) represent results from 3 individual donors. Two technical replicates were used for each condition per donor.

Inhibition of monocyte adhesion to activated endothelium using neutralizing antibodies against integrins 4.3.4

As previously illustrated in **Figure 4.4 B**, all monocyte sub-populations demonstrated increased adherence to TNF-α-activated compared to resting endothelium. In **Chapter 3,** phenotypic characterisation of monocyte sub-populations revealed differential expression across the sub-populations of integrins involved in endothelial adherence: CD11a (alpha chain of LFA-1), CD11b (alpha chain of MAC-1), CD11c and CD49d/CD29 (VLA-4). It is possible, therefore, that the individual monocyte sub-populations differentially employ these integrin receptors during their adherence to inflamed endothelium and that differences in integrin-mediated endothelial adherence contribute to specific in vivo functional characteristics of circulating monocyte subsets and sub-populations in the setting of infection, trauma of chronic inflammation.

To assess the role of different integrin receptors in monocyte sub-population endothelial adhesion, HAECs were seeded onto fibronectin-coated tissue culture wells and pre-activated with TNF-α (2.5ng/ml for 6 hours). Freshly isolated PBMCs from healthy adult volunteers were then co-cultured with the activated endothelium for 1 hour in the presence of blocking antibodies to CD11a, CD11b, CD11c, CD49d/CD29 or of matching concentrations of the appropriate isotype control antibodies. Floating and endothelial adherent cells were retrieved, stained with a monocyte-specific antibody panel and analysed by flow cytometry with quantification using added counting beads. The results of series of such experiments carried out with PBMCs from 3 individual donors are summarised in **Figure 4.6**. As shown, the four monocyte sub-populations displayed similar relative adherence rates to those observed in the Transwell assays (**Figure 4.4 B**). Thus, Classical monocytes had the lowest rate of adherence (82.8±8.4%) with DR^{mid} Intermediate (93.5±2.6%), DR^{hi} Intermediate (95.2±3.3%) and Non-Classical (95.6±2.7%) sub-populations all having comparably high rates of adherence to activated endothelium (**Figure 4.6 A**).

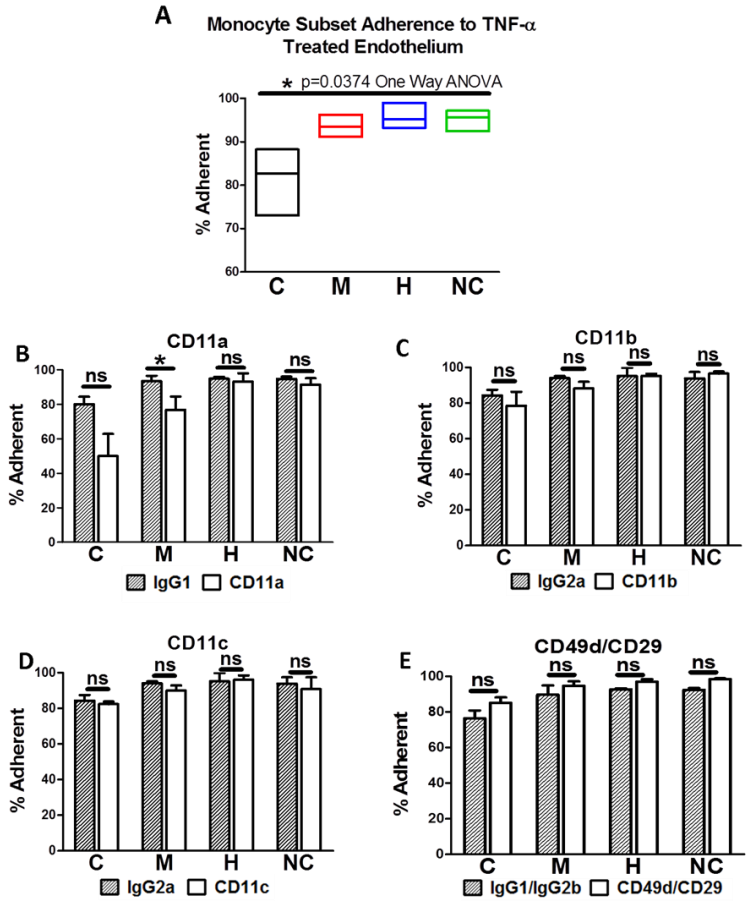

Figure 4. 6 Adherence rates of monocyte sub-populations to TNF-a-activated endothelium in the presence of anti-integrin and control antibodies.

(**A**) Adherence rates of four monocyte subpopulations to TNF-α activated endothelium. Data presented as box plots: Box limits = upper and lower interquartile range, median line = median. Effect of anti-CD11a (**B**), anti-CD11b (**C**), anti-CD11c (**D**) and anti-CD49d/CD29 on monocyte sub-population adherence to TNF-α activated endothelium. . Legend: (**C**) Classical, (**M**) DR^{mid}, (**H**) DR^{hi}, (**NC**) Non-Classical monocytes. Grey bar indicates relevant isotype control; white bar represents blocking antibody. Data derived from n = 3 healthy adult PBMC samples. Data presented as mean ± standard deviation for **B**,**C**,**D** and **E**. Statistical comparisons performed using two-sided paired t test and ANOVA. ns = $p>0.05$, * = $p<0.05$; ** = $p<0.01$; *** = $p<0.001$.

Discussion 4.4

In this Chapter, we have assessed the in vitro transmigratory responses of the Classical, DR^{mid}, DR^{hi} and Non-Classical monocyte sub-populations with a focus on chemokines known to serve as ligands for CCR2. Despite the numerous studies on human monocyte subsets since their most recent classification, only a few have looked in-depth at the transmigration properties of the Intermediate subset. As outlined in the introduction, specific transmigratory responses are strong defining characterisitcs of the the well-established Classical and Non-Classical monocytes in both human and mouse. A quantifiable, in vitro transmigration Transwell assay was, therefore, created in order to assess DR^{mid} and DR^{hi} Intermediate monocyte transmigaton to specific relevant chemokines. This assay was also modified to incorporate a human aortic endothelial cell monolayer to assess monocyte-endothelial interactions and monocyte transendothelial migration. Addtionally, as we had observed that the four defined monocyte sub-populations display varying surface expression of integrin receptors involved in endothelial adhesion, we also sought to determine whether there were any defining functional differences among the sub-populations in regard to integrin-mediated adhesion.

The initial establishment of a quantifiable transmigration Transwell assay was an essential pre-requisite to the experiments in this Chapter. The addtion of flow cytometry-compatible counting beads combined with multi-colour surface staining of the retrieved fractions allowed accurate quantification of transmigration for all monocyte sub-populations. In a series of optimisation experiments not presented in the thesis, we were able to demonstrate that an incubation time of 1 hour of the Transwells was sufficent to allow for monocyte transmigration while avoiding changes to the defining surface markers for the monocyte sub-populations (especially CD16).

The primary aim of this Chapter was to quantfy the transmigratory response of DR^{mid} and DR^{hi} Intermediate monocytes in response to chemokines. Our results indicate that neither Intermediate subset transmigrates robustly to CCL2

(MCP-1), CCL8 (MCP-2) or CCL7 (MCP-3) when compared to the strong response elicted in Classical monocytes (**Figure 4.1 C, D and E**). The MCP family was selected because these chemokines induce robust, and importantly, rapid migration of human (and mouse) monocytes. Speed of transmigration was of particular importance when designing the in vitro transmigration assays. Monocytes are a dynamic cell, and short term culture (2-5 hours) at 37°C induces phenotypic changes, predominatly the shedding of the CD16 receptor, which makes it impossible to accurately identify monocyte subsets during flow cytometry (MC Dennedy, EP Connaughton and M Griffin, unpublished observations) (Picozza et al., 2013). Addtionally, in migration assays carried out using the described protocol, we observed no significant transmigration of monocyte subpopulations toward CX3CL1 or SDF-1α (data not shown), despite the fact that these chemokines have previously been shown to provoke monocyte migration (Ancuta et al., 2004, Ancuta et al., 2003). However, these studies used incubation tie of 2.5-4 hours, and, in our migration assay, 1 hour have been insufficient for migration to occur in response to these chemokines.

Even though DR^{mid} and DR^{hi} Intermediate monocytes do not transmigrate robustly to MCP family chemokines, neither do they transmigrate as weakly as Non-Classical monocytes (**Figure 4.1 C, D and E**). This poor response to chemokines, specifically CCL2, by Intermediate monocytes has been repeatedly reported in the literature with Intermediate monocyte migration variously reported as occurring at an 'intermediate' level between Classical (high CCL2 induced transmigration) and Non-Classical (weak to no CCL2 induced transmigration) monocytes (Krankel et al., 2011, Thiesen et al., 2014). The transmigration responses of DR^{mid} and DR^{hi} Interemdiate monocytes to CCL2 are quite similar, and, with the notable exception of the DR^{mid} Intermediate subset , the responses observed for the sub-populations were consistent with their respective cell surface expression of CCR2. From the CCR2 expression on the subsets, it is clear that the reduced receptor levels on the DR^{hi} subsets, and even more so on Non-Classical monocytes and may partly or completely explain the observed reduced transmigration toward MCP family chemokines. Interestingly, however, Classical and DR^{mid} monocytes express similar amount

of the cell surface receptor CCR2, but this clearly does not correlate with their transmigration responses to CCL2 and other MCP family chemokines. In several studies, it has been highlighted that Intermediate monocytes display less CCR2 than Classical monocytes, and, in some they have even been reported as having lower surface CCR2 than Non-Classical monocytes (Cros et al., 2010, Wong et al., 2011). Our results suggest that these reports may have over-simplified the situation as it would appear that the currently recognised Intermediate monocyte gate for human PBMCs contains sub-populations with higer and lower CCR2 expression. It is tempting to speculate that down-regulation of CCR2 is a feature of a step-wise transition from Classical to Intermediate to Non-Classical. Furthermore, the results of our transmigration experiments suggest that, even prior to receptor down-regulation, Classical monocytes transitioning to the DR^{mid} Intermediate state, initally become significantly less responsive to CCR2 ligands.

The transwell assay utilised to determine monocyte subsets transmigration towards chemokines may not represent true migration toward a chemokine gradient. It is not clear how much time elapses before chemokine from the basal well of the transwell diffuses into the apical well, eventually resulting in equilibration of the chemokine throughtout each compartment of the transwell. In this case, if the chemokine is equally dispersed throughout the transwell, then transmigrating monocytes may be exhibitng chemokinesis rather than chemotaxis in reponse to a chemokine gradient. This may be overcome by the use of assays where migration is horizontal rather vertical, ideally toward increasing gradients of immobilised or tethered chemokines.

Monocyte subset interactions with and transmigration through endothelium was also partly assessed in this Chapter. Human aortic endothelial cells were treated with TNF-α to mimic in vivo inflammation, which stimulates endothelial upregulation of adhesion receptors, such as ICAM-1 and VCAM-1, with which monocytes interact. Our results indicate that DR^{mid} and DR^{hi} Intermediate monocytes are more adherent to resting endothelium than are Classical and Non-Classical monocytes and that their adherence is further

increased when the endothelial cells are TNF-α activated. Addtionally, In the absence of chemokine stimulus, the DR^{mid} and DR^{hi} Intermediate monocytes exhibited similar, poor transendothelial migration responses through both resting and activated endothelium when compared with Classical monocytes (**Figure 4.3**). The TNF-α activated endothelium was more permissive to monocyte transmigration, as greater transmigration of all monocyte subsets was observed in comparison to resting endothelium. In a small number of published studies, Intermediate human monocytes have been reported to be highly adherent to endothelium and to exhibit low rates of transendothelial migration (Collison et al., 2015, Krankel et al., 2011). These reports are consistent with our observations that both DR^{mid} and DR^{hi} Intermediate subsets exhibit poor transendothelial migration and are strongly adherent to endothelium. This relatively strong adherence to both resting and activated endothelium and apparent limited tendency to transmigrate through activated endothelium may point toward an endothelial monitoring function, similar to that described by Non-Classical monocytes (Carlin et al., 2013). However, it is important to acknowledge that our experiments did not extend to experimental systems which better model the intravascular environment by incorporating flow and shear stress. In this regard, a study by Collison et al., in which human Intermediate monocytes were perfused over endothelium, indicated that Intermediate monocytes, while highly adherent, exhibit little long range endothelial crawling behaviour and remained tightly bound (Collison et al., 2015). This suggests that in vivo surveillenace functions of Intermediate monocytes differs from those of Non-classical monocytes. It also raises the interesting questions of whether DR^{mid} and DR^{hi} Intermediate monocytes behave differently under conditions of flow when intereacting with healthy or “inflamed” endothelium.

However, there are caveats to our monocyte transdendothelial migration and adhesion assays. Firstly, in the transendothelial migration assay, we utilize a simple crystal violet stain to determine the presence of a confluent endothelial cell layer. However, this may only provide information on endotheilal cell coverage, as opposed to the endothelial cell layer integrity. In this regard,

transendothelial electrical resistance (TEER), which measures electrical resistance across a endothelial monolayer and is directly related to monolayer permeability. In future, endothelial monolayer permiability and integrity may be best assessed using TEER rather than crystal violet staining. Secondly, many studies have shown that in order to re-create an endothelial monolayer with tight junctions, similar to in-vivo, the monolayer must be cultured under sheer flow. Our assays utilize endothelial cells grown in static culture, and may not reflect the same properties as cells grown in the presence of sheer flow. However, despite this, static cultures are still widely used, with culture of endothelial cells under sheer flow technically challenging and costly reagents/equipment.

With the use of neutralizing antibodies, we sought to determine whether either of the Intermediate sub-populations preferentially uses certain integrins to mediate their adherence to activated endothelium. The results indicated that only blocakde of CD11a (the α-chain of LFA-1) interfered with monocyte subset adherence. Specifically, addition of anti-CD11a reduced adherence of Classical and DR^{mid} but not that of DR^{hi} and Non-Classical monocytes. This may suggest a similar utilization of LFA-1 by Classical and DR^{mid} monocytes for endothelial adherence. In the study by Collison et al., long-range crawling of Classical monocyte was blocked neutalizing antibody to ICAM-1 (to endothelial co-receptor for LFA-1), but the study report does not indicate whether ICAM-1 blockade had any effect on Intermediate and Non-Classical monocyte adhesion.

Somewhat unexpectedly, we observed no reduction in endothelial adherence of any monocyte sub-population with addition of neutralising antibodies against other integrin receptors that are reported to mediate such effects in one or more subset. For example, Collison et al. observed strong reduction in Non-Classical monocyte adhesion and crawling when VCAM-1 [the endothelial co-receptor for CD29/CD49d (VLA4)]. This may be explained by some of our selected experimental conditions and, with the benefit of hindsight, it could have been important to carry out additional experiments utlizing neutalising

antibodies against ICAM-1 and VCAM-1 and to develop a flow-based experimental system.

In summary, the results reported in this Chpater suggest that DR^{mid} and DR^{hi} Intermediate monocytes transmigrate weakly toward MCP family chemokines in comparision to Classical monocytes whether in the presence or absence of an endothelial layer. Nonetheless, the low migratory rate of the Intermediate sub-populations was demonstrably greater than that of Non-Classical monocytes. The DR^{mid} and DR^{hi} subpopulations both exhibited characterisitcally high adherence to endothelium, both resting and activated. However, our results for integrin blockade experiments, while relatively limited in scope, do indicate that LFA-1/ICAM-1-mediated binding of DR^{mid} Intermediates to activated endothelium is more important for, or possibly less stable than, that of the DR^{hi} sub-population – a difference that would be particularly interesting to explore in more dynamic experimental systems. Interestingly, Classical and DR^{mid} monocytes display similar cell surface levels of CCR2, despite the observation of a substantially lower rate of CCL2-mediated transendothelial migration of the DR^{mid} sub-population.

Taking this evidence into account, we felt that the evidence has been strengthened further for a model whereby DR^{mid} and DR^{hi} Intermediate monocytes represent individual stages in a monocyte phenotypic transition from a state of high trans-endothelial migratory capacity in the setting of tissue inflammation/endothelial activation to one of progressively greater endothelial adherence and blunted transmigratory response to classical pro-inflammatory chemokines. In the final part of the project, we elected to focus further on comparing the nature of the transmigratory signal mediated by CCL2 among the four defined monocyte sub-populations.

Chapter 5

Regulation of Chemokine Induced Transmigaration in Human Monocytes 5.0

Introduction 5.1

Regulation of immune cell trafficking is a critical aspect of immune and inflammatory responses. Many diseases are linked with dysfunctional immune cell transmigration in response to initial inflammation. A prime example of this is the uncontrolled accumulation of monocytes (and other immune cells) in atherosclerotic plaques, into which monocytes are attracted by stimuli associated with tissue inflammation. However, in spite of monocytes 'best intentions' to aid tissue repair by scavenging lipids and the by-products of necrotic cells, they become converted to lipid-laden 'foam cells', chemotactically defunct - in particular poorly responsive to CCL2 (Han et al., 2000, Ingersoll et al., 2011). Additionally, lipid-laden monocyte/macrophages "trapped" in atherosclerotic plaques contribute to the on-going tissue inflammation by secreting cytokines and chemokines that cause further immune cell infiltration and drive plaque growth (Hansson and Libby, 2006). One mechanism underlying the regulation of monocyte subset transmigration is differential expression of chemokine receptors. However, monocytes display a range of chemokine receptors and inflammation produces a wide range of chemokines specific for these receptors. So how does a monocyte determine which signal to follow?

Chemokine receptors are G-protein coupled receptors (GPCRs) and are regulated by G-protein receptor kinases (GRKs), arrestins and regulator of G-protein signalling (RGS) proteins as described in **Chapter 1, Section 1.6**. The latter, RGS proteins, are negative regulators of GPCR signalling. The expression of RGS proteins in immune cells is also greatly influenced by inflammatory stimuli, producing an increase or decrease depending on the cell type and stimulus. RGS proteins regulate G-protein signalling by decreasing the amount of time the G-protein Gα subunit and GβϒY sub complex are dissociated. This results in termination of downstream signalling cascades such as intracellular calcium release, protein phosphorylation and cytoskeletal rearrangement (Ross and Wilkie, 2000, Ritter and Hall, 2009). RGS proteins have been implicated in reduced chemokine induced transmigration in a range of immune

cells. For example, RGS16 overexpression in murine T-cells was found to inhibit CXCL12 induced transmigration (Lippert et al., 2003), while in a RGS1 was found to be essential in retention of antigen-stimulated B-cell retention in germinal centres, as evidenced aberrant germinal centre formation following immunization in $RGS1^{-/-}$ mice (Moratz et al., 2004). In particular, separate studies have implicated RGS1 in decreased CCL2 induced transmigration in myeloid cells (Patel et al., 2015, Denecke et al., 1999)

As also discussed in **Chapter 1**, human Intermediate blood monocytes are expanded in a range of inflammatory diseases and we have specifically shown that, under our proposed Intermediate monocyte sub-division into DR^{mid} and DR^{hi} Intermediate, the DR^{mid} subpopulation is specifically expanded in the setting of obesity compared to lean controls. Furthermore, as we now show in the current project (**Chapter 4**), DR^{mid} Intermediate monocytes do not migrate as robustly as Classical monocytes to CCL2 in in vitro transmigration assays, despite expressing similar surface levels of CCR2.

In this Chapter, to better understand CCL2-induced chemokine receptor activation in the four defined monocyte sub-populations, we elected to measure a key early signalling event - intracellular calcium release - as well as a downstream event - filamentous actin polymerisation - in response to CCL2 in live, freshly isolated PBMCs from healthy adult volunteers. Additionally, we sought to test whether differential expression of RGS proteins might explain the observed differences in CCL2-induced transmigration of the monocyte sub-populations.

Hypothesis and Objectives 5.2

Hypothesis 5.2.1

The differential migratory response of individual monocyte sub-populations to CCL2 is explained by variation in the regulation of proximal GPCR signalling events by RGS proteins.

Objectives 5.2.2

1. To compare CCL2-induced intracellular calcium flux and filamentous actin polymerisation in healthy human monocyte sub-populations using real-time, live-cell assays.
2. To determine the expression of a panel of RGS proteins in healthy human monocytes and compare their expression levels among four defined monocyte sub-populations.

Results 5.3

Lower CCL2-induced intracellular calcium flux in DR^{mid} monocytes 5.3.1

When a chemokine binds to its cognate GPCR, it triggers a rapid series of intracellular molecular events including calcium release from the ER and activation of signalling mediators like phospholipase C (PLC), diacylglycerol (DAG), calmodulin and protein kinase C (PKC) (see **Chapter 1, Section 1.6.1**). These, in turn, induce phosphorylation of target proteins culminating in cytoskeletal re-arrangement and transmigration (Imhof and Aurrand-Lions, 2004). In order to investigate GPCR-proximate signalling in response to CCL2, monocyte sub-populations were analysed for intracellular calcium flux (Ca[i]) by a flow cytometric method described in **Chapter 2**. A series of such experiments was performed with PBMCs from a total of 4 healthy adults.

Examples of the calcium flux kinetics in response to CCL2 for Classical, DR^{mid}, DR^{hi} and Non-Classical monocytes are illustrated in **Figure 5.1 A and B**, with the dashed line representing Ca[i] in response to ionomycin (a positive control for prolonged calcium release from the ER). As shown, ionomycin provoked a

strong, protracted increase in Ca[i] in all monocyte subsets. However, only Classical and DR^{mid} Intermediate monocytes demonstrated a significant peak in Ca[i] in response to CCL2 which then gradually declined to baseline over approximately 120 seconds. When expressed as an index (calculated as described in **Chapter 2**), the values for CCL2-induced Ca[i] for the full dataset from 3 separate experiments were significantly higher than carrier-only control values for Classical and DR^{mid} Intermediate monocytes but not for DR^{hi} Intermediate and Non-classical monocytes (**Figure 5.1 A-C**). Comparing CCL2-induced Ca[i] across the four monocyte sub-populations, Classical monocytes displayed the highest value (1.9±0.1), followed by DR^{mid} (1.6±0.06), DR^{hi} (1.2±0.07) and Non-Classical (1.1±0.03) monocytes (Figure 5.1D). In contrast, after loading with Fluo-4 calcium indicator, Non-Classical monocytes displayed the highest baseline fluorescence (**Figure 5.1 E**). Thus, despite similar surface expression of CCR2, DR^{mid} Intermediate monocytes had lower CCL2-induced Ca[i] than Classical monocytes.

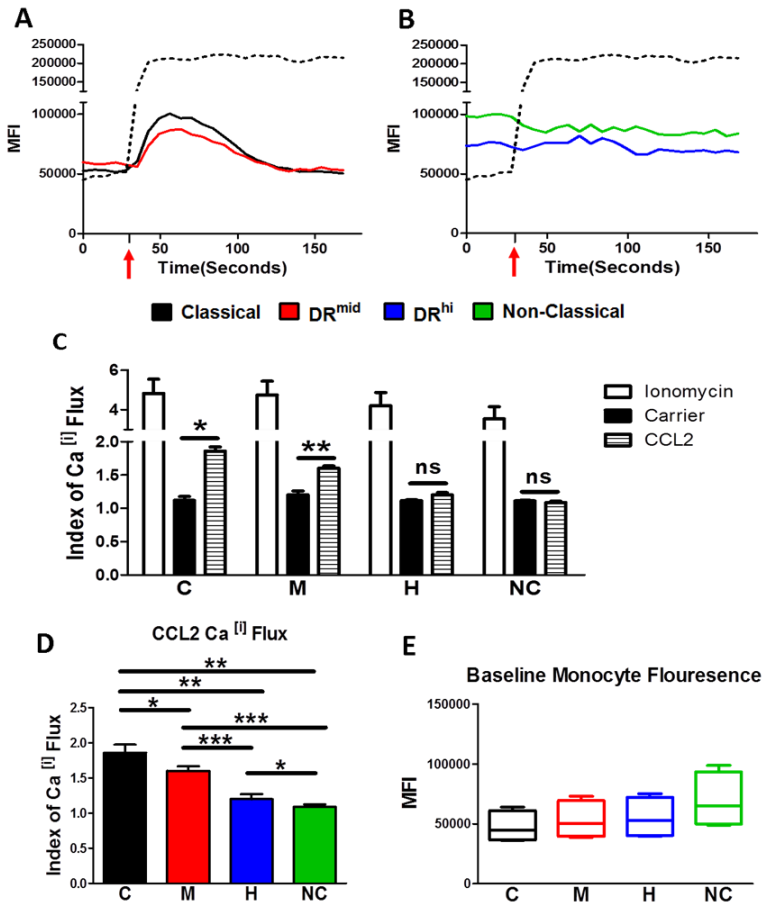

Figure 5. 1 CCL2-induced Ca[i] in human monocyte sub-populations.

Intracellular calcium flux was measured in real-time by flow cytometry in PBMCs loaded with Fluo-4. (**A**) Time-course of Ca[i] in Classical (black) and DR^{mid} Intermediate (red) monocytes in response to CCL2. (**B**) Time-course of Ca[i] in DR^{hi} Intermediate (blue) and Non-Classical (green) monocytes. The dashed lines represent total monocyte Ca[i] in response to ionomycin (positive control). (**C**) Indices of Ca[i] in monocyte sub-populations induced by ionomycin, carrier or CCL2. (**D**) Comparison of CCL2-induced Indices Ca[i] among the four monocytes sub-populations. (**E**) Comparison of baseline Ca[i] among the four monocytes sub-populations, presented as box plots: Box limits = upper and lower interquartile range, median line = median, whiskers represent smallest and largest values that are not outliers. Legend: (**C**) Classical, (**M**) DR^{mid}, (**H**) DR^{hi}, (**NC**) Non-Classical monocytes. Data derived from n = 4 healthy adult PBMC samples. Data presented as mean ± standard deviation for **C** and **D**. Statistical comparisons performed using two-sided paired t test. ns = $p>0.05$, * = $p<0.05$; ** = $p<0.01$; *** = $p<0.001$.

Attenuated CCL2-induced F-actin polymerization in DR^{mid} intermediate monocytes 5.3.2

As shown in **Chapter 2** and previously reported by others, CCL2 induces transmigration of $CCR2^{+}$ monocytes through endothelial monolayers (Thiesen et al., 2014, Krankel et al., 2011). Transmigration is initiated after CCL2 binding to one or more GPCRs on the monocyte cell surface and the resulting intracellular signalling triggers cytoskeletal re-arrangement, cell polarisation and polymerisation of filamentous actin (F-actin) toward the chemokine gradient (Imhof and Aurrand-Lions, 2004).

F-actin polymerisation induced by CCL2 was separately quantified in the four defined monocyte sub-populations within freshly isolated healthy adult PBMCs using a previously described method combined with surface marker staining and adapted for flow cytometry (Hu et al., 2008). As described in detail in **Chapter 2**, aliquots of PBMCs were stimulated with CCL2 for 0, 15, 30, 60 and 120 seconds before fixation and staining with phalloidin-FITC.

Figure 5.2 A illustrates a representative example of the response for each monocyte sub-population with CCL2-induced F-actin polymerisation expressed as a percentage increase over the fluorescence value for unstimulated cells. **Figure 5.2 B** summarises the combined results for a series of such assays carried out on PBMCs from a total of 3 healthy volunteers. As shown, peaks in F-actin polymerisation of variable magnitude occurred in Classical (125.3±3.5%), DR^{mid} Intermediate (118.6±3.2%), and DR^{hi} Intermediate (110.6±8.0%) at 15 seconds after CCL2 stimulation, with Non-Classical monocytes showing no increase in F-actin polymerisation (95.41±4.405%). In addition, however, Classical monocytes also exhibited significantly prolonged F-actin polymerisation when compared with DR^{mid} and DR^{hi} Intermediate monocytes ($p=0.02$ and $p=0.0008$ respectively at 120 seconds after CCL2 stimulation) (**Figure 5.2 C**).

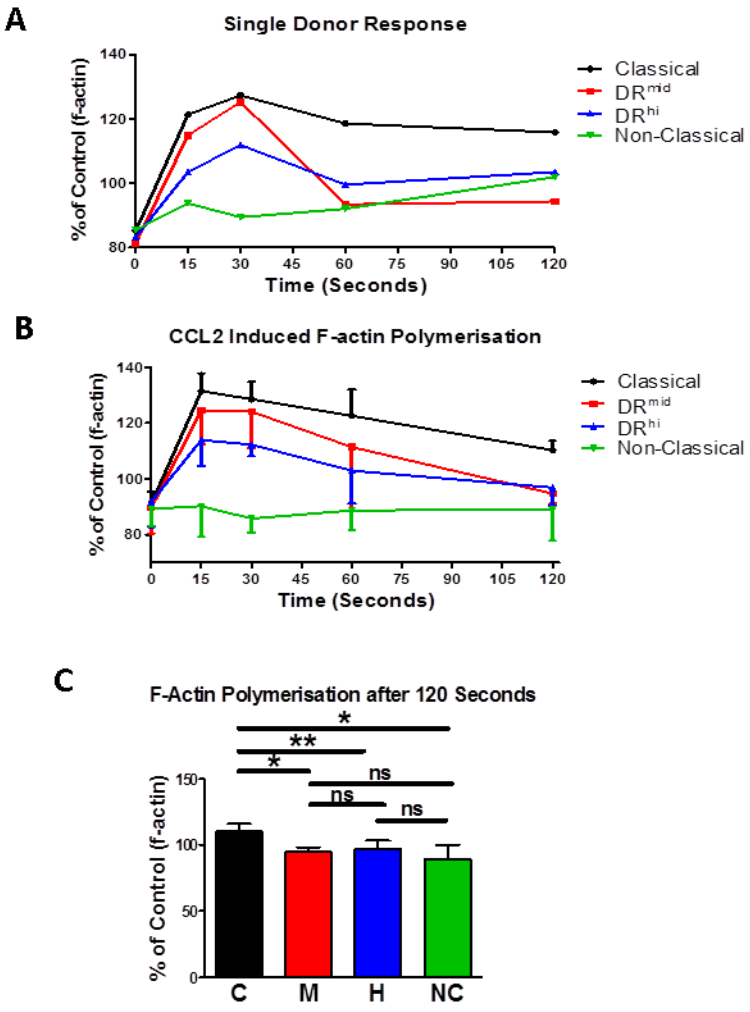

Figure 5. 2 CCL2 induced F-actin polymerisation in monocyte sub-populations.

F-actin polymerisation of monocyte subsets was measured at 0, 15, 30, 60 and 120 seconds after addition of CCL2 or carrier alone. Phalloidin-FITC fluorescence at each time-point was expressed as % of the unstimulated control sample for the same time-point. (**A**) Graphical representation of the data for PBMCs from one representative donor. (**B**) Graphical representation of the data for PBMCs from three individual donors. (**C**) Comparison of F-actin polymerisation quantitation at 120 seconds after addtion CCL2 for Classical (**C**), DR^{mid} Intermediate (**M**), DR^{hi} Interemdiate (**H**) and Non-Classical (**NC**) monocytes. Data derived from n = 3 healthy adult PBMC samples. Data presented as mean ± standard deviation. Statistical comparisons performed using two-sided paired t test. ns = $p>0.05$, * = $p<0.05$; ** = $p<0.01$; *** = $p<0.001$.

Expression of mRNA for RGS protein in primary human monocytes 5.3.3

As described previously, RGS proteins regulate the duration of signalling following binding of a chemokine (or other ligand) to its cognate GPCR. Thus, we hypothesised that differential expression of one or more RGS proteins in the monocyte sub-populations may account for their variable migration characteristics – in particular, the attenuated CCL2-induced transmigration of $CCR2^{+}$ DR^{mid} and $CCR2^{int}$ DR^{hi} monocytes compared to Classical monocytes.

A literature review indicated that RGS1, 2, 3, 4, 12, 16, and 18 were potential regulators of G-protein signalling present in monocyte/macrophages (Shi et al., 2004, Denecke et al., 1999, Suurvali et al., 2015, Tran et al., 2010, Yuan et al., 2015). A RT-PCR screen was, therefore, performed to determine their expression in a $CD14^{+}$-enriched monocyte preparation. Results of this analysis, shown in **Figure 5.3**, indicated that freshly isolated, resting $CD14^{+}$ monocytes do not express RGS3, 4 and 16, express RGS1 and 18 at low levels and express RGS2 and 12 at higher levels.

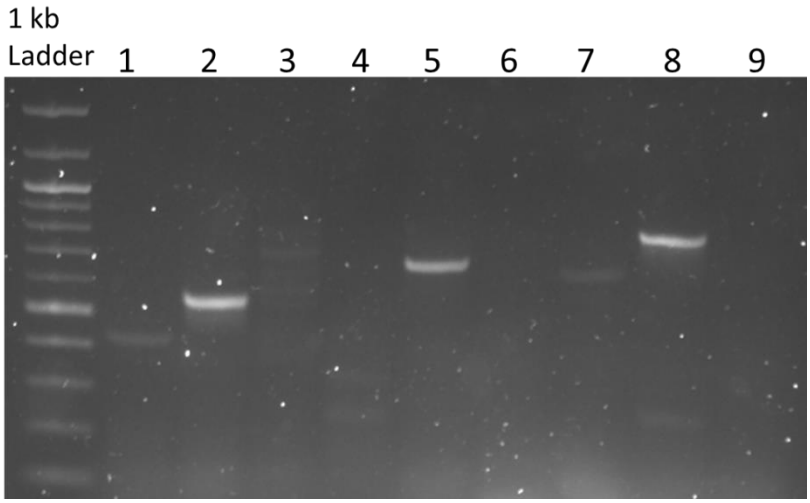

Figure 5. 3 RT-PCR of RGS protein transcripts in $CD14^{+}$ monocytes

A Sybr-Green-stained agarose gel is shown with amplified bands for candidate RGS gene and housekeeping gene mRNAs from PCR reactions using cDNA from healthy adult $CD14^{+}$ monocytes. Lane **1**: RGS1 (460bp), Lane **2**: RGS2 (590bp), Lane **3**: RGS3 (1300bp), Lane **4**: RGS4 (590bp), Lane **5**: RGS12 (710bp), Lane **6**: RGS16 (540bp), Lane **7**: RGS18 (708bp), Lane **8**: HPRT (867bp), Lane **9**: No-RT control. The result is representative of three separate experiments carried out with samples from seperate donors.

Purification of individual monocytes sub-populations 5.3.4

With the PCR screen for RGS genes in $CD14^+$ monocytes having reduced the initial RGS gene candidates to just four (RGS1, 2, 12 and 18), we next sought to quantify mRNA levels of these genes within the individual monocyte sub-populations using qRT-PCR. To achieve this, however, it was necessary to develop a method to enrich monocytes from PBMC preparations prior to full purification by FACS. An important consideration was the requirement to preserve all four defined sub-populations and to maintain them in an unactivated state. The two methods assessed were counter current centrifugal elutriation (referred to as "elutriation") and a commercially-available no-touch magnetic bead isolation kit (see **Chapter 2** for methodological details).

As shown in **Figure 5.4**, elutriation with collection and flow cytometric analysis of 14 individual fractions, effectively depleted lymphocytes during higher speed centrifugation (2700-2000 rpm) resulting in enrichment of monocytes from a baseline of approximately 5% of to an average of 70% of the total cells retrieved from the lower-speed fractions (1800-0 rpm).

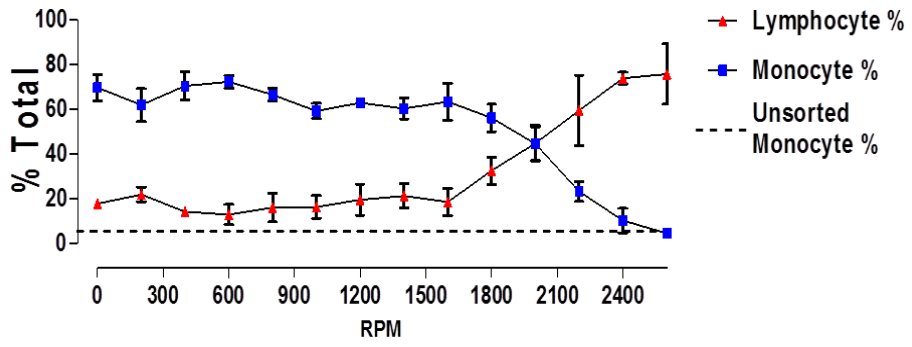

Figure 5. 4 Elutriation enriches monocytes from PBMC

The percentages of monocytes and lymphocytes within 14 individual elutriation fractions collected during deceleration from 2700 to 0 rpm are shown graphically. Data derived from n = 3 healthy adult PBMC samples. Data presented as mean ± standard deviation.

By staining each fraction with a 4-colour panel to identify individual sub-populations, we also observed that their elutriation profiles were distinctive and were in keeping with their respective morphological characteristics (see **Chapter 3, Figure 3.6**). As shown in **Figure 5.5 (A-D)**, the smaller-sized Non-Classical and DR^{hi} Intermediate monocytes peaked in their frequency earlier in the deceleration process (1800 and 2000rpm respectively) compared to the larger Classical and DR^{mid} Intermediate sub-populations (600rpm and 1200-1800 rpm respectively).

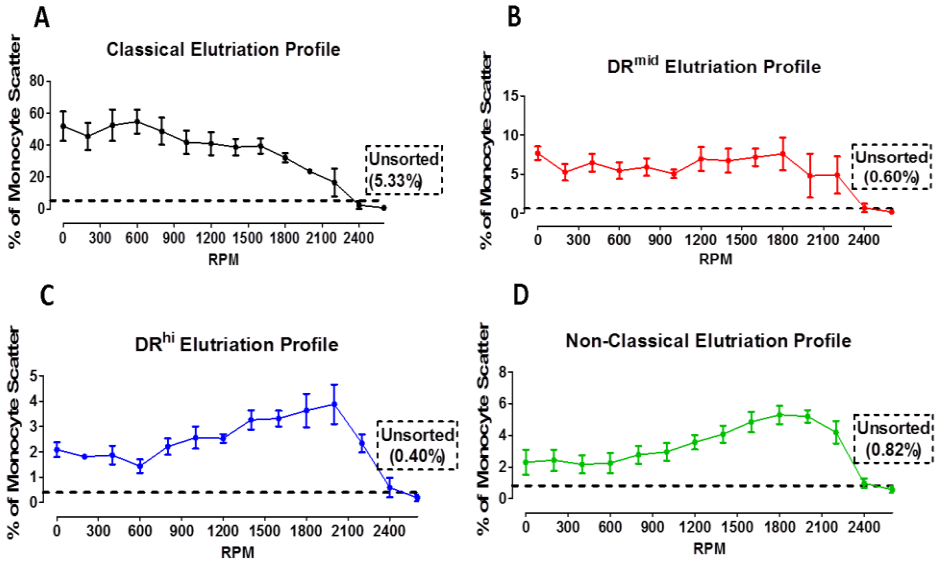

Figure 5. 5 Monocyte subpopulation elutriation profiles.
The percentages of the four individual monocytes sub-populations and within 14 individual elutriation fractions collected during deceleration from 2700 to 0 rpm are shown graphically along with their baseline frequencies in the unsorted PBMC samples. (**A**) Classical (**B**) DR^{mid} Intermediate (**C**) DR^{hi} Intermediate (**D**) Non-classical monocytes. . Data derived from n = 3 healthy adult PBMC samples. Data presented as mean ± standard deviation.

We also evaluated whether the elutriation process resulted in activation or unresponsiveness of the enriched monocytes. Equal numbers of elutriated monocytes and non-elutriated PBMCs were cultured in the presence or absence of LPS and the supernatants were analysed by ELISA for TNF-α and IL-

10. As shown in **Figures 5.6A and B**, TNF-α and IL-10 production by unstimulated PBMCs and elutriation-enriched monocytes were comparably low. Additionally, both non-elutriated PBMCs and elutriation-enriched monocytes produced significantly higher TNF-α and IL-10 levels following LPS stimulation. The higher TNF-α and lower IL-10 production of the samples generated by elutriation was in keeping with enrichment of monocytes in comparison to unfractionated PBMCs. Viability of elutriated cells was not adversely affected by the separation process, as evidenced by 99.4% viability within the monocyte and lymphocyte gates post-elutriation (**Figure 5.6 C**)

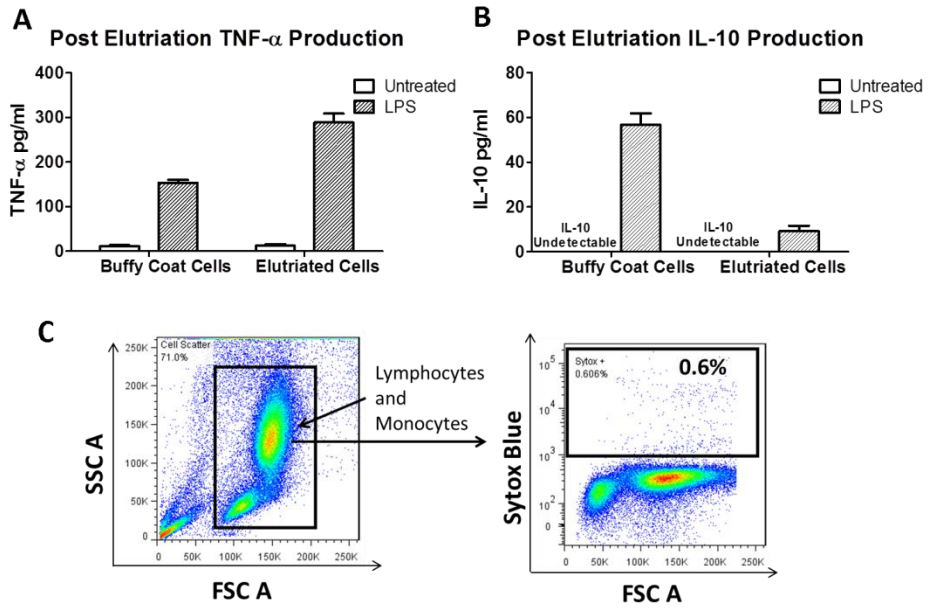

Figure 5. 6 Monocyte activation and viability post-elutriation

Graphical representation of the results of ELISAs for TNF-α (**A**) and IL-10 (**B**) of supernatants from unstimulated and LPS-stimulated cultures of non-elutriated PBMCs ("buffy coat cells") and elutriation-enriched monocytes ("Elutriated Cells"). Cells were stimulated with 5 ng/ml LPS for 8 hrs (TNF-α) and 16 hrs (IL-10). **C.** Representative example of viability analysis of post-elutriation monocyte-enriched fraction by flow cytometry using viability dye Sytox Blue®. Data derived from n = 1 healthy adult PBMC samples. Three technical replicates were carried out for each condition in (**A**) and (**B**). Data presented as mean ± standard deviation.

Monocyte enrichment was also evaluated using a commercial magnetic activated cell sorting (MACS)-based enrichment kit which was applied to

freshly isolated PBMCs from healthy adult volunteers according to the manufacturer's protocol as described in **Chapter 2**. Although it was expected that this approach would provide equal enrichment of all four defined sub-populations, in our hands the kit resulted in specific depletion of the DR^{mid} Intermediate sub-population. As illustrated in **Figure 5.7**, when the monocyte sub-population proportions within the enriched fraction were compared by flow cytometry with those of the pre-enrichment PBMC sample, a decrease in the percentage of DR^{mid} Intermediate monocytes was observed. Overall a reduction of DR^{mid} Intermediate monocytes from 5.5±1.2% to 2.9±1.9% (n=3) was observed, although the decrease following 3 enrichments was not statistically significant. Classical (un-sorted 75.2±6.5% vs sorted 83.1±1.9%), DR^{hi} Intermediate (un-sorted 2.1±0.7% vs sorted 1.9±0.6%) and Non-Classical (un-sorted 3.6±0.3% vs sorted 5.2±0.8%) (all n=3) monocyte proportions were not similarly affected by the MACs enrichment process (**Figure 5.7A**).

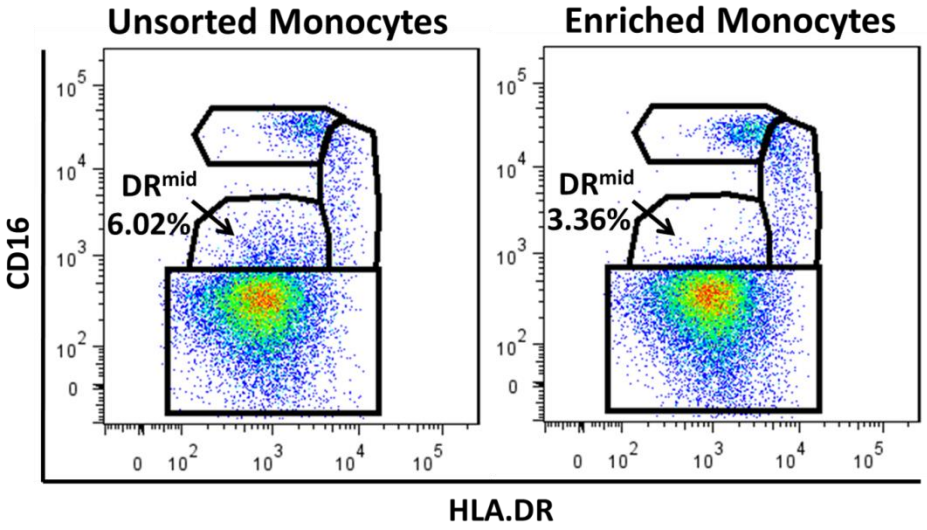

Figure 5. 7 Depletion of DR^{mid} monocytes after enriching for monocytes with MACs 'no-touch' sorting kit.

Representative HLA.DR vs CD16 dot-plot showing a decreased % DR^{mid} with 'no-touch' monocyte enrichment kit (6.02% before to 3.36% after enrichment). Plot is representative of one of a total of three MACS enrichments performed.

Taking all of these results into account it was decided not to persist with further MACS-based enrichments and the elutriation was chosen as the preferred monocyte pre-enrichment method prior to FACS purification of the four defined monocyte sub-populations.

Purification of individual monocytes sub-populations by FACS and comparison of RGS protein mRNA expression 5.3.5

Elutriation-enriched monocytes were then purified into the individual monocyte subsets from freshly-isolated PBMCs of healthy adult volunteers using FACS and mRNA levels for RGS 1, 2, 12 , 18, FCGR3B (CD16) and the housekeeping gene GAPDH were assessed using qRT-PCR as described in **Chapter 2**. In total, 8 individual sorts were performed using PBMCs from different volunteers.

Initially, because of the low amounts of total RNA retrieved from the less frequent Intermediate and Non-Classical subpopulations, a cDNA titration was completed to determine the minimum amount of template required to achieve sufficient amplification of target genes for quantification of the target mRNAs. For this optimisation step, RNA was prepared from a MACS-isolated whole monocyte preparation and serial dilutions (from 5 to 0.0005 ng) of the resulting cDNA were subjected to qPCR for GAPDH, FCGR3B, RGS1, RGS2, RGS12 and RGS1 as described in **Chapter 2**. The results of this titration are shown in **Figure 5.8**.

A 100% efficient PCR should have co-efficient of determination of 1 with a ten-fold increase in gene expression represented by 3.32 cycles. A shown, the R^2 values the various targets were: (**A**) GAPDH (0.9999), (**B**) FCGR3B (0.9978), (**C**) RGS1 (0.9927), (**D**) RGS2 (0.9968), (**E**) RGS12 (**I**) and (**F**) RGS18 (0.9938). These suggested a high PCR efficiency and absence of any inhibition.

Based on the amplification thresholds (C_T) values for the individual targets at the different dilutions, the minimum amount of cDNA required to quantify all targets in samples of monocyte-derived RNA was determined to be 2 ng. This

selected minimum amount was primarily influenced by the lowest-abundance transcript RGS12 for which the C_T values at 5 ng and 0.5 ng were approximately 33 and 36 respectively (**Figure 5.8**).

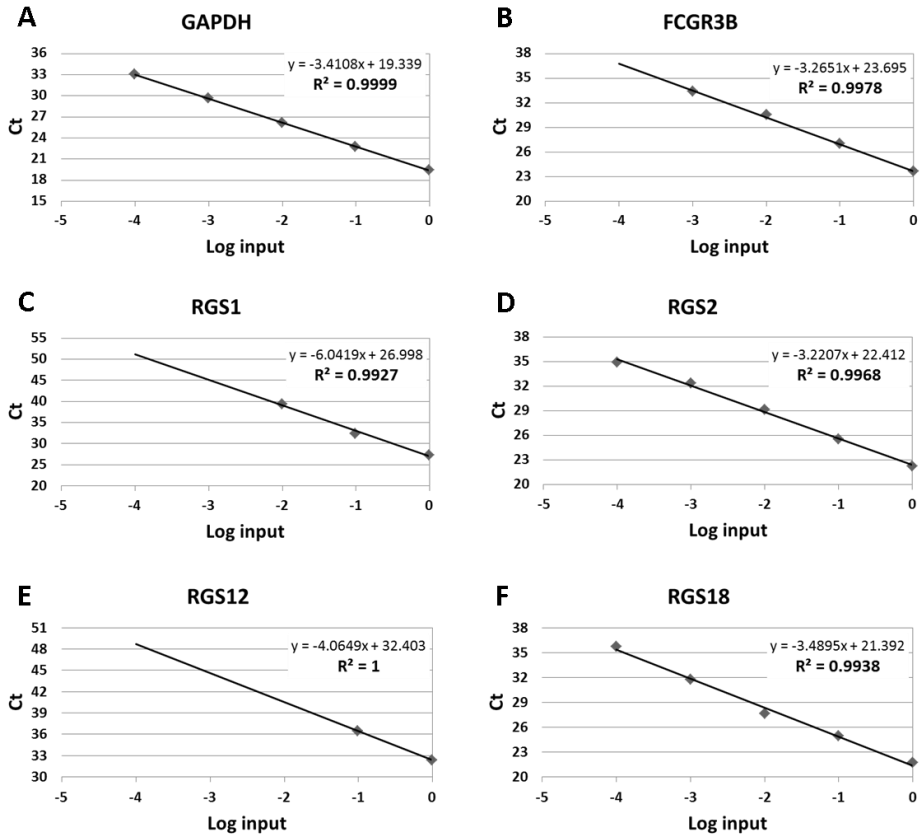

Figure 5. 8 Titration of cDNA for qRT-PCR of eight target genes
Titration of cDNA to determine the minimum amount of template required to detect a signal for each target gene. Data represents Ct values for qRT-PCR reactions across a five-point ten-fold dilution of cDNA template derived from a single purified total monocyte preparation. Dilutions (in ng of cDNA) were: 5 ng (0), 0.5 ng (-1), 0.05 ng (-2), 0.005 ng (-3) and 0.0005 ng (-4).

Monocytes were purified into the individual subsets using FACS. A total of 7 individual sorts were performed. For 5 of these, it was possible to quantify all target mRNAs from all 4 defined monocyte sub-populations. For an additional 2, it was possible to quantify all targets from Classical and DR^{mid} Intermediate only. For each set of sorted monocytes, quantification of the target mRNAs in each sub-population was calculated by the $2^{-\Delta\Delta CT}$ method with normalisation

to GAPDH and expressed relative to the value for the Classical monocyte sample. The results of these analyses are summarised in **Figure 5.9** for: (**A**) RGS1,(**B**) RGS2, (**C**) RGS12, (**D**) RGS18 and (**E**) FCG3RB.

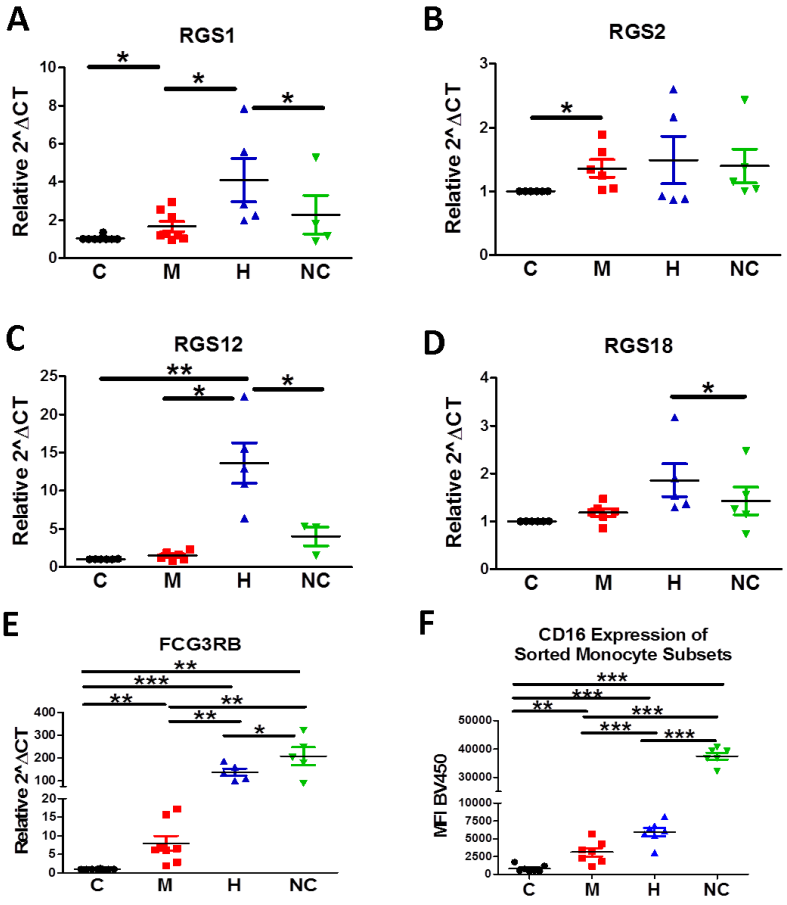

Figure 5. 9 Results of qRT-PCR from FACS-purified monocyte sub-populations
Relative mRNA quantities in purified monocytes sub-populations from 5-7 healthy adult PBMC samples for: (**A**) RGS1, (**B**) RGS2, (**C**) RGS12, (**D**) RGS18, (**E**) FCG3RB (CD16). GAPDH was used for normalisation and Classical monocytes as the reference sample with quantification by the $2^{-\Delta\Delta CT}$ method. Legend: (**C**) Classical, (**M**) DRmid, (**H**) DRhi, (**NC**) Non-Classical monocytes. Data derived from n= (RGS1 C, M n=8,′ H n=5, NC n=4) (RGS2 C, M n=6, H, NC n=5) (RGS12 C, M n=6, H n=5, NC n=3) (RGS18 C, M n=6, H, NC n=5), (FCG3RB C, M n=8,′ H, NC n=5). Error bars represent mean ± SD. Statistical comparisons performed using two-sided paired t test. * = p<0.05; ** = p<0.01; *** = p<0.001.

The results for FCG3RB (CD16) provided confirmation of sort purity of the individual sub-populations with DR^{mid} Intermediate, DR^{hi} Intermediate and Non-classical having sequentially higher expression relative to the ($CD16^{-}$)

Classical monocytes. The mRNA levels of FCG3RB reflect the cell surface CD16 expression on the sorted monocyte subsets (**Figure 5.9 F**).

The results for RGS protein transcripts also demonstrated multiple differences among the monocyte sub-populations including two RGS protein transcripts – RGS1 and RGS2 – which were significantly more highly expressed by DR^{mid} Intermediate than Classical monocytes (1.66±0.77 and 1.36±0.34 respectively for DR^{mid} Intermediate relative to Classical). In the case of RGS1, the expression level was further increased in the DR^{hi} Intermediate sub-population (4.10±2.54) then reduced again in the Non-Classical subset (2.28±2.03). In the case of RGS2, there was no further increase in DR^{hi} Intermediate and Non-Classical compared to DR^{mid} Intermediate.

For the two other RGS protein transcripts analysed, there was no significant difference between Classical and DR^{mid} Intermediate monocytes. However, both demonstrated highest expression in DR^{hi} Intermediate monocytes with the result for RGS12 (13.64±5.92) being statistically significantly different to all other sub-populations.

From these analyses it was concluded that: (**a**) Intermediate and Non-Classical monocyte sub-populations exhibited a general trend of increased expression of RGS proteins previously reported to be associated with regulation of chemokine receptor signalling. (**b**) More specifically, DR^{mid} Intermediate monocytes express higher levels of mRNA for RGS1 and RGS2 – both of which, as discussed below, may be implicated in responsiveness to CCR2 ligands such as CCL2. (**c**) The DR^{hi} Intermediate sub-population demonstrated highest expression of 3 of the 4 selected RGS proteins at mRNA level with significant differences to both DR^{mid} Intermediate and Non-classical monocytes for some of these. Although preliminary in nature, this novel finding appears compatible with a distinct functional profile for this monocyte subpopulation in regard to chemokine-induced transmigration and, potentially, other GPCR-regulated processes.

Discussion 5.4

In this chapter, we have presented experimental results directed toward better understanding why DR^{mid} and DR^{hi} Intermediate monocytes transmigrate at a low rate to CCL2, depsite their respective $CCR2^{+}$ and $CCR2^{int}$ phenotypes. Having observed blunted CCL2-induced transmigration (including transendothelial migration) in **Chapter 4**, we sought to quantify the intracellular responses in the Intermediate subsets that occur initially after CCL2 binding to CCR2 and which culminate in cytoskeletal re-arrangement and transmigration. The two such intracellular responses that we selected for "real time" analysis on intact primary human monocytes were release of calcium from the ER and, further downstream, the polymerisation of F-actin. Additionally, we assessed the role regulator of G-protein signalling (RGS) proteins may play in the attenuated transmigratory response of DR^{mid} and DR^{hi} Intermediate subsets by profiling expression of candidate family-members at RNA level in highly purified sub-populations.

With the use of qRT-PCR, we sought to determine the presence of RGS1, 2, 12 and 18 in the monocyte subsets. Interestingly, our results indicate that there are higher mRNA levels for RGS1 in both DR^{mid} and DR^{hi} Intermediate monocyte subsets when compared to Classical monocytes. RGS1 is well described as a negative regulator of transmigration in a range of immune cells. It was the focus of a recent study by Patel et al., in which the authors demonstrated that RGS1 negatively regulates CCL2-induced transmigration of monocytes, resulting in decreased monocyte accumulation in atherosclerotic lesions (Patel et al., 2015). In this study, monocyte accumulation in atherosclerotic lesions was abrogated in $RGS1^{-/-}$ mice and this observation was attributed to increased chemokine-induced signalling in the absence of RGS1 (Patel et al., 2015). Thus, the higher mRNA expression of RGS1 in the Intermediate subsets may account for or contribute to their blunted transmigration toward CCL2 in comparison with Classical monocytes. Of the Intermediate subsets, the DR^{hi} subset displayed higher levels of RGS1 than the DR^{mid} subset. The higher expression of RGS1 in the DR^{hi} subset may therefore,

also explain the lack of CCL2-induced calcium flux in this sub-population as well as their reduced transmigration when compared to the DR^{mid} subset. However, the differences in the CCL2-induced transmigratory responses of the two Intermediate sub-populations could also be explained by differences in CCR2 surface expression and differences in the strength of their adherence to activated endothelium.

We also found that RGS2 was elevated in the Intermediate sub-populations compared to Classical monocytes. In contrast to RGS1, RGS2 has not been implicated in blunting chemokine receptor signalling and has been reported to preferentially bind to Gαq G-protein subunits rather than the Gαi subunits which are predominantly coupled with chemokine receptors (Park et al., 2001). The physiological role of RGS2 in monocytes is not clear, although some studies have linked it to negative regulation of calcium oscillations (Wang et al., 2004, Semplicini et al., 2006) and CCL2 production (Boelte et al., 2011) – both being of potential relevance to our experimental findings in this project. Whether RGS2 impacts on CCL2-induced GPCR signalling is unclear, but calcium is essential to many cell signalling pathways and regulation of calcium oscillations is likely to exert a broad effect on other signalling events (Vig and Kinet, 2009, Chaigne-Delalande and Lenardo, 2014).

Higher levels of RGS12 were specifically detected in the DR^{hi} intermediate monocyte compared to the other three sub-populations. To date, RGS12 has been implicated in in vivo osteoclast differentiation as mice that are genetically deficient in RGS12 mice exhibit impaired osteoclast generation (Yuan et al., 2015). Additionally, RGS12 has been implicated in co-ordinating nerve growth factor (NGF) signalling through tropomyosin receptor kinase A (TrkA), prolonging Ras-Raf-MEK-ERK signalling (Willard et al., 2007). Notably, NGF signalling through TrkA has been associated with sustained survival of monocytes and other immune cells, through the expression of the anti-apoptotic protein B-cell lymphoma 2 (BCL-2) (la Sala et al., 2000). It is tempting, therefore, to speculate that RGS12 expression in DR^{hi} Intermediate monocytes reflects a maturing phenotype as cells undergoing maturation or

differentiation often have enhanced anti-apoptotic mechanisms (Tardivel et al., 2004). In future work, it would be interesting to assess cell surface levels of the TrkA receptor, BCL-2 expression and response to pro-apoptotic stimuli in the monocyte subsets to test this possibility. Interestingly, in the study by Wong et al., RGS12 expression was reported highest in the Intermediate subset compared to Classical and Non-Classical monocytes (Wong et al., 2011) (supplemental data, table S3). This correlates with our observation that RGS12 mRNA expression is specifically elevated in the DR^{hi} sub-population of Intermediate monocytes.

Similarly, RGS18 was detected at the highest levels in the DR^{hi} sub-population. The physiological role of RGS18 is unknown, but it is reported to be highly expressed in long- and short-term hematopoietic stem cells and its expression is decreased as the cells become more lineage-committed (Park et al., 2001). With this in mind, it is unclear what function RGS18 may contribute to the function DR^{hi} Intermediate monocytes but its documented expression in hematopoietic progenitors fits, at least loosely, with the concept that this monocyte sub-population possesses a distinct set of functional capabilities.

The reduced CCL2-induced calcium flux in the Intermediate subsets is indicative of early termination of G-protein mediated signals required to open ion-gated channels on the ER and, as a result, attenuated calcium release into the cytoplasm. The elevated level of RGS1 in the Intermediate monocytes correlates with reduced CCL2-induced calcium release although further experiments would be required to prove this mechanistic link. In a study by Moratz et al., $RGS1^{-/-}$ B cells exhibited increased calcium signalling and enhanced transmigration in response CXCL12 and CXCL13 (Moratz et al., 2004). This data suggests that the quantification of calcium release may be directly indicative of attenuated G-protein signalling mediated by RGS1. To our knowledge, there is no published data on CCL2-induced calcium release in the recently classified monocyte subsets. However, the ability of bulk human monocytes to flux calcium in response to CCL2 is well established (Hu et al., 2008, Fox et al., 2011).

But does decreased calcium release contribute to reduced transmigration of Intermediate monocyte sub-populations or is it simply just a reflection of the duration of G-protein signalling? Chemokine-induced released calcium ions bind to protein kinase C (PKC) and Ca^{2+}/calmodulin-dependant protein kinases (CaM-kinases) which require calcium binding in in order to become activated. Activated PKC has been shown to be required for immune cell migration, and is involved in phosphorylation of several proteins involved in controlling the morphology of the actin cytoskeleton (Larsson, 2006). In a study by Carnevale et al., CCL2-induced human monocyte migration was found to be heavily dependent on PKC (specifically PKCβ) (Carnevale and Cathcart, 2003). The CaM-kinases have a broad range of cellular functions including regulation of cell survival and activation of transcription factors (Soderling, 1999). However, inhibition of calmodulin has been shown to abrogate chemokine-induced migration of neutrophils (Verploegen et al., 2002) and lymphocytes (Matheny et al., 2000). It is possible, if not likely, therefore, that reduced calcium release, mediated by RGS1, directly contributes to a reduced transmigratory response of the Intermediate monocyte subsets by limiting the activation of PKC and calmodulin.

The reduced CCL2-induced F-actin polymerisation that we observed in the Intermediate monocyte sub-populations is also consistent with a role for RGS1 in blunting G-protein signalling (**Figure 5.2**). It is well recognised that CCL2-triggered G-protein signalling can induce F-actin polymerization by activation of phosphoinositide 3-kinase (PI3K) signalling (via interaction with the G-protein GβϒY subunit) which can then activate members of the Rho family of GTPases including Rho, Rac and Cdc42 (Curnock et al., 2002). These GTPases are important regulators of actin cytoskeleton assembly/disassembly, controlling the formation of filopodia and lamellipodia during migration (Vicente-Manzanares et al., 2009). Additionally, as mentioned above, PKC can also assist in actin cytoskeleton re-arrangement by interacting with proteins such as GAP43 which affect actin stabilisation (He et al., 1997). Early termination of the G-protein signal, by RGS1 for example, would result in reduced PI3K signalling with downstream negative effects on the activation of

the Rho family of GTPases and on actin assembly/disassembly (Vicente-Manzanares et al., 2009). In our experiments, the DR^{mid} and DR^{hi} Intermediate monocyte sub-populations exhibited trends toward F-actin polymerisation compared to Classical monocytes at the earlier time points (15 and 30 second time points) and this became significantly lower at 120 seconds. When migrating along a chemokine gradient, a cell is constantly assembling/disassembling actin and redistributing adhesion-mediating integrins in the tail and leading edge of the cell. As it encounters more chemokine ligand, more chemokine receptors are engaged, resulting in greater intracellular signalling involving PKC, calmodulin and PI3K, all of which are required for cytoskeletal rearrangement and migration. Despite the presence of RGS1, our results have shown there is still a quantifiable response to CCL2 by the DR^{mid} and DR^{hi} monocytes (including in vitro transmigration and F-actin polymerisation). Perhaps it is the scenario described above, whereby a cell is sensing CCL2 gradient, where RGS1 or other negative regulators of GPCR signalling truly exert their effects, with a culmination of attenuated CCR2 signalling resulting in inefficient migration of the DR^{mid} and DR^{hi} Intermediate subsets. We believe that the low rates of CCL2-induced transendothelial migration we observed in freshly-isolated human Intermediate monocytes are likely to be linked to receptor-proximal termination of the intracellular signals that mediate F-actin polymerisation in one or both of the defined sub-populations. Nevertheless, additional experimental approaches would be needed to formally prove this concept.

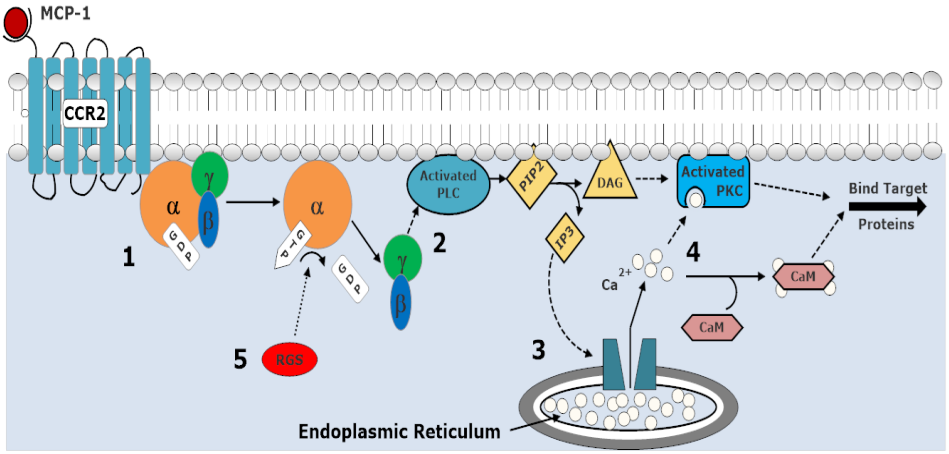

Figure 5. 10 Overview of attenuated GPCR signalling mediated by RGS proteins

(1) MCP-1 binds to the CCR2 receptor and the G-protein subunits dissociate. The free Gα and GβϒY subunits are then involved in cell signalling cascades (2) The free GβϒY sub complex activates Phospholipase C (PLC). Phosphoinositol 4,5 diphosphate (PI(4,5)P2; PIP2) is hydrolyzed by activated PLC producing diaglycerol (DAG) and inositol 1,4,5-trisphosphate (IP3). (3) The latter binds to IP3-gated Ca^{2+} in the endoplasmic reticulum (ER) membrane resulting in the release of Ca^{2+} into the cytosol. (4) The released Ca^{2+} can activate Protein Kinase C (PKC). Released Ca^{2+} may also bind to Calmodulin. Both Ca^{2+}-bound Calmodulin and activated PKC can then phosphorylate target proteins that promote actin polymerisation resulting in polarisation and cell movement toward the chemokine gradient. (5) However, if RGS proteins are present, they may bind to the activated Gα subunit and increase its intrinsic GTPase activity. This results Gα-bound GTP being replaced with GDP, resulting in re-association of the Gα and GβϒY subunits. When the G-protein subunits are associated, they can no longer be involved in signalling. RGS proteins essentially result in early termination of G-protein signalling, resulting in decreased Ca^{2+} release, activation of PKC and calmodulin.

While the results point toward a role of RGS1 in the inefficient CCL2-induced transmigration, there are other mechanisms which may be involved. The expression of G-protein receptor kinases (GRKs), which mediate chemokine receptor desensitisation and internalisation, may also play an important role. As reported by others, increased levels of GRK2 and 5 may result in increased CCR2 receptor internalisation and blunted CCL2-induced chemotaxis in monocyte/macrophages (Wu et al., 2012, Aragay et al., 1998).

When working with human monocytes, the choice of isolation method may have a major impact on downstream applications and on the final interpretation of experimental results. In our experience, a commercial "no-touch" magnetic bead-based kit for enrichment of monocytes from PBMCs appeared to selectively deplete the DR^{mid} Intermediate sub-population from the enriched monocyte population. The reason for this is not clear (the manufacturer does not provide a list of the depleting antibodies used in the kit) but, in a broader sense, inadvertent loss or activation of specific monocyte sub-populations associated with enrichment/purification procedures could explain current discrepancies in the literature. For example, in widely-cited the studies of Wong et al. and Cros et al., TNF-α production was found to be highest in Non-Classical and Intermediate monocytes respectively (Wong et al., 2011, Cros et al., 2010). The study by Wong et al. relied on an initial microbead-based depletion method to remove $CD56^+$ and $CD15^+$ NK cells and granulocytes, while Cros et al. used no enrichment step, instead relying on a large panel of antibodies to achieve pure monocyte subsets during FACS sorting (Cros et al., 2010, Wong et al., 2011). Indeed, a recent study assessing the effects of FACS as well as positive and negative microbead isolation on the effect of gene expression in various immune cells, including monocytes, indicated that both positive and negative microbead selection induced high-level expression of genes involved in stress compared to FACS (Beliakova-Bethell et al., 2014). Although this study did not directly examine cytokine production, it does serve to highlight the modifying effects that microbead isolation can exert on monocytes. In the end, we chose counter current elutriation as our preferred enrichment method. This method has been used by other recent studies to enrich monocytes before FACS sorting for transcriptional analysis of the monocyte subsets (Schmidl et al., 2014). While the process is technically challenging, we have shown that the elutriation process did not have a detrimental effect on monocyte viability or cytokine production under either resting or stimulated conditions.

In summary of Chapter 5, we sought to assess the intracellular signalling events shortly after CCL2 stimulation of the four defined monocyte sub-populations. Quantification of mRNAs for selected RGS proteins in the revealed higher levels of RGS1 in DR^{mid} and DR^{hi} Intermediates compared to Classical monocytes. RGS1 is a well described negative regulator of G-protein induced chemotaxis and its expression has been directly shown to blunt CCL2 induced transmigration in mouse myeloid cells (Patel et al., 2015) and human monocyte cell lines (Denecke et al., 1999). Intracellular quantification of CCL2 induced calcium release and F-actin polymerisation revealed these responses were attenuated in the DR^{mid} and DR^{hi} Intermediate monocytes in comparison to Classical monocytes. The reduced calcium release and F-actin polymerisation are likely the result of early termination of CCL2-induced G-protein signalling. These phenomena are consistent with the low transendothelial migration rate of DR^{mid} Intermediate subset compared to Classical monocytes and may result partially or entirely from elevated expression of one or more RGS proteins. At the time of writing, to the best of our knowledge, this is the first study to specifically address mechanistic underpinnings of the inefficient transmigration of human Intermediate monocytes. Although less readily interpreted, the differential expression of RGS2, RGS12 and RGS18 across the monocyte sub-populations we have studied also raises interesting questions about their responses to chemokines and other GPCR ligands.

Chapter 6

Overall Discussion and Implications of the Results 6.0

Overall discussion 6.1

The aim of this project was to investigate Intermediate monocyte heterogenity. Based on previous work by our group, we proposed that the Intermdiate monocyte subset consists of two distinct sub-populations based on HLA-DR expression - namely DR^{mid} and DR^{hi} sub-populations. The data presented in this study argue that the DR^{mid} and DR^{hi} Intermediate monocyte subsets are distinct populations based on the following observations: (**i**) Cell surface expression of chemokine, integrin and selectin receptors are expressed at significantly different levels between the two (**ii**) The DR^{mid} sub-population appear more granular than the DR^{hi} sub-population, (**iii**) DR^{mid} intermediate monocytes exihibt higher migratory rate toward CCL2 than their DR^{hi} counterparts, (**iv**) Adhesion of the DR^{mid} sub-population to activated primary endothelium is partialy inhibited by blocking CD11a, while that of the DR^{hi} sub-population is not (**v**) The DR^{mid} sub-population displays greater CCL2-induced intracellular calcium release and filamentous actin polymerisation, and (**vi**) the DR^{hi} sub-population has significantly higher mRNA levels of RGS1 and RGS12.

Little was known about the biological function of these cells at the time the project was initiated. We firstly, and importantly, ruled out the possibilty that the Intermediate sub-populations might represent “spill-over” of lymphocytes into the monocyte gates. However, a stringent flow cytometry gating strategy indicated the Intermediate subsets were free from lymphocyte populations, and addtionally, morphological analysis of the subsets following FACS revealed characteristic monocytic nuclear morphology on all sorted cells providing further evidence that these sub-populations are bona-fide monocytes. Phenotyping for various cell surface receptors involved in chemotaxis and endothelial adherence indicated that, for several receptors, the DR^{mid} and DR^{hi} sub-populations expressed levels that were ‘intermediate’ between those of Classical and Non-Classical monocyte subsets. It has been suggested that Intermediate monocytes may represent cells that are in the process of maturing from Classical to Non-Classical. Interstingly, in mouse models, it has been elegantly demonstrated that “Classical” ($Ly6C^{hi}$) monocytes may mature

directly to “Non-Classical” (Ly6C^{lo}) monocytes. Although mice currently lack an identifiable equivalent of the human Intermediate subset, this fits with a model whereby Intermediate monocytes represent a stage in a stepwise transition from Classical to Non-Classical.

This consideration raises the question of how our proposed DR^{mid} and DR^{hi} Intermediate sub-populations fit into such a stepwise progression model. At present, we believe that our data are consistent with an hypothesis that some Classsical monocytes initially mature to or are stimulated toward the DR^{mid} Intermediate phenotpye within the bloodstream and that these Intermediate monocytes subsequently further mature/differentiate to DR^{hi} Intermediate and then to Non-Classical monocytes. Thus, it is tempting to suggest that DR^{mid} Intermediate moncytes represent an activated form of Classcial blood monocytes. In keeping with this, Classical and DR^{mid} Intermediate monocytes display similar levels of many cell surface receptors. In fact, we found no specific cell surface receptor which could readily distinguish these two apart from CD16 itself. If the transition from Classical to DR^{mid} Interemdiate phenotype were accelerated by scavenging of modified lipoproteins or other diet-related factors, this could explain why the latter sub-population is specifically expanded in obesity. In this regard, an initial pilot experiment assessing the influence of a high fat meal on blood monocyte proportions in a healthy adult revealed a direct expansion of the DR^{mid} sub-population 3 hours after ingestion (see **Appendix 4**). This correlates with data generated by our group implicating the DR^{mid} subset as an avid scavenger of lipid in vitro. On the other hand, in further preliminary work, high levels of transcription factors implicated in Non-Classical monocyte devleopment, namely PU.1, Nurr1 and Nurr77 in the DR^{hi} monocytes may suggest these could the true ‘Intermediate’ subset in transition to Non-Classical monocytes (see **Appendix 5**). The DR^{hi} Intermediate and Non-Classical sub-populations also share similar expression of cell surface receptors. Addtionally, we obesrved high levels of RGS12, which has been implicated in maturation and differentiation in other myeloid-derived cells and may be involved in generation of anti-apoptotic signals, in the DR^{hi} sub-population. Addtionally, monocytes are known to migrate to tissue and,

under various stimuli, adopt either a macrophage or dendritic like cell phenotype and carry out mcarophage and DC functions. It is possible that the Intermediate substets may represent monocytes adopting a macrophage or DC like phenotype. For example, cell surface phenotyping of DR^{hi} monocytes revealed high expression of CD11c, a marker expressed on human myeloid DCs (Kelly et al., 2014). The DR^{mid} subset was found to have high cell surface levels of macrophage antigen-1 (MAC-1), which may reflect a macrophage like-phenotype. However, further experimental evidence is required to determine the macrophage-DC like plasticity of the Intermediate monocyte subsets.

Intermediate human monocytes have been shown to migrate poorly toward chemokine gradients in several studies (Krankel et al., 2011, Thiesen et al., 2014), but to our knowledge, no study has delved deeper into the mechanisms underlying this reduced transmigration. In keeping with prior reports, our results indicate a reduced migratory role, via blunted chemokine signalling, in the Intermediate sub-populations with associated up-regulation of mRNA for multiple RGS proteins. Increased expression of RGS1 in particular is likely to result in reduced chemotaxis to CCL2. This mechanism could function to limit the egress of DR^{mid} and DR^{hi} Intermediate monocytes from the intravascular compartment, thus promoting ongoing maturation of a subpopulation of monocytes toward a “patrolling” Non-Classical phenotype.

Regulation of RGS1 has been linked to certain inflammatory stimuli, particularly its upregulation in atheroscelrotic lesions (Patel et al., 2015). Based on our group’s previous observations in subjects with obesity and type 2 diabetes, it will be of high interest to test whether scavenging of modifed lipoproteins or exposure to specific inflammatory stimuli result in Classical monocyte upregulation of RGS1 and blunting of chemotactic responses similar to the observed phenotype of DR^{mid} Intermediate monocytes in this project. It could also be informative to more directly compare DR^{mid} Intermediate monocytes in the circulation with lipid-laden, RGS1-expressing monocytes in atherosclerotic lesions. Furthermore, it remains to be clearly determined whether the DR^{mid} sub-population represents a more potent producer than

Classical monocytes of cytokines after encountering stimuli in the cirulation. In this scenario, upregulation of RGS proteins and, potentially, other negative regulators of GPCR signalling may be important in preventing unwanted migration of an activated cytokine-producing blood cells to the tissues.

Alternatively, as proposed by Collison et al., the increased adherence of TNF-α-producing Intermediate monocytes to endothelium might allow precise delivery of cytokines to areas of localised endothelial injury (Cros et al., 2010), (Collison et al., 2015). Based on our own results, high capacity for endothelial adherence may specifically play a role in the retention of Intermediate monocytes, in particular DR^{hi} Intermediates, in the circulation. We observed strong adherence of this sub-population to both resting and inflamed endothelium in vitro. Unlike Classical and DR^{mid} Intermediate monocytes, static endothelial adherence of DR^{hi} Intermediates was not disrupted by addition of anti-CD11a neutralising antibody.

It has been extensively documented that Intermediate monocytes are expanded in a range of diseases. In a study by Koch et al, the authors observed increased $CD16^{+}CD14^{+}$ monocytes in the lamina propira and blood of Crohn's disease patients with high disease activity and they reasoned that the these cells were entering inflamed tissue and driving inflammation (Koch et al., 2010). However, isolated $CD16^{+}CD14^{+}$ monocytes were found to be poor migrators through intestinal endothelial cells, in keeping with our results. As an alternative explanation, therefore, it was suggested that highly migratory $CD16^{-}$ Classical monocytes were entering the inflamed tissue, transitioning to an Intermediate-like phenotype and then "reverse migrating" back into circulation, resulting in an apparent expansion of Intermediate blood monocytes. This model whereby Classical monocytes switch to a $CD16^{+}$ Intermediate phenotype following migration into inflamed tissue provides a potentially interesting interpretation of our own results in healthy and obese adults as abdominal/visceral adipose tissue has been shown to be a significant site of chronic inflammation in metabolically unhealthy obese individuals. Whether such transition were to occur in the bloodstream or following

Classical monocytes migration into inflamed peripheral tissues, we belive that that the DR^{mid} sub-population is likely to represent an activated form of the Classical monocyte and, as such, may be a useful biomarker of chronic inflammatory disorders and risk for metabolic and cardiovascular disease complications. It would also be fascinating to test the hypothesis that Intermediate monocytes, and DR^{mid} Intermediates in particular, may be imprinted with a distnict genetic signature confered by the tissue inflammation that they encountered.

The development of therapeutic agents that target RGS proteins and their upregulation in monocyte sub-populations could be of interest for modulating disease associated with altered monocyte repertoire and migration. For example, in Crohn's disease, reduction in the cycling of monocytes into and out of the intestine may decrease monocyte-mediated tissue inflammation. In this regard, Interferon β-1b (IFN-β), which is used to treat multiple sclerosis - a disease driven by migration of immune effector cells into the central nervous system, has been shown to induce RGS1 expression in PBMCs, particularly monocytes. This effect has been proposed as a mechanisim of action for IFN-β in reducing monocyte-mediated inflammation in the brain (Tran et al., 2010).

The evidence presented in this thesis has contibuted novel insights into the phenotypes of multiple monocyte sub-populations in the circulation during health and reveals potentially important features of the regulation of chemokine-induced migration of Intermediate human monocytes. Our results pertaining to the endothelial adherence of the Intermediate monocytes is consistent with a recetly published study (Collison et al., 2015) and builds toward a clearer understanding of the range of functional effects of Intermediate monocytes within the circulation during health and disease. Most importantly, we have built upon previous work by our group to demonstrate that Intermediate human monocytes represent a heterogeneous population consisting of two distinct sub-populations, DR^{mid} and DR^{hi}. We have confirmed their status as bona fide monocytes with many similarities but also with distinct phenotypic and functional differences. We propose a model whereby

the DR^{mid} sub-population represents an activated form of Classical monocytes while the DR^{hi} sub-population represents a true 'intermediate' phenotype, potentially in transition to the fully-mature "patrolling" Non-Classical monocyte.

Future Directions 6.2

There are a number of experimental investigations which we did not have adequate time to address in this study. Thus far, we have only documented elevated mRNA levels for specific RGS proteins in the defined monocyte sub-populations and confirmation of over-expression in Intermediate monocytes at the protein level will be important. Furthermore, it could be very informative to overexpress or deplete RGS1 in human monocytes to determine whether such interventions mediate predicted effects on CCL2-induced transmigration. Additionally, it would be interesting to assess mRNA levels for RGS1 and other RGS proteins in the monocyte sub-populations after various stimuli as this has not yet been reported in the literature.

A feature of Intermediate monocytes may be their strong inflammatory cytokine production but this has varied among reported studies (Thiesen et al., 2014, Wong et al., 2011, Cros et al., 2010). This variation may be explained in part by heterogeneity among Intermediate monocytes. Therefore, it would be of great interest to compare the cytokine responses of the DR^{mid} and DR^{hi} sub-populations following exposure to various inflammatory stimuli. In fact, we made several attempts at stimulating FACS-purified DR^{mid} and DR^{hi} Intermediate monocytes with the TLR4 agonist LPS. However, in these experiments, the sorted cells were poorly responsive to LPS, producing low amounts of TNF-α as determined by ELISA. We speculated that the responsiveness of rare monocyte subpopulations is negatively affected by the sorting process, but, due to time and resource constraints we did not persist with this line of investigation. Nevertheless, with further optimisation, an approach to individually profiling the inflammatory responses of the two Intermediate monocyte sub-populations should be feasible and revealing.

As described above, we have recently generated preliminary data indicating that mRNA levels of transcription factors PU.1, Nurr1, Nurr77 may differ among the four defined monocyte sub-populations. Clearly, analysis of a greater number of sorted monocyte samples and confirmation at protein level

will be required to determine whether this observation is valid. However, we believe that further profiling of growth factor and differentiation-dependent gene products in the DR^{hi} Intermediate in particular may help to better understand their relationship with Non-Classical monocytes and their functional distinctions from Classical and DR^{mid} Intermediate monocytes.

In regard to the in vivo dynamics and functions of the individual monocyte subpopulations, the use of humanised mice, such as NOD/SCID/IL2rϒ^{null} mice engrafted with $CD34^{+}$ cord blood hematopoietic stem cells, have been shown to support the development of functional myeloid subsets (Tanaka et al., 2012). Using these mice it may be possible to track the development of monocytes subsets in bone marrow, blood and tissue. Coupled with models of inflammatory disease, this may prove to be the best technological approach for advancing knowledge of human monocyte kinetics and activation/maturation pathways in health and disease.

From a clinical view, it would be desirable to phenotype the DR^{mid} and DR^{hi} subsets in the context of a broader range of physiological conditions and inflammatory disorders. Initially, it would be of interest to determine whether DR^{mid} expansion predominantly accounts for the proportionate increases in Intermediate monocyte expansion reported for various disease states. Our preliminary experiment indicating that the DR^{mid} Intermediate subpopulation rapidly expands in the blood in a healthy person after a high fat meal is in keeping with a direct relationship between Classical and DR^{mid} Intermediate monocytes and provides a striking example of the influence of unhealthy diet on cells of the innate immune system. Clearly it will be of interest to more carefully study this phenomenon and its implications for health.

Having completed this project, we feel that additional experiments are needed to make definitive conclusions regarding the nature of DR^{mid} and DR^{hi} Intermediate monocytes. Rather than challenging the current classification system, our work perhaps advances the emerging concept of heterogeneity among Intermediate monocytes. We hope that this body of work will contribute to future studies and discoveries of human monocyte biology.

Appendices

Appendix 1: Antibodies and Reagents

All antibodies used were targeted against cell surface receptors.

Appendix Table 1- 1 Antibody information

Fluorochrome	Clone	Vendor	Code	Vol. (µl / $5x10^5$ cells)
FITC				
CD16	Clone 3G8	BD Biosciences	555406	2
PE				
CD45	HI30	BD Biosciences	555483	2.5
HLA.DR	TU36	BD Biosciences	555561	2
CD11c	B-ly6	BD Biosciences	555392	3
CD114/G-MCSF	LMM741	Miltenyi	130-097-309	5
CD162/PSGL-1	KPL-1	BD Biosciences	556055	5
CD115/CSF-1R	12-3A3-1 B10	eBioscience	12-1159-42	5
CCR5	eBioT21/8	eBioscience	12-1957-42	
CD33	HIM3-4	Immunotools	21270334	5
CD31	MEM-05	Immunotools	21270314	2
CD49d	BU49	Immunotools	21488494	5
CD11b	MEM-174	Immunotools	21279114	5
CD18	MEM-48	Immunotools	21270184	5
CXCR4	12G5	eBioscience	12-9999-42	5
CD106 (VCAM-1)	STA	eBioscience	12-1069-42	2.5
PerCP Cy5.5				
CD14	TÜK4	Miltenyi	130-094-969	1.5
Pe-Cy7				
CD45		BD Biosciences	557748	2.5
APC				
CD45	HI30	BD Biosciences	555485	2.5
CX_3CR_1	2A9-1	eBioscience	17-6099-42	2
CCR6	R6H1	eBioscience	17-1969-41	5
CD11a	MEM-25	Immunotools	21270116	5
CD54 (ICAM-1)	1H4	Immunotools	2127946	2.5
CD62L	LT-TD180	Immunotools	21279626	2.5
CCR2	REA264	Miltenyi	130-103-830	10
APC H7				
HLA-DR	G46-6	BD Biosciences	561358	2
BV421/Pacific Blue				
CD56	NCAM16.2	BD Biosciences	562751	2
BV450/Brilliant Violet				
CD16	eBioCB16	eBioscience	48-0168-42	2

Appendix Table 1- 2 Reagents

Item Description	Vendor	Code
Count Bright Beads for Flow Cytometry	Life Technologies	C36950
Sytox Red	Life Technologies	S34859
Flow cytometry compensation beads	Life Technologies	A-10344
Fluo-4 probe	Invitrogen	F-14201
CD14 microbeads	Miltenyi	130-050-201
Pan-monocyte Microbeads	Miltenyi	130-096-537
RevertAid First Strand cDNA Synthesis Kit	ThermoScientific	K1632
RNeasy Micro RNA isolation kit	Qiagen	74004
Phalloidin FITC	Sigma-Aldrich	P5282-.1MG

Appendix 2: Additional data on primers used for PCR and qRT-PCR

PCR primers data sheet 2.1

Batch #	Oligo Name	Oligo #	LerPur	Scale	MW	Tm°	µg/OD	OD	µg	nmol	Epsilon 1/(mMcm)	Dimer	2ndry	GC %	µl for 100µM	Sequence(5'-3')
HA0734611	RGS1 Fwd	801862938O-000010	27 DST	0.025	8219	69.8	31.8	16.2	515.8	62.7	258.1	No	Moderate	48.1	627	ACCTGAGATCTATGATCCCACATCTGG
HA0734612	RGS1 Rev	801862938O-000020	21 DST	0.025	6437	64.2	32.4	17.4	565.1	87.7	198.2	No	Strong	52.3	877	GGCTATTAGCCTGCAGGTCAT
HA0734613	RGS2 Fwd	801862938O-000030	21 DST	0.025	6434	71.3	31.0	17.2	533.8	82.9	207.3	Yes	None	61.9	829	CAGACCCATGGACAAGAGCGC
HA0734614	RGS2 Rev	801862938O-000040	21 DST	0.025	6517	66.0	31.8	13.6	432.5	66.3	204.9	No	Weak	52.3	663	TAGCATGAGGCTCTGTGGTGA
HA0734615	RGS4 Fwd	801862938O-000050	21 DST	0.025	6469	71.3	34.0	13.4	455.7	70.4	190.2	No	None	61.9	704	GCCGGCTTCTTGCTTGAGGAG
HA0734616	RGS4 Rev	801862938O-000060	21 DST	0.025	6514	70.9	30.4	15.4	468.5	71.9	214.1	No	Weak	61.9	719	CACTGAGGGACCAGGGAAGCA
HA0734617	RGS12 Fwd	801862938O-000070	21 DST	0.025	6466	74.7	31.4	15.5	487.7	75.4	205.5	No	Weak	71.4	754	ACCAGGAGGCACCGGGAGGTCC
HA0734618	RGS12 Rev	801862938O-000080	21 DST	0.025	6389	68.6	33.8	14.7	498.2	77.9	188.5	No	Weak	61.9	779	CTCTCCCGTAGCCGAGTGGTT
HA0734619	RGS16 Fwd	801862938O-000090	21 DST	0.025	6425	71.1	31.6	15.3	484.7	75.4	202.8	No	Weak	61.9	754	CACCTGCCTGGAGAGAGCCAA
HA0734620	RGS16 Rev	801862938O-000100	21 DST	0.025	6543	76.3	32.9	12.4	408.9	62.5	198.4	No	Weak	66.6	625	TGGCAGAGGCGGCTGAGGGTT
HA0734621	RGS18 Fwd	801862938O-000110	22 DST	0.025	6706	61.3	31.7	20.8	680.0	98.3	211.4	No	Weak	31.8	983	ATGGAAACAACATTGCTTTTCT
HA0734622	RGS18 Rev	801862938O-000120	24 DST	0.025	7329	63.9	30.2	12.7	383.9	52.3	242.4	No	Very Weak	33.3	523	TTATAACCAAATGGCACACATCTGA
HA0734623	Actin Fwd	801862938O-000130	20 DST	0.025	6037	61.0	32.5	15.4	501.1	83.0	185.5	No	Weak	50	830	GTTTGAGACCTTCAACACCC
HA0734624	Actin Rev	801862938O-000140	20 DST	0.025	6019	60.9	34.1	11.9	406.4	67.5	176.2	No	None	50	675	ATACTCCTGCTTGCTGATCC
HA0734625	RGS3 Fwd	801862938O-000150	30 DST	0.025	9318	77.0	32.1	18.1	581.3	62.3	290.1	No	Strong	53.3	623	TTGGCTGTCAGGGCAGCTGTACAATAGTGG
HA0734626	RGS3 Rev	801862938O-000160	30 DST	0.025	9305	78.3	31.2	24.0	750.1	80.6	297.7	No	Moderate	53.3	806	CACTGAACTCAGTGCGAAGGAAGGCTTGGA
HA0734627	HPRT A Fwd	801862938O-000170	20 DST	0.025	6164	66.2	32.2	12.7	410.0	66.5	190.9	No	None	55	665	CCTGGCGTCGTGATTAGTGA
HA0734628	HPRT A Rev	801862938O-000180	20 DST	0.025	6113	69.4	29.7	12.9	383.7	62.7	205.5	No	Moderate	50	627	AACAATCCGCCCAAAGGGAA
HA0734629	HPRT B Fwd	801862938O-000190	20 DST	0.025	6157	62.4	31.7	15.3	486.3	78.9	193.7	No	Weak	50	789	TGGACAGGACTGAACGTCTT
HA0734630	HPRT B Rev	801862938O-000200	20 DST	0.025	6080	69.1	31.4	15.8	496.9	81.7	193.3	No	Moderate	55	817	CAATCCGCCCAAAGGGAACT
HA0734631	GADPH A Fwd	801862938O-000210	20 DST	0.025	6044	62.2	34.1	16.0	546.6	90.4	176.9	No	None	55	904	CACTAGGCGCTCACTGTTCT
HA0734632	GADPH A Rev	801862938O-000220	23 DST	0.025	7024	68.1	31.7	19.1	605.6	86.2	221.5	No	None	47.8	862	GCCAAATTCGTTGTCATACCAGG
HA0734633	GADPH B Fwd	801862938O-000230	20 DST	0.025	6029	64.9	34.1	13.4	458.2	76.0	176.3	No	None	60	760	CCACTAGGCGCTCACTGTTC

Batch #	Oligo Name	Oligo #	LerPur	Scale	MW	Tm°	µg/OD	OD	µg	nmol	Epsilon 1/(mMcm)	Dimer	2ndry	GC %	µl for 100µM	Sequence(5'-3')
HA0734634	GADPH B Rev	801862938O-000240	24 DST	0.025	7386	64.7	30.7	16.6	510.0	69.0	240.4	No	Moderate	45.8	690	GTCATACCAGGAAATGAGCTTGAC

Figure 6. 1 PCR primers data sheet

qRT-PCR primer data sheets 2.2

Batch #	Oligo Name	Oligo #	Len	Pur	Scale	MW	Tm°	µg/OD	OD	µg	nmol	Epsilon 1/(mMcm)	Dime	2ndry	GC %	µl for 100µM	Sequence(5'-3')
HA07700676	FH1_RGS12	801924378-70/0	20	RP1	0.025	5996	58.0	32.6	15.0	489.8	81.7	183.6		None	0	817	TAAACTTTTCTCACGCAC
																	Forward Human 1 RGS12
HA07700677	RH1_RGS12	801924378-70/1	20	RP1	0.025	6141	56.3	31.2	15.5	484.4	78.8	196.5	No	Weak	45	788	GACTGCTGGTCATTAGAAAC
																	Reverse Human 1 RGS12
HA07700678	FH1_SPI1	801924378-80/0	18	RP1	0.025	5453	-1	30.8	12.6	388.1	71.1	177	No	None	0	711	AGCCATAGCGACCATTAC
																	Forward Human 1 SPI1
HA07700679	RH1_SPI1	801924378-80/1	18	RP1	0.025	5457	55.6	33.9	15.1	512.0	93.8	160.9	No	Very Weak	0	938	CTCCGTGAAGTTGTTCTC
																	Reverse Human 1 SPI1
HA07700680	FH1_RGS18	801924378-90/0	21	RP1	0.025	6484	55.8	30.8	16.6	512.0	78.9	210.2		None	0	789	AGATGGACTAGAGGCTTTTAC
																	Forward Human 1 RGS18
HA07700681	RH1_RGS18	801924378-90/1	20	RP1	0.025	6067	59.4	32.6	15.9	519.4	85.6	185.7	No	Weak	40	856	TTCTTGAAATCTTCACAGGC
																	Reverse Human 1 RGS18
HA07700682	FH1_CSF1R	801924378-100/0	22	RP1	0.025	6677	-1	31.4	18.8	591.0	88.5	212.4	No		40.9	885	GAATGAGTCCAACTACATTGTC
																	Forward Human 1 CSF1R
HA07700683	RH1_CSF1R	801924378-100/1	21	RP1	0.025	6503	-1	29.5	14.1	416.0	63.9	220.4		Weak	42.8	639	GTGTAGACACAGTCAAAGATG
																	Reverse Human 1 CSF1R
HA07700684	FH1_CSF3R	801924378-110/0	20	RP1	0.025	6083	55.7	32.9	15.9	523.3	86.0	184.8			45	860	GCTTCACTCTGAAGAGTTTC
																	Forward Human 1 CSF3R
HA07700685	RH1_CSF3R	801924378-110/1	21	RP1	0.025	6414	57.3	30.8	16.7	514.9	80.2	208	No	Weak	42.8	802	CATATTCTGGTACAACAGCAG
																	Reverse Human 1 CSF3R
HA07700686	FH1_FCGR3B	801924378-120/0	20	RP1	0.025	6039	58.0	30.5	15.4	470.8	77.9	197.5		None	45	779	GAACATCACCATCACTCAAG
																	Forward Human 1 FCGR3B
HA07700687	RH1_FCGR3B	801924378-120/1	22	RP1	0.025	6758	55.5	30.2	19.3	584.6	86.5	223.1	No	None	40.9	865	AGAGAAATATAGTCCTGTGTCC
																	Reverse Human 1 FCGR3B

Figure 6. 2 qRT-PCR primer data sheet 1

Batch #	Oligo Name	Oligo #	Len	Pur	Scale	MW	Tm°	µg/OD	OD	µg	nmol	Epsilon 1/(mMcm)	Dime	2ndry	GC %	µl for 100µM	Sequence(5'-3')
HA07700664	FH1_GAPDH	801924378-10/0	18	RP1	0.025	5484	55.7	31.1	18.2	567.6	103.5	175.8	No	Very Weak	50	1035	ACAGTTGCCATGTAGACC
																	Forward Human 1 GAPDH
HA07700665	RH1_GAPDH	801924378-10/1	18	RP1	0.025	5561	59.9	32.5	13.0	422.9	76.0	170.9	No	None	44.4	760	TTTTTGGTTGAGCACAGG
																	Reverse Human 1 GAPDH
HA07700666	FH1_NR4A1	801924378-20/0	18	RP1	0.025	5444	53.9	31.6	15.7	496.3	91.1	172.2	No	Very Weak	50	911	ACTACTCCAAGTTCCAGG
																	Forward Human 1 NR4A1
HA07700667	RH1_NR4A1	801924378-20/1	18	RP1	0.025	5478	56.9	30.8	14.8	456.7	83.3	177.5	No	None	55.5	833	GATGACCTCCAGAGAACC
																	Reverse Human 1 NR4A1
HA07700668	FH1_HPRT1	801924378-30/0	19	RP1	0.025	5843	56.8	31.3	12.9	403.9	69.1	186.6	No	Weak	42.1	691	ATAAGCCAGACTTTGTTGG
																	Forward Human 1 HPRT1
HA07700669	RH1_HPRT1	801924378-30/1	20	RP1	0.025	6092	57.0	31.4	18.2	573.2	94.1	193.4	No	Weak	45	941	ATAGGACTCCAGATGTTTCC
																	Reverse Human 1 HPRT1
HA07700670	FH1_NR4A2	801924378-40/0	22	RP1	0.025	6847	57.7	29.6	19.2	569.6	83.1	230.8			0	831	GACTATCAAATGAGTGGAGATG
																	Forward Human 1 NR4A2
HA07700671	RH1_NR4A2	801924378-40/1	20	RP1	0.025	6141	56.4	30.9	14.4	445.2	72.5	198.6	No	None	45	725	GACCTGTATGCTAATCGAAG
																	Reverse Human 1 NR4A2
HA07700672	FH1_RGS1	801924378-50/0	20	RP1	0.025	6147	59.1	31.8	16.3	518.3	84.3	193.3	No	Weak	0	843	ACTGGTCAAAATGTCTTTGG
																	Forward Human 1 RGS1
HA07700673	RH1_RGS1	801924378-50/1	21	RP1	0.025	6364	55.8	31.6	14.4	456.3	71.7	200.8	No	Very Weak	42.8	717	CTTATAGTCTTCACAAGCCAG
																	Reverse Human 1 RGS1
HA07700674	FH1_RGS2	801924378-60/0	20	RP1	0.025	6098	59.2	32.6	16.7	545.7	89.4	186.6	No	Very Weak	40	894	AATATGGTCTTGCTGCATTC
																	Forward Human 1 RGS2
HA07700675	RH1_RGS2	801924378-60/1	20	RP1	0.025	6079	60.8	34.6	10.5	364.1	59.8	175.3		Moderate	0	598	TTTTCCTTGCTTTTGAGGAC
																	Reverse Human 1 RGS2

Figure 6. 3 qRT-PCR primer data sheet 2

Appendix 3: Consent form for blood donation

Study Number:

Participant Identification Number:

Consent Form

Title of Project: Immunological research using healthy human blood cells

Name of Principal Researcher: Prof. Matthew Griffin

Please Initial Box

1. I confirm that I have read the information sheet dated 09/01/14, Version 1 for the above study and have had the opportunity to ask questions. ☐

2. I am satisfied that I understand the information provided and have had enough time to consider the information. ☐

3. I understand that my participation is voluntary and that I am free to withdraw at any time, without giving any reason, without my legal rights being affected. ☐

4. I agree to take part in the above study. ☐

Name of Participant: _____ Date: _____

Signature: _____

Person taking consent (if different from researcher): _____
Date: _____

Signature: _____

Name of Researcher: _____ Date: _____

Signature: _____

1 copy for participant; 1 copy for researcher; 1 to be kept with research notes

HEALTH QUESTIONNAIRE: ***Immunological research using healthy human blood cells***

Name: _____

Date: _____

Please answer all questions

1. **Are you feeling sick or unwell today?**

   YES ☐ **NO** ☐

2. **Are you currently taking any prescription medication?**

   YES ☐ **NO** ☐

3. **Have you ever been diagnosed or treated for anaemia or any other blood condition?**

YES ☐ **NO** ☐

4. **Have you ever had a problem with excessive bleeding?**

YES ☐ **NO** ☐

5. **Have you ever experienced a problem or complication from having a blood sample taken?**

YES ☐ **NO** ☐

Participant Information Sheet

Title of Project: Immunological research using healthy human blood cells

Objective of the Study:

Name of Principal Researchers: Prof. Matthew Griffin and Prof. Rhodri Ceredig

You are being invited to take part in a research study. Before you decide, it is important for you to understand why the research is being done and what it will involve. This Participant Information Sheet will tell you about the purpose, risks and benefits of this research study. If you agree to take part, we will ask you to sign a Consent Form. If there is anything that you are not clear about, we will be happy to explain it to you. Please take as much time as you need to read it. You should only consent to participate in this research study when you feel that you understand what is being asked of you, and you have had enough time to think about your decision.

Purpose of the Study

The purpose of the study is to learn more about the types and functions of immune cells (white blood cells) present in the bloodstream by performing experiments on cells freshly isolated from blood samples of healthy people. Prof. Griffin, Prof. Ceredig and researchers working with him have several active research projects that are currently investigating new aspects of human immune cell function and the ways in which these cells behave differently in people with a variety of diseases. The goals of these projects are to find new ways of testing blood cells for changes that indicate risk for disease or severity of disease and to discover new strategies for treating diseases by targeting immune cells function. In order to understand immune cell changes associated with disease, it is essential to define immune cell functions in healthy people.

You are being asked to participate in the study because you are a healthy adult (aged more than 18 years) who may be willing to provide blood samples for this research.

Taking Part in the Study

Do I have to take part?

It is up to you to decide whether or not to take part. If you do decide to take part you will be given this information sheet to keep and be asked to sign a consent form. If you decide to take part you are still free to withdraw at any time and without giving a reason. A decision to withdraw at any time, or a decision not to take part, will not affect your rights in any way.

What will happen if I take part?

If you decide to participate you will be asked to sign a consent form. After this, a time will be arranged for you to have a blood sample taken by an experienced member of the research team in a private area of the Biosciences Research Building or the Orbsen Building on the NUI Galway campus.

When you arrive for the appointment, you will be given a short, confidential health questionnaire to complete and this will then be reviewed by the researcher. If the answer to all questions is NO then a blood sample will be taken If one or more questions is answered YES then a blood sample will not be taken but you will be given appropriate information about future suitability for providing a blood sample.

If a blood sample is taken, you will be seated comfortably and asked about any allergies to antiseptics or adhesives or any other concerns before proceeding. Your left or right arm will be rested on a flat surface and the skin over a suitable vein on the inner surface of the elbow cleaned with an antiseptic swab. A tourniquet will be applied to the upper arm and tightened until the veins are prominent but no discomfort is felt in the arm and hand. A small needle will be inserted and connected to one or more vacuum tubes to collect a total volume of blood between 5 and 50 millilitres. Following completion of blood collection, the tourniquet will be removed, the needle withdrawn and a piece of cotton wool applied to the area. You will be asked to raise the arm and apply gentle pressure to the cotton wool for 1-2 minutes following which a clean adhesive bandage will be applied. You will then be allowed to rest for 2-5 minutes and will be questioned about lightheadedness/weakness before you leave.

You will be assigned an identification number and this number will be used to label the collected blood sample and all subsequent experimental containers and data derived from the sample. A written record of the time, date and volume of the blood draw along with your name, age, gender and unique subject number will be kept in a locked cabinet in Prof. Griffin's office in the BRB.

If you have previously consented and provided blood samples you may be asked to provide subsequent samples at intervals of no less than 2 weeks but you will under no obligation to do so.

For these subsequent blood draws, a suitable time and date will be arranged following which administration of the Health Questionnaire and blood sampling will be carried out by the same procedure described above. You will not be asked to provide more than 50 millilitres of blood in total in a given 4 week period.

How long will my part in the study last?

If you agree to participate, you will be kept on a list of healthy volunteers and may be asked to provide a blood sample from time to time for a maximum period of five years.

What are the possible benefits of taking part?

There will be no direct benefits to you in taking part.

What are the possible disadvantages of taking part?

There is a small risk that you will suffer harm by participating in the study. The two possible causes of harm are (a) pain, discomfort or weakness at the time of blood sampling and (b) loss of confidentiality of personal information. Careful measures will be taken by the researchers to minimise these risks.

(a) *Pain and discomfort at the time of blood sampling*: Having a blood sample taken is usually associated with momentary sharp pain when the needle is inserted and removed. To minimise this, blood sampling will only be performed by experienced researchers trained in the procedure and the smallest size needle that allows for efficient collection of blood will be used.

(b) *Weakness or fainting at the time of blood sampling*: Occasionally, a person will feel weak or faint during or immediately after having a blood sample taken. The risk of this will be minimised by not taking blood if you have previously had this experience, by ensuring that you are sitting comfortably throughout the process, by limiting the amount of blood taken at one time to 50 millilitres and by allowing you the rest for a short while after the sample is taken. In addition, the researcher taking the blood sample will remain with you until you are ready to leave.

(c) *Loss of confidentiality of personal information*: A limited amount of personal information will be recorded if you agree to participate. This will include your name, age, gender and your response to 5 questions on a health questionnaire. Any time you provide personal information, there is a risk that it will be seen by people for whom it is not intended. This risk will be minimised by having all documents containing personal information kept in a locked cabinet in Prof. Griffin's office, by using an anonymous identification number on all sample tubes, laboratory samples and notebooks and by limiting the questions on the questionnaire to the

minimum basic details required to ensure that you are in good health and that it is safe for you to have a blood sample taken.

Can women of childbearing potential participate in the study?

Yes, women of childbearing potential can participate. They are not at increased risk from having a blood sample taken and it is scientifically important to include both men and women in the study. However, if you have any concerns or questions about providing a blood sample that relate to possible pregnancy you should ask one of the researchers about this.

What if something goes wrong?

If you have excessive pain, discomfort or weakness during the blood sampling procedure, the procedure will be stopped and the researcher will stay with you until you feel better. If you do not feel better within 10 minutes, assessment and appropriate help from a medically trained person (doctor or nurse) will be arranged for you.

What happens at the end of the study?

After your blood sample is taken you will be able to leave. You may be asked to provide additional blood samples from time to time at intervals of no less than 2 weeks for a period of time up to five years. Your blood samples and cells from it will be used for experiments on the same day and, sometimes at later time-points after a period of storage in a freezer. The maximum period of time for which samples from your blood cells may be stored is ten years. At the end of ten years, all paper records of your participation in the study and all remaining samples derived from your blood will be destroyed. The results of experiments carried out with cells from your blood sample may be published in one or more scientific journals although you will not be identified in the publication if this is the case. You will be able to obtain a copy of the published results by contacting Prof. Griffin or Prof. Ceredig.

What if I change my mind during the study?

You can change your mind about participating in the study at any time without any disadvantage or loss of rights. At any time you can request that documents and samples related to your participation in the study be destroyed immediately.

What if I have a complaint during my participation in the study?

If you have a complaint about the study during your participation you should contact Prof. Griffin or Prof. Ceredig to discuss the complaint. If you do not wish to do this, you may also contact the Chairperson of the NUI Galway Research Ethics Committee (c/o Office of the Vice President for Research, NUI Galway, ethics@nuigalway.ie) to discuss your concerns. Your complaint will be listened to carefully and confidentially and every effort will be made to address it including changes to study procedure if that is appropriate.

Whom do I contact for more information if I have further concerns?

For more information about the study you may contact: Prof. Matthew Griffin (matthew.griffin@nuigalway.ie, phone: +353-91-495436) or Prof. Rhodri Ceredig (rhodri.ceredig@nuigalway,ie, phone: +353-91- 49 59 16).

If you have any concerns about this study and wish to contact someone independent and in confidence, you may contact 'the Chairperson of the NUI

Galway Research Ethics Committee, c/o Office of the Vice President for Research, NUI Galway, ethics@nuigalway.ie.

Appendix 4: Influence of high fat meal on monocyte subset proportions

Previous work generated by our group (MC Dennedy, EP Connaughton and M Griffin, unpublished observations) indicated the DR^{mid} subset is expanded in an obese patient cohort and are avid scavengers of modified lipid in vitro. This led us to speculate that either lipid uptake or inflammation generated by a high fat diet may contribute to the specific expansion of the DR^{mid} subset in circulation.

In a study by Gower et al., healthy individuals were given a high fat meal and 3.5 hours postprandial (the period that coincides with the peak in triglycerides after ingestion of a high fat meal) blood was drawn and monocytes isolated and found to have increased lipid content in contrast to monocytes isolated from fasting donors (Gower et al., 2011). A range of inflammatory cytokines, such as TNF-α and IL-1β, were also significantly increased in the serum after the high fat meal in contrast to fasting state (Gower et al., 2011). In a separate study by den Hartigh et al, a similar high fat meal was given to fasting individuals, and blood drawn 3.5 hours postprandial, with results also indicating increased lipid accumulation in monocytes (den Hartigh et al., 2010). Additionally, PBMCs were isolated from blood and gene expression of inflammatory cytokines TNF-α, IL-1β and IL-8 were assessed by qRT-PCR. Interestingly, mRNA levels of all three cytokines were significantly elevated in PBMCs isolated from postprandial versus fasting blood samples (den Hartigh et al., 2010).

With the evidence provided by these studies, it posed intriguing questions as to how the Intermediate DR^{mid} subset would respond. To test this, we designed a similar experimental setup as outlined in the previous studies. Briefly, the donor had fasting bloods drawn three hours before ingestion of a high fat meal, and 3.5 hours postprandial. PBMCs were isolated as described in **Section 2.1** and monocyte subsets analysed using flow cytometry. Strikingly, the DR^{mid} subset was expanded, comprising 23% of total monocytes in postprandial blood, in comparison to fasting blood (14%) (**Appendix 4.1**). Of note, the DR^{hi}

subset was also expanded postprandial (4.5%) compared to fasting (3.3%), with Classical monocyte reducing from 75.5% of total monocytes in fasting bloods to 65% in postprandial blood. This is preliminary data and warrants further investigation before concrete conclusions can be made, but it suggests a dynamic response between the DR^{mid} subset and increased triglycerides or inflammatory mediators in the circulation (den Hartigh et al., 2010, Gower et al., 2011).

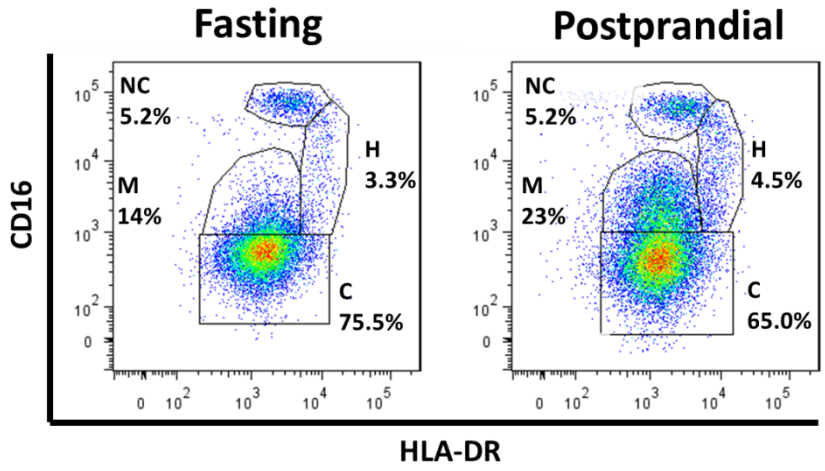

Appendix 4. 1 Expansion of blood monocyte sub-populations after high fat meal.

HLA-DR vs CD16 flow cytometry plots illustrating the expansion of the monocyte sub-populations isolated from fasting or postprandial bloods. Monocyte sub-population expansion is expressed as a percentage of the total monocyte population. (**C**) Classical (**M**) DR^{mid} (**H**) DR^{hi} (**NC**) Non-Classical. n=1.

Appendix 5: Human monocyte subset mRNA levels of transcription factors NR4A1 (Nurr77), NR4A2 (Nurr1) and SPI1 (PU.1)

Monocytes were purified by FACS, RNA isolated and mRNA levels of the transcription factors NR4A1 (Nurr77), NR4A2 (Nurr1) and SPI1 (PU.1) were measured using qRT-PCR in the same manner as indicated in **Section 2.9**. In mouse models, NR4A1 (Nurr77) (Hanna et al., 2011, Carlin et al., 2013) and SPI1 (PU.1) (Anderson et al., 1998) were found essential of development of Non-Classical monocytes and myeloid cells respectively.

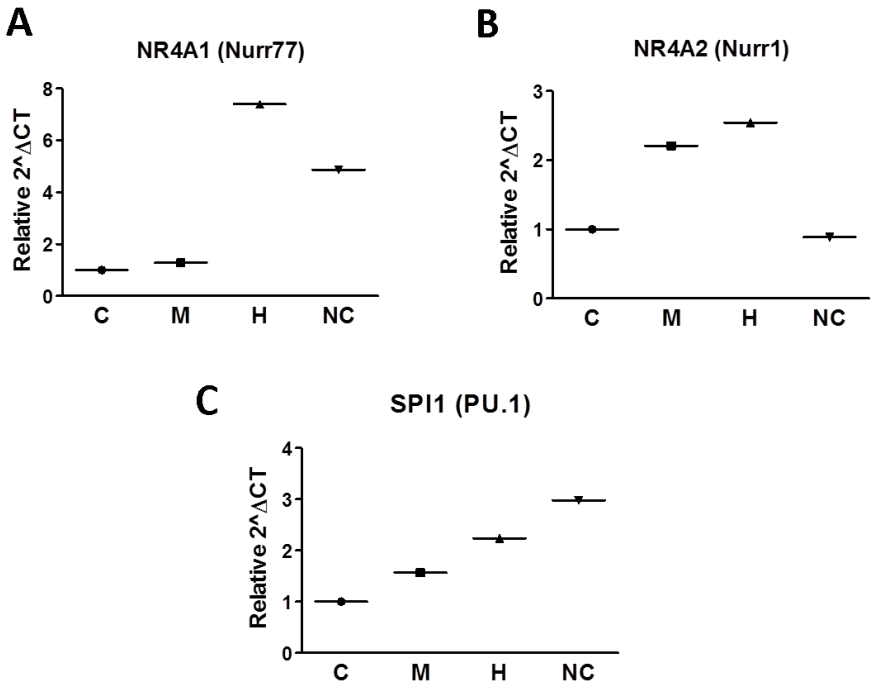

Appendix 5. 1 mRNA levels of transcription factors in human monocyte subsets

mRNA levels of transcription factors NR4A1 (Nurr77), NR4A2 (Nurr1) and SPI1 (PU.1) in sorted human monocyte subsets. GAPDH was used as housekeeping gene, and Classical monocytes are set as the reference sample. (**C**) Classical (**M**) DR^{mid} (**H**) DR^{hi} (**NC**) Non-Classical. n=1

Appendix 6: Publications, presentations and achievements.

Publications:

Dennedy MC, Connaughton EP, Hanley SA, Slevin S, O'Shea D, Ceredig R, O'Brien T, Griffin MD. Intermediate Monocytes are Expanded in Obesity and are Associated with Scavenger-receptor-Mediated Uptake of Modified Lipoproteins and Adverse Cardiometabolic Risk. *Under Revision.*

Presentations:

1. **Phenotypic, Functional and Molecular Analysis of Novel Human Monocyte Subpopulations.** Eanna Connaughton, Shirley A Hanley, Conall Dennedy, Rhodri Ceredig & Matthew D Griffin. Trinity College Dublin, May 2013. *Poster Presentation*.

2. **Phenotypic, Functional and Molecular Analysis of Novel Human Monocyte Subpopulations.** Eanna Connaughton, Shirley A Hanley, Conall Dennedy, Rhodri Ceredig & Matthew D Griffin. School of Medicine Research Day. National University of Ireland, Galway, May 2013. *Poster Presentation*.

3. **The human intermediate monocyte subset can be further subdivided on the basis of HLA-DR expression revealing a distinct abnormality in obesity and diabetes.** M. Conall Dennedy, Eanna Connaughton, Stephanie Slevin, Shirley A. Hanley, Timothy O'Brien, Rhodri Ceredig, Matthew D Griffin. International Congress of Immunology, Milano Congressi, Milan, Italy, August 2013. *Poster Presentation*.

4. **Phenotypic, Functional and Molecular Analysis of Novel Human Monocyte Subpopulations.** Eanna Connaughton, Shirley A Hanley, Conall Dennedy, Rhodri Ceredig & Matthew D Griffin. Irish Society of Immunology, Dublin, September 2013. *Poster Presentation*.

5. **Leukocyte Fractionation by Centrifugal Elutriation to Facilitate Fluorescent Activated Cell Sorting (FACS) of Human Monocyte Subsets.** Eanna Connaughton, Shirley A Hanley, Conall Dennedy, Rhodri Ceredig & Matthew D Griffin. Irish Cytometry Society Annual Meeting, University College of Dublin, February 2014. *Poster Presentation*.

6. **Phenotypic, functional and molecular analysis of novel human monocyte subpopulations.** Eanna Connaughton, Shirley A Hanley, Conall Dennedy, Rhodri Ceredig & Matthew D Griffin. Molecular Medicine Ireland, Annual Meeting, Trinity College Dublin, March 2014. *Oral presentation* (Winner, MMI Medal).

7. **Development of a Quantitative, Flow Cytometry-based Assay for Human Blood Monocyte Adhesion to and Transmigration through an Endothelial Layer.** Eanna Connaughton, Shirley A Hanley, Conall Dennedy, Rhodri Ceredig & Matthew D Griffin. School of Medicine Research Day. National University of Ireland, Galway, May 2014. *Poster Presentation*.

8. **Phenotypic, Functional and Molecular Analysis of Novel Human Monocyte Subpopulations.** Eanna Connaughton, Shirley A Hanley, Conall Dennedy, Rhodri Ceredig & Matthew D Griffin. Molecular Medicine Ireland Annual Meeting, Trinity College Dublin, March 2015. *Poster Presentation*.

9. **Phenotypic, Functional and Molecular Analysis of Novel Human Monocyte Subpopulations.** Eanna Connaughton, Shirley A Hanley, Conall Dennedy, Rhodri Ceredig & Matthew D Griffin. Evolve Biomed, RDS Dublin, Ireland, April 2015. *Poster Presentation*.

Achievements:

1. Winner, Immunotools Award 2012.

2. Awarded Molecular Medicine Ireland (MMI) medal for best oral presentation at MMI open day, Trinity Science Gallery, Dublin, 2014.

References

AGENES, F., BOSCO, N., MASCARELL, L., FRITAH, S. & CEREDIG, R. 2005. Differential expression of regulator of G-protein signalling transcripts and in vivo migration of CD4+ naive and regulatory T cells. *Immunology,* 115**,** 179-88.

ALBERTS, B., JOHNSON, A., LEWIS, J., RAFF, M., ROBERTS, K., WALTER, PETER,. 2008. *Molecular Biology of The Cell*.

ANCUTA, P., MOSES, A. & GABUZDA, D. 2004. Transendothelial migration of CD16+ monocytes in response to fractalkine under constitutive and inflammatory conditions. *Immunobiology,* 209**,** 11-20.

ANCUTA, P., RAO, R., MOSES, A., MEHLE, A., SHAW, S. K., LUSCINSKAS, F. W. & GABUZDA, D. 2003. Fractalkine preferentially mediates arrest and migration of CD16+ monocytes. *J Exp Med,* 197**,** 1701-7.

ANDERSON, K. L., SMITH, K. A., CONNERS, K., MCKERCHER, S. R., MAKI, R. A. & TORBETT, B. E. 1998. Myeloid development is selectively disrupted in PU.1 null mice. *Blood,* 91**,** 3702-10.

ANGER, T., EL-CHAFCHAK, J., HABIB, A., STUMPF, C., WEYAND, M., DANIEL, W. G., HOMBACH, V., HOEHER, M. & GARLICHS, C. D. 2008. Statins stimulate RGS-regulated ERK 1/2 activation in human calcified and stenotic aortic valves. *Exp Mol Pathol,* 85**,** 101-11.

ARAGAY, A. M., MELLADO, M., FRADE, J. M., MARTIN, A. M., JIMENEZ-SAINZ, M. C., MARTINEZ, A. C. & MAYOR, F., JR. 1998. Monocyte chemoattractant protein-1-induced CCR2B receptor desensitization mediated by the G protein-coupled receptor kinase 2. *Proc Natl Acad Sci U S A,* 95**,** 2985-90.

ARAI, H., TSOU, C. L. & CHARO, I. F. 1997. Chemotaxis in a lymphocyte cell line transfected with C-C chemokine receptor 2B: evidence that directed migration is mediated by betagamma dimers released by activation of Galphai-coupled receptors. *Proc Natl Acad Sci U S A,* 94**,** 14495-9.

AUFFRAY, C., FOGG, D., GARFA, M., ELAIN, G., JOIN-LAMBERT, O., KAYAL, S., SARNACKI, S., CUMANO, A., LAUVAU, G. & GEISSMANN, F. 2007. Monitoring of blood vessels and tissues by a population of monocytes with patrolling behavior. *Science,* 317**,** 666-70.

BELIAKOVA-BETHELL, N., MASSANELLA, M., WHITE, C., LADA, S. M., DU, P., VAIDA, F., BLANCO, J., SPINA, C. A. & WOELK, C. H. 2014. The effect of cell subset isolation method on gene expression in leukocytes. *Cytometry A,* 85**,** 94-104.

BENZING, T., BRANDES, R., SELLIN, L., SCHERMER, B., LECKER, S., WALZ, G. & KIM, E. 1999. Upregulation of RGS7 may contribute to tumor necrosis factor-induced changes in central nervous function. *Nat Med,* 5**,** 913-8.

BOELTE, K. C., GORDY, L. E., JOYCE, S., THOMPSON, M. A., YANG, L. & LIN, P. C. 2011. Rgs2 mediates pro-angiogenic function of myeloid derived suppressor cells in the tumor microenvironment via upregulation of MCP-1. *PLoS One,* 6**,** e18534.

BORRONI, E. M., MANTOVANI, A., LOCATI, M. & BONECCHI, R. 2010. Chemokine receptors intracellular trafficking. *Pharmacol Ther,* 127**,** 1-8.

BRIDGES, T. M. & LINDSLEY, C. W. 2008. G-protein-coupled receptors: from classical modes of modulation to allosteric mechanisms. *ACS Chem Biol,* 3**,** 530-41.

BYERS, M. A., CALLOWAY, P. A., SHANNON, L., CUNNINGHAM, H. D., SMITH, S., LI, F., FASSOLD, B. C. & VINES, C. M. 2008. Arrestin 3 mediates endocytosis of CCR7 following ligation of CCL19 but not CCL21. *J Immunol,* 181**,** 4723-32.

CARLIN, L. M., STAMATIADES, E. G., AUFFRAY, C., HANNA, R. N., GLOVER, L., VIZCAY-BARRENA, G., HEDRICK, C. C., COOK, H. T., DIEBOLD, S. & GEISSMANN, F. 2013. Nr4a1-dependent Ly6C(low) monocytes monitor endothelial cells and orchestrate their disposal. *Cell,* 153**,** 362-75.

CARMAN, C. V. & SPRINGER, T. A. 2004. A transmigratory cup in leukocyte diapedesis both through individual vascular endothelial cells and between them. *J Cell Biol,* 167**,** 377-88.

CARNEVALE, K. A. & CATHCART, M. K. 2003. Protein kinase C beta is required for human monocyte chemotaxis to MCP-1. *J Biol Chem,* 278**,** 25317-22.

CHAIGNE-DELALANDE, B. & LENARDO, M. J. 2014. Divalent cation signaling in immune cells. *Trends Immunol,* 35**,** 332-44.

COLLISON, J. L., CARLIN, L. M., EICHMANN, M., GEISSMANN, F. & PEAKMAN, M. 2015. Heterogeneity in the Locomotory Behavior of Human Monocyte Subsets over Human Vascular Endothelium In Vitro. *J Immunol,* 195**,** 1162-70.

COMBADIERE, C., POTTEAUX, S., RODERO, M., SIMON, T., PEZARD, A., ESPOSITO, B., MERVAL, R., PROUDFOOT, A., TEDGUI, A. & MALLAT, Z. 2008. Combined inhibition of CCL2, CX3CR1, and CCR5 abrogates Ly6C(hi) and Ly6C(lo) monocytosis and almost abolishes atherosclerosis in hypercholesterolemic mice. *Circulation,* 117**,** 1649-57.

COULAIS, D., PANTERNE, C., FONTENEAU, J. F. & GREGOIRE, M. 2012. Purification of circulating plasmacytoid dendritic cells using counterflow centrifugal elutriation and immunomagnetic beads. *Cytotherapy,* 14**,** 887-96.

CROS, J., CAGNARD, N., WOOLLARD, K., PATEY, N., ZHANG, S. Y., SENECHAL, B., PUEL, A., BISWAS, S. K., MOSHOUS, D., PICARD, C., JAIS, J. P., D'CRUZ, D., CASANOVA, J. L., TROUILLET, C. & GEISSMANN, F. 2010. Human CD14dim monocytes patrol and sense nucleic acids and viruses via TLR7 and TLR8 receptors. *Immunity,* 33**,** 375-86.

CURNOCK, A. P., LOGAN, M. K. & WARD, S. G. 2002. Chemokine signalling: pivoting around multiple phosphoinositide 3-kinases. *Immunology,* 105**,** 125-36.

DE VRIES, L., ZHENG, B., FISCHER, T., ELENKO, E. & FARQUHAR, M. G. 2000. The regulator of G protein signaling family. *Annu Rev Pharmacol Toxicol,* 40**,** 235-71.

DEBIEN, E., MAYOL, K., BIAJOUX, V., DAUSSY, C., DE AGUERO, M. G., TAILLARDET, M., DAGANY, N., BRINZA, L., HENRY, T., DUBOIS, B., KAISERLIAN, D., MARVEL, J., BALABANIAN, K. & WALZER, T. 2013. S1PR5 is pivotal for the homeostasis of patrolling monocytes. *Eur J Immunol,* 43**,** 1667-75.

DEN HARTIGH, L. J., CONNOLLY-ROHRBACH, J. E., FORE, S., HUSER, T. R. & RUTLEDGE, J. C. 2010. Fatty acids from very low-density lipoprotein lipolysis products induce lipid droplet accumulation in human monocytes. *J Immunol,* 184**,** 3927-36.

DENECKE, B., MEYERDIERKS, A. & BOTTGER, E. C. 1999. RGS1 is expressed in monocytes and acts as a GTPase-activating protein for G-protein-coupled chemoattractant receptors. *J Biol Chem,* 274**,** 26860-8.

DESMEULES, P., DUFOUR, M. & FERNANDES, M. J. 2009. A rapid flow cytometry assay for the assessment of calcium mobilization in human neutrophils in a small volume of lysed whole-blood. *J Immunol Methods,* 340**,** 154-7.

DOHLMAN, H. G., APANIESK, D., CHEN, Y., SONG, J. & NUSSKERN, D. 1995. Inhibition of G-protein signaling by dominant gain-of-function mutations in Sst2p, a pheromone desensitization factor in Saccharomyces cerevisiae. *Mol Cell Biol,* 15**,** 3635-43.

DOULATOV, S., NOTTA, F., LAURENTI, E. & DICK, J. E. 2012. Hematopoiesis: a human perspective. *Cell Stem Cell,* 10**,** 120-36.

DVORAK, A. M. & FENG, D. 2001. The vesiculo-vacuolar organelle (VVO). A new endothelial cell permeability organelle. *J Histochem Cytochem,* 49**,** 419-32.

FAN, J. & MALIK, A. B. 2003. Toll-like receptor-4 (TLR4) signaling augments chemokine-induced neutrophil migration by modulating cell surface expression of chemokine receptors. *Nat Med,* 9**,** 315-21.

FERGUSON, S. S. 2001. Evolving concepts in G protein-coupled receptor endocytosis: the role in receptor desensitization and signaling. *Pharmacol Rev,* 53**,** 1-24.

FIGDOR, C. G., BONT, W. S., TOUW, I., DE ROOS, J., ROOSNEK, E. E. & DE VRIES, J. E. 1982. Isolation of functionally different human monocytes by counterflow centrifugation elutriation. *Blood,* 60**,** 46-53.

FONG, A. M., PREMONT, R. T., RICHARDSON, R. M., YU, Y. R., LEFKOWITZ, R. J. & PATEL, D. D. 2002. Defective lymphocyte chemotaxis in beta-arrestin2- and GRK6-deficient mice. *Proc Natl Acad Sci U S A,* 99**,** 7478-83.

FOX, J. M., LETELLIER, E., OLIPHANT, C. J. & SIGNORET, N. 2011. TLR2-dependent pathway of heterologous down-modulation for the CC chemokine receptors 1, 2, and 5 in human blood monocytes. *Blood,* 117**,** 1851-60.

GEISSMANN, F., JUNG, S. & LITTMAN, D. R. 2003. Blood monocytes consist of two principal subsets with distinct migratory properties. *Immunity,* 19**,** 71-82.

GIORELLI, M., LIVREA, P. & TROJANO, M. 2004. Post-receptorial mechanisms underlie functional disregulation of beta2-adrenergic receptors in

lymphocytes from Multiple Sclerosis patients. *J Neuroimmunol,* 155**,** 143-9.
GORDON, S. & TAYLOR, P. R. 2005. Monocyte and macrophage heterogeneity. *Nat Rev Immunol,* 5**,** 953-64.
GOWER, R. M., WU, H., FOSTER, G. A., DEVARAJ, S., JIALAL, I., BALLANTYNE, C. M., KNOWLTON, A. A. & SIMON, S. I. 2011. CD11c/CD18 expression is upregulated on blood monocytes during hypertriglyceridemia and enhances adhesion to vascular cell adhesion molecule-1. *Arterioscler Thromb Vasc Biol,* 31**,** 160-6.
GRIP, O., BREDBERG, A., LINDGREN, S. & HENRIKSSON, G. 2007. Increased subpopulations of CD16(+) and CD56(+) blood monocytes in patients with active Crohn's disease. *Inflamm Bowel Dis,* 13**,** 566-72.
GUNZER, M., RIEMANN, H., BASOGLU, Y., HILLMER, A., WEISHAUPT, C., BALKOW, S., BENNINGHOFF, B., ERNST, B., STEINERT, M., SCHOLZEN, T., SUNDERKOTTER, C. & GRABBE, S. 2005. Systemic administration of a TLR7 ligand leads to transient immune incompetence due to peripheral-blood leukocyte depletion. *Blood,* 106**,** 2424-32.
HAN, J., WANG, B., HAN, N., ZHAO, Y., SONG, C., FENG, X., MAO, Y., ZHANG, F., ZHAO, H. & ZENG, H. 2009. CD14(high)CD16(+) rather than CD14(low)CD16(+) monocytes correlate with disease progression in chronic HIV-infected patients. *J Acquir Immune Defic Syndr,* 52**,** 553-9.
HAN, K. H., CHANG, M. K., BOULLIER, A., GREEN, S. R., LI, A., GLASS, C. K. & QUEHENBERGER, O. 2000. Oxidized LDL reduces monocyte CCR2 expression through pathways involving peroxisome proliferator-activated receptor gamma. *J Clin Invest,* 106**,** 793-802.
HANNA, R. N., CARLIN, L. M., HUBBELING, H. G., NACKIEWICZ, D., GREEN, A. M., PUNT, J. A., GEISSMANN, F. & HEDRICK, C. C. 2011. The transcription factor NR4A1 (Nur77) controls bone marrow differentiation and the survival of Ly6C- monocytes. *Nat Immunol,* 12**,** 778-85.
HANSSON, G. K. & LIBBY, P. 2006. The immune response in atherosclerosis: a double-edged sword. *Nat Rev Immunol,* 6**,** 508-19.
HARKINS, A. B., KUREBAYASHI, N. & BAYLOR, S. M. 1993. Resting myoplasmic free calcium in frog skeletal muscle fibers estimated with fluo-3. *Biophys J,* 65**,** 865-81.
HASHIMOTO, D., CHOW, A., NOIZAT, C., TEO, P., BEASLEY, M. B., LEBOEUF, M., BECKER, C. D., SEE, P., PRICE, J., LUCAS, D., GRETER, M., MORTHA, A., BOYER, S. W., FORSBERG, E. C., TANAKA, M., VAN ROOIJEN, N., GARCIA-SASTRE, A., STANLEY, E. R., GINHOUX, F., FRENETTE, P. S. & MERAD, M. 2013. Tissue-resident macrophages self-maintain locally throughout adult life with minimal contribution from circulating monocytes. *Immunity,* 38**,** 792-804.
HE, Q., DENT, E. W. & MEIRI, K. F. 1997. Modulation of actin filament behavior by GAP-43 (neuromodulin) is dependent on the phosphorylation status of serine 41, the protein kinase C site. *J Neurosci,* 17**,** 3515-24.
HEINE, G. H., ULRICH, C., SEIBERT, E., SEILER, S., MARELL, J., REICHART, B., KRAUSE, M., SCHLITT, A., KOHLER, H. & GIRNDT, M. 2008.

CD14(++)CD16+ monocytes but not total monocyte numbers predict cardiovascular events in dialysis patients. *Kidney Int,* 73**,** 622-9.
HETTINGER, J., RICHARDS, D. M., HANSSON, J., BARRA, M. M., JOSCHKO, A. C., KRIJGSVELD, J. & FEUERER, M. 2013. Origin of monocytes and macrophages in a committed progenitor. *Nat Immunol,* 14**,** 821-30.
HIJDRA, D., VORSELAARS, A. D., GRUTTERS, J. C., CLAESSEN, A. M. & RIJKERS, G. T. 2013. Phenotypic characterization of human intermediate monocytes. *Front Immunol,* 4**,** 339.
HOEFFEL, G., WANG, Y., GRETER, M., SEE, P., TEO, P., MALLERET, B., LEBOEUF, M., LOW, D., OLLER, G., ALMEIDA, F., CHOY, S. H., GRISOTTO, M., RENIA, L., CONWAY, S. J., STANLEY, E. R., CHAN, J. K., NG, L. G., SAMOKHVALOV, I. M., MERAD, M. & GINHOUX, F. 2012. Adult Langerhans cells derive predominantly from embryonic fetal liver monocytes with a minor contribution of yolk sac-derived macrophages. *J Exp Med,* 209**,** 1167-81.
HOLLINGER, S. & HEPLER, J. R. 2002. Cellular regulation of RGS proteins: modulators and integrators of G protein signaling. *Pharmacol Rev,* 54**,** 527-59.
HU, Y., HU, X., BOUMSELL, L. & IVASHKIV, L. B. 2008. IFN-gamma and STAT1 arrest monocyte migration and modulate RAC/CDC42 pathways. *J Immunol,* 180**,** 8057-65.
IMHOF, B. A. & AURRAND-LIONS, M. 2004. Adhesion mechanisms regulating the migration of monocytes. *Nat Rev Immunol,* 4**,** 432-44.
INGERSOLL, M. A., PLATT, A. M., POTTEAUX, S. & RANDOLPH, G. J. 2011. Monocyte trafficking in acute and chronic inflammation. *Trends Immunol,* 32**,** 470-7.
INGERSOLL, M. A., SPANBROEK, R., LOTTAZ, C., GAUTIER, E. L., FRANKENBERGER, M., HOFFMANN, R., LANG, R., HANIFFA, M., COLLIN, M., TACKE, F., HABENICHT, A. J., ZIEGLER-HEITBROCK, L. & RANDOLPH, G. J. 2010. Comparison of gene expression profiles between human and mouse monocyte subsets. *Blood,* 115**,** e10-9.
JAKUBZICK, C., GAUTIER, E. L., GIBBINGS, S. L., SOJKA, D. K., SCHLITZER, A., JOHNSON, T. E., IVANOV, S., DUAN, Q., BALA, S., CONDON, T., VAN ROOIJEN, N., GRAINGER, J. R., BELKAID, Y., MA'AYAN, A., RICHES, D. W., YOKOYAMA, W. M., GINHOUX, F., HENSON, P. M. & RANDOLPH, G. J. 2013. Minimal differentiation of classical monocytes as they survey steady-state tissues and transport antigen to lymph nodes. *Immunity,* 39**,** 599-610.
KELLY, A., FAHEY, R., FLETCHER, J. M., KEOGH, C., CARROLL, A. G., SIDDACHARI, R., GEOGHEGAN, J., HEGARTY, J. E., RYAN, E. J. & O'FARRELLY, C. 2014. CD141(+) myeloid dendritic cells are enriched in healthy human liver. *J Hepatol,* 60**,** 135-42.
KELLY, E., BAILEY, C. P. & HENDERSON, G. 2008. Agonist-selective mechanisms of GPCR desensitization. *Br J Pharmacol,* 153 Suppl 1**,** S379-88.
KOCH, S., KUCHARZIK, T., HEIDEMANN, J., NUSRAT, A. & LUEGERING, A. 2010. Investigating the role of proinflammatory CD16+ monocytes in the pathogenesis of inflammatory bowel disease. *Clin Exp Immunol,* 161**,** 332-41.

KRANKEL, N., KUSCHNERUS, K., MADEDDU, P., LUSCHER, T. F. & LANDMESSER, U. 2011. A novel flow cytometry-based assay to study leukocyte-endothelial cell interactions in vitro. *Cytometry A,* 79**,** 256-62.

LA SALA, A., CORINTI, S., FEDERICI, M., SARAGOVI, H. U. & GIROLOMONI, G. 2000. Ligand activation of nerve growth factor receptor TrkA protects monocytes from apoptosis. *J Leukoc Biol,* 68**,** 104-10.

LANDSMAN, L., BAR-ON, L., ZERNECKE, A., KIM, K. W., KRAUTHGAMER, R., SHAGDARSUREN, E., LIRA, S. A., WEISSMAN, I. L., WEBER, C. & JUNG, S. 2009. CX3CR1 is required for monocyte homeostasis and atherogenesis by promoting cell survival. *Blood,* 113**,** 963-72.

LARSSON, C. 2006. Protein kinase C and the regulation of the actin cytoskeleton. *Cell Signal,* 18**,** 276-84.

LATTIN, J., ZIDAR, D. A., SCHRODER, K., KELLIE, S., HUME, D. A. & SWEET, M. J. 2007. G-protein-coupled receptor expression, function, and signaling in macrophages. *J Leukoc Biol,* 82**,** 16-32.

LAUDANNA, C., KIM, J. Y., CONSTANTIN, G. & BUTCHER, E. 2002. Rapid leukocyte integrin activation by chemokines. *Immunol Rev,* 186**,** 37-46.

LEUSCHNER, F., RAUCH, P. J., UENO, T., GORBATOV, R., MARINELLI, B., LEE, W. W., DUTTA, P., WEI, Y., ROBBINS, C., IWAMOTO, Y., SENA, B., CHUDNOVSKIY, A., PANIZZI, P., KELIHER, E., HIGGINS, J. M., LIBBY, P., MOSKOWITZ, M. A., PITTET, M. J., SWIRSKI, F. K., WEISSLEDER, R. & NAHRENDORF, M. 2012. Rapid monocyte kinetics in acute myocardial infarction are sustained by extramedullary monocytopoiesis. *J Exp Med,* 209**,** 123-37.

LEY, K., LAUDANNA, C., CYBULSKY, M. I. & NOURSHARGH, S. 2007. Getting to the site of inflammation: the leukocyte adhesion cascade updated. *Nat Rev Immunol,* 7**,** 678-89.

LI, H., SUN, X., LESAGE, G., ZHANG, Y., LIANG, Z., CHEN, J., HANLEY, G., HE, L., SUN, S. & YIN, D. 2010. beta-arrestin 2 regulates Toll-like receptor 4-mediated apoptotic signalling through glycogen synthase kinase-3beta. *Immunology,* 130**,** 556-63.

LIASKOU, E., ZIMMERMANN, H. W., LI, K. K., OO, Y. H., SURESH, S., STAMATAKI, Z., QURESHI, O., LALOR, P. F., SHAW, J., SYN, W. K., CURBISHLEY, S. M. & ADAMS, D. H. 2013. Monocyte subsets in human liver disease show distinct phenotypic and functional characteristics. *Hepatology,* 57**,** 385-98.

LIPPERT, E., YOWE, D. L., GONZALO, J. A., JUSTICE, J. P., WEBSTER, J. M., FEDYK, E. R., HODGE, M., MILLER, C., GUTIERREZ-RAMOS, J. C., BORREGO, F., KEANE-MYERS, A. & DRUEY, K. M. 2003. Role of regulator of G protein signaling 16 in inflammation-induced T lymphocyte migration and activation. *J Immunol,* 171**,** 1542-55.

LIU, Z., JIANG, Y., LI, Y., WANG, J., FAN, L., SCOTT, M. J., XIAO, G., LI, S., BILLIAR, T. R., WILSON, M. A. & FAN, J. 2013. TLR4 Signaling augments monocyte chemotaxis by regulating G protein-coupled receptor kinase 2 translocation. *J Immunol,* 191**,** 857-64.

LOMBARDI, M. S., KAVELAARS, A., SCHEDLOWSKI, M., BIJLSMA, J. W., OKIHARA, K. L., VAN DE POL, M., OCHSMANN, S., PAWLAK, C., SCHMIDT, R. E. & HEIJNEN, C. J. 1999. Decreased expression and

activity of G-protein-coupled receptor kinases in peripheral blood mononuclear cells of patients with rheumatoid arthritis. *FASEB J,* 13**,** 715-25.

LUTTRELL, L. M. & LEFKOWITZ, R. J. 2002. The role of beta-arrestins in the termination and transduction of G-protein-coupled receptor signals. *J Cell Sci,* 115**,** 455-65.

MACEY, M. G. 2007. Flow Cytometry Prinicpals and Applications.

MARSHALL, B. T., LONG, M., PIPER, J. W., YAGO, T., MCEVER, R. P. & ZHU, C. 2003. Direct observation of catch bonds involving cell-adhesion molecules. *Nature,* 423**,** 190-3.

MATHENY, H. E., DEEM, T. L. & COOK-MILLS, J. M. 2000. Lymphocyte migration through monolayers of endothelial cell lines involves VCAM-1 signaling via endothelial cell NADPH oxidase. *J Immunol,* 164**,** 6550-9.

MITTMANN, C., CHUNG, C. H., HOPPNER, G., MICHALEK, C., NOSE, M., SCHULER, C., SCHUH, A., ESCHENHAGEN, T., WEIL, J., PIESKE, B., HIRT, S. & WIELAND, T. 2002. Expression of ten RGS proteins in human myocardium: functional characterization of an upregulation of RGS4 in heart failure. *Cardiovasc Res,* 55**,** 778-86.

MOORE, C. A., MILANO, S. K. & BENOVIC, J. L. 2007. Regulation of receptor trafficking by GRKs and arrestins. *Annu Rev Physiol,* 69**,** 451-82.

MORATZ, C., HAYMAN, J. R., GU, H. & KEHRL, J. H. 2004. Abnormal B-cell responses to chemokines, disturbed plasma cell localization, and distorted immune tissue architecture in Rgs1-/- mice. *Mol Cell Biol,* 24**,** 5767-75.

MOSSER, D. M. & EDWARDS, J. P. 2008. Exploring the full spectrum of macrophage activation. *Nat Rev Immunol,* 8**,** 958-69.

MULLER, W. A. 2003. Leukocyte-endothelial-cell interactions in leukocyte transmigration and the inflammatory response. *Trends Immunol,* 24**,** 327-34.

OPPERMANN, M., MACK, M., PROUDFOOT, A. E. & OLBRICH, H. 1999. Differential effects of CC chemokines on CC chemokine receptor 5 (CCR5) phosphorylation and identification of phosphorylation sites on the CCR5 carboxyl terminus. *J Biol Chem,* 274**,** 8875-85.

PARK, I. K., KLUG, C. A., LI, K., JERABEK, L., LI, L., NANAMORI, M., NEUBIG, R. R., HOOD, L., WEISSMAN, I. L. & CLARKE, M. F. 2001. Molecular cloning and characterization of a novel regulator of G-protein signaling from mouse hematopoietic stem cells. *J Biol Chem,* 276**,** 915-23.

PATEL, J., MCNEILL, E., DOUGLAS, G., HALE, A. B., DE BONO, J., LEE, R., IQBAL, A. J., REGAN-KOMITO, D., STYLIANOU, E., GREAVES, D. R. & CHANNON, K. M. 2015. RGS1 regulates myeloid cell accumulation in atherosclerosis and aortic aneurysm rupture through altered chemokine signalling. *Nat Commun,* 6**,** 6614.

PICOZZA, M., BATTISTINI, L. & BORSELLINO, G. 2013. Mononuclear phagocytes and marker modulation: when CD16 disappears, CD38 takes the stage. *Blood,* 122**,** 456-7.

PITCHER, J. A., FREEDMAN, N. J. & LEFKOWITZ, R. J. 1998. G protein-coupled receptor kinases. *Annu Rev Biochem,* 67**,** 653-92.

POEHLMANN, H., SCHEFOLD, J. C., ZUCKERMANN-BECKER, H., VOLK, H. D. & MEISEL, C. 2009. Phenotype changes and impaired function of dendritic cell subsets in patients with sepsis: a prospective observational analysis. *Crit Care,* 13**,** R119.

PORTER, K. J., GONIPETA, B., PARVATANENI, S., APPLEDORN, D. M., PATIAL, S., SHARMA, D., GANGUR, V., AMALFITANO, A. & PARAMESWARAN, N. 2010. Regulation of lipopolysaccharide-induced inflammatory response and endotoxemia by beta-arrestins. *J Cell Physiol,* 225**,** 406-16.

PREMONT, R. T. & GAINETDINOV, R. R. 2007. Physiological roles of G protein-coupled receptor kinases and arrestins. *Annu Rev Physiol,* 69**,** 511-34.

REITER, E. & LEFKOWITZ, R. J. 2006. GRKs and beta-arrestins: roles in receptor silencing, trafficking and signaling. *Trends Endocrinol Metab,* 17**,** 159-65.

RITTER, S. L. & HALL, R. A. 2009. Fine-tuning of GPCR activity by receptor-interacting proteins. *Nat Rev Mol Cell Biol,* 10**,** 819-30.

ROGACEV, K. S., CREMERS, B., ZAWADA, A. M., SEILER, S., BINDER, N., EGE, P., GROSSE-DUNKER, G., HEISEL, I., HORNOF, F., JEKEN, J., REBLING, N. M., ULRICH, C., SCHELLER, B., BOHM, M., FLISER, D. & HEINE, G. H. 2012. CD14++CD16+ monocytes independently predict cardiovascular events: a cohort study of 951 patients referred for elective coronary angiography. *J Am Coll Cardiol,* 60**,** 1512-20.

ROGACEV, K. S., ZAWADA, A. M., EMRICH, I., SEILER, S., BOHM, M., FLISER, D., WOOLLARD, K. J. & HEINE, G. H. 2014. Lower Apo A-I and lower HDL-C levels are associated with higher intermediate CD14++CD16+ monocyte counts that predict cardiovascular events in chronic kidney disease. *Arterioscler Thromb Vasc Biol,* 34**,** 2120-7.

ROSS, E. M. & WILKIE, T. M. 2000. GTPase-activating proteins for heterotrimeric G proteins: regulators of G protein signaling (RGS) and RGS-like proteins. *Annu Rev Biochem,* 69**,** 795-827.

SCHENKEL, A. R., MAMDOUH, Z. & MULLER, W. A. 2004. Locomotion of monocytes on endothelium is a critical step during extravasation. *Nat Immunol,* 5**,** 393-400.

SCHMIDL, C., RENNER, K., PETER, K., EDER, R., LASSMANN, T., BALWIERZ, P. J., ITOH, M., NAGAO-SATO, S., KAWAJI, H., CARNINCI, P., SUZUKI, H., HAYASHIZAKI, Y., ANDREESEN, R., HUME, D. A., HOFFMANN, P., FORREST, A. R., KREUTZ, M. P., EDINGER, M., REHLI, M. & CONSORTIUM, F. 2014. Transcription and enhancer profiling in human monocyte subsets. *Blood,* 123**,** e90-9.

SEMPLICINI, A., LENZINI, L., SARTORI, M., PAPPARELLA, I., CALO, L. A., PAGNIN, E., STRAPAZZON, G., BENNA, C., COSTA, R., AVOGARO, A., CEOLOTTO, G. & PESSINA, A. C. 2006. Reduced expression of regulator of G-protein signaling 2 (RGS2) in hypertensive patients increases calcium mobilization and ERK1/2 phosphorylation induced by angiotensin II. *J Hypertens,* 24**,** 1115-24.

SERBINA, N. V. & PAMER, E. G. 2006. Monocyte emigration from bone marrow during bacterial infection requires signals mediated by chemokine receptor CCR2. *Nat Immunol,* 7**,** 311-7.

SHI, C., JIA, T., MENDEZ-FERRER, S., HOHL, T. M., SERBINA, N. V., LIPUMA, L., LEINER, I., LI, M. O., FRENETTE, P. S. & PAMER, E. G. 2011. Bone marrow mesenchymal stem and progenitor cells induce monocyte emigration in response to circulating toll-like receptor ligands. *Immunity,* 34**,** 590-601.

SHI, G. X., HARRISON, K., HAN, S. B., MORATZ, C. & KEHRL, J. H. 2004. Toll-like receptor signaling alters the expression of regulator of G protein signaling proteins in dendritic cells: implications for G protein-coupled receptor signaling. *J Immunol,* 172**,** 5175-84.

SIVAPALARATNAM, S., BASART, H., WATKINS, N. A., MAIWALD, S., RENDON, A., KRISHNAN, U., SONDERMEIJER, B. M., CREEMERS, E. E., PINTO-SIETSMA, S. J., HOVINGH, K., OUWEHAND, W. H., KASTELEIN, J. J., GOODALL, A. H. & TRIP, M. D. 2012. Monocyte gene expression signature of patients with early onset coronary artery disease. *PLoS One,* 7**,** e32166.

SODERLING, T. R. 1999. The Ca-calmodulin-dependent protein kinase cascade. *Trends Biochem Sci,* 24**,** 232-6.

SORKIN, A. & VON ZASTROW, M. 2002. Signal transduction and endocytosis: close encounters of many kinds. *Nat Rev Mol Cell Biol,* 3**,** 600-14.

SU, Y., RAGHUWANSHI, S. K., YU, Y., NANNEY, L. B., RICHARDSON, R. M. & RICHMOND, A. 2005. Altered CXCR2 signaling in beta-arrestin-2-deficient mouse models. *J Immunol,* 175**,** 5396-402.

SUMAGIN, R., PRIZANT, H., LOMAKINA, E., WAUGH, R. E. & SARELIUS, I. H. 2010. LFA-1 and Mac-1 define characteristically different intralumenal crawling and emigration patterns for monocytes and neutrophils in situ. *J Immunol,* 185**,** 7057-66.

SUNDERKOTTER, C., NIKOLIC, T., DILLON, M. J., VAN ROOIJEN, N., STEHLING, M., DREVETS, D. A. & LEENEN, P. J. 2004. Subpopulations of mouse blood monocytes differ in maturation stage and inflammatory response. *J Immunol,* 172**,** 4410-7.

SUURVALI, J., PAHTMA, M., SAAR, R., PAALME, V., NUTT, A., TIIVEL, T., SAAREMAE, M., FITTING, C., CAVAILLON, J. M. & RUUTEL BOUDINOT, S. 2015. RGS16 restricts the pro-inflammatory response of monocytes. *Scand J Immunol,* 81**,** 23-30.

TACKE, F., ALVAREZ, D., KAPLAN, T. J., JAKUBZICK, C., SPANBROEK, R., LLODRA, J., GARIN, A., LIU, J., MACK, M., VAN ROOIJEN, N., LIRA, S. A., HABENICHT, A. J. & RANDOLPH, G. J. 2007. Monocyte subsets differentially employ CCR2, CCR5, and CX3CR1 to accumulate within atherosclerotic plaques. *J Clin Invest,* 117**,** 185-94.

TANAKA, S., SAITO, Y., KUNISAWA, J., KURASHIMA, Y., WAKE, T., SUZUKI, N., SHULTZ, L. D., KIYONO, H. & ISHIKAWA, F. 2012. Development of mature and functional human myeloid subsets in hematopoietic stem cell-engrafted NOD/SCID/IL2rgammaKO mice. *J Immunol,* 188**,** 6145-55.

TARDIVEL, A., TINEL, A., LENS, S., STEINER, Q. G., SAUBERLI, E., WILSON, A., MACKAY, F., ROLINK, A. G., BEERMANN, F., TSCHOPP, J. & SCHNEIDER, P. 2004. The anti-apoptotic factor Bcl-2 can functionally substitute for

the B cell survival but not for the marginal zone B cell differentiation activity of BAFF. *Eur J Immunol,* 34**,** 509-18.

THATHIAH, A., HORRE, K., SNELLINX, A., VANDEWYER, E., HUANG, Y., CIESIELSKA, M., DE KLOE, G., MUNCK, S. & DE STROOPER, B. 2013. beta-arrestin 2 regulates Abeta generation and gamma-secretase activity in Alzheimer's disease. *Nat Med,* 19**,** 43-9.

THIESEN, S., JANCIAUSKIENE, S., URONEN-HANSSON, H., AGACE, W., HOGERKORP, C. M., SPEE, P., HAKANSSON, K. & GRIP, O. 2014. CD14(hi)HLA-DR(dim) macrophages, with a resemblance to classical blood monocytes, dominate inflamed mucosa in Crohn's disease. *J Leukoc Biol,* 95**,** 531-41.

TRAN, T., PAZ, P., VELICHKO, S., CIFRESE, J., BELUR, P., YAMAGUCHI, K. D., KU, K., MIRSHAHPANAH, P., REDER, A. T. & CROZE, E. 2010. Interferonbeta-1b Induces the Expression of RGS1 a Negative Regulator of G-Protein Signaling. *Int J Cell Biol,* 2010**,** 529376.

TSOU, C. L., PETERS, W., SI, Y., SLAYMAKER, S., ASLANIAN, A. M., WEISBERG, S. P., MACK, M. & CHARO, I. F. 2007. Critical roles for CCR2 and MCP-3 in monocyte mobilization from bone marrow and recruitment to inflammatory sites. *J Clin Invest,* 117**,** 902-9.

ULRICH, C., HEINE, G. H., SEIBERT, E., FLISER, D. & GIRNDT, M. 2010. Circulating monocyte subpopulations with high expression of angiotensin-converting enzyme predict mortality in patients with end-stage renal disease. *Nephrol Dial Transplant,* 25**,** 2265-72.

VAN FURTH, R. & COHN, Z. A. 1968. The origin and kinetics of mononuclear phagocytes. *J Exp Med,* 128**,** 415-35.

VERPLOEGEN, S., VAN LEEUWEN, C. M., VAN DEUTEKOM, H. W., LAMMERS, J. W., KOENDERMAN, L. & COFFER, P. J. 2002. Role of Ca2+/calmodulin regulated signaling pathways in chemoattractant induced neutrophil effector functions. Comparison with the role of phosphotidylinositol-3 kinase. *Eur J Biochem,* 269**,** 4625-34.

VICENTE-MANZANARES, M., CHOI, C. K. & HORWITZ, A. R. 2009. Integrins in cell migration--the actin connection. *J Cell Sci,* 122**,** 199-206.

VIDOVIC, D., GRADDIS, T. J., STEPAN, L. P., ZALLER, D. M. & LAUS, R. 2003. Specific stimulation of MHC-transgenic mouse T-cell hybridomas with xenogeneic APC. *Hum Immunol,* 64**,** 238-44.

VIG, M. & KINET, J. P. 2009. Calcium signaling in immune cells. *Nat Immunol,* 10**,** 21-7.

VROON, A., HEIJNEN, C. J., RAATGEVER, R., TOUW, I. P., PLOEMACHER, R. E., PREMONT, R. T. & KAVELAARS, A. 2004. GRK6 deficiency is associated with enhanced CXCR4-mediated neutrophil chemotaxis in vitro and impaired responsiveness to G-CSF in vivo. *J Leukoc Biol,* 75**,** 698-704.

VROON, A., KAVELAARS, A., LIMMROTH, V., LOMBARDI, M. S., GOEBEL, M. U., VAN DAM, A. M., CARON, M. G., SCHEDLOWSKI, M. & HEIJNEN, C. J. 2005. G protein-coupled receptor kinase 2 in multiple sclerosis and experimental autoimmune encephalomyelitis. *J Immunol,* 174**,** 4400-6.

WALKER, J. K., FONG, A. M., LAWSON, B. L., SAVOV, J. D., PATEL, D. D., SCHWARTZ, D. A. & LEFKOWITZ, R. J. 2003. Beta-arrestin-2 regulates the development of allergic asthma. *J Clin Invest,* 112**,** 566-74.

WANG, X., HUANG, G., LUO, X., PENNINGER, J. M. & MUALLEM, S. 2004. Role of regulator of G protein signaling 2 (RGS2) in Ca(2+) oscillations and adaptation of Ca(2+) signaling to reduce excitability of RGS2-/- cells. *J Biol Chem,* 279**,** 41642-9.

WATSON, N., LINDER, M. E., DRUEY, K. M., KEHRL, J. H. & BLUMER, K. J. 1996. RGS family members: GTPase-activating proteins for heterotrimeric G-protein alpha-subunits. *Nature,* 383**,** 172-5.

WEBER, C., ZERNECKE, A. & LIBBY, P. 2008. The multifaceted contributions of leukocyte subsets to atherosclerosis: lessons from mouse models. *Nat Rev Immunol,* 8**,** 802-15.

WEI, C., WANG, X., CHEN, M., OUYANG, K., SONG, L. S. & CHENG, H. 2009. Calcium flickers steer cell migration. *Nature,* 457**,** 901-5.

WEINER, J. L., GUTTIEREZ-STEIL, C. & BLUMER, K. J. 1993. Disruption of receptor-G protein coupling in yeast promotes the function of an SST2-dependent adaptation pathway. *J Biol Chem,* 268**,** 8070-7.

WILLARD, M. D., WILLARD, F. S., LI, X., CAPPELL, S. D., SNIDER, W. D. & SIDEROVSKI, D. P. 2007. Selective role for RGS12 as a Ras/Raf/MEK scaffold in nerve growth factor-mediated differentiation. *EMBO J,* 26**,** 2029-40.

WONG, K. L., TAI, J. J., WONG, W. C., HAN, H., SEM, X., YEAP, W. H., KOURILSKY, P. & WONG, S. C. 2011. Gene expression profiling reveals the defining features of the classical, intermediate, and nonclassical human monocyte subsets. *Blood,* 118**,** e16-31.

WU, J. H., ZHANG, L., FANAROFF, A. C., CAI, X., SHARMA, K. C., BRIAN, L., EXUM, S. T., SHENOY, S. K., PEPPEL, K. & FREEDMAN, N. J. 2012. G protein-coupled receptor kinase-5 attenuates atherosclerosis by regulating receptor tyrosine kinases and 7-transmembrane receptors. *Arterioscler Thromb Vasc Biol,* 32**,** 308-16.

WYNN, T. A., CHAWLA, A. & POLLARD, J. W. 2013. Macrophage biology in development, homeostasis and disease. *Nature,* 496**,** 445-55.

YONA, S., KIM, K. W., WOLF, Y., MILDNER, A., VAROL, D., BREKER, M., STRAUSS-AYALI, D., VIUKOV, S., GUILLIAMS, M., MISHARIN, A., HUME, D. A., PERLMAN, H., MALISSEN, B., ZELZER, E. & JUNG, S. 2013. Fate mapping reveals origins and dynamics of monocytes and tissue macrophages under homeostasis. *Immunity,* 38**,** 79-91.

YUAN, X., CAO, J., LIU, T., LI, Y. P., SCANNAPIECO, F., HE, X., OURSLER, M. J., ZHANG, X., VACHER, J., LI, C., OLSON, D. & YANG, S. 2015. Regulators of G protein signaling 12 promotes osteoclastogenesis in bone remodeling and pathological bone loss. *Cell Death Differ*.

ZAWADA, A. M., ROGACEV, K. S., ROTTER, B., WINTER, P., MARELL, R. R., FLISER, D. & HEINE, G. H. 2011. SuperSAGE evidence for CD14++CD16+ monocytes as a third monocyte subset. *Blood,* 118**,** e50-61.

ZHANG, J. Y., ZOU, Z. S., HUANG, A., ZHANG, Z., FU, J. L., XU, X. S., CHEN, L. M., LI, B. S. & WANG, F. S. 2011. Hyper-activated pro-inflammatory CD16 monocytes correlate with the severity of liver injury and fibrosis in patients with chronic hepatitis B. *PLoS One,* 6**,** e17484.

ZHOU, J., FENG, G., BEESON, J., HOGARTH, P. M., ROGERSON, S. J., YAN, Y. & JAWOROWSKI, A. 2015. CD14(hi)CD16+ monocytes phagocytose

antibody-opsonised Plasmodium falciparum infected erythrocytes more efficiently than other monocyte subsets, and require CD16 and complement to do so. *BMC Med,* 13**,** 154.

ZIEGLER-HEITBROCK, L. 2014. Monocyte subsets in man and other species. *Cell Immunol,* 289**,** 135-9.

ZIEGLER-HEITBROCK, L., ANCUTA, P., CROWE, S., DALOD, M., GRAU, V., HART, D. N., LEENEN, P. J., LIU, Y. J., MACPHERSON, G., RANDOLPH, G. J., SCHERBERICH, J., SCHMITZ, J., SHORTMAN, K., SOZZANI, S., STROBL, H., ZEMBALA, M., AUSTYN, J. M. & LUTZ, M. B. 2010. Nomenclature of monocytes and dendritic cells in blood. *Blood,* 116**,** e74-80.

ZIGMOND, E. & JUNG, S. 2013. Intestinal macrophages: well educated exceptions from the rule. *Trends Immunol,* 34**,** 162-8.

ZIMMERMANN, H. W., SEIDLER, S., NATTERMANN, J., GASSLER, N., HELLERBRAND, C., ZERNECKE, A., TISCHENDORF, J. J., LUEDDE, T., WEISKIRCHEN, R., TRAUTWEIN, C. & TACKE, F. 2010. Functional contribution of elevated circulating and hepatic non-classical CD14CD16 monocytes to inflammation and human liver fibrosis. *PLoS One,* 5**,** e11049.

ZIMMERMANN, N., CONKRIGHT, J. J. & ROTHENBERG, M. E. 1999. CC chemokine receptor-3 undergoes prolonged ligand-induced internalization. *J Biol Chem,* 274**,** 12611-8.

ZOUDILOVA, M., MIN, J., RICHARDS, H. L., CARTER, D., HUANG, T. & DEFEA, K. A. 2010. beta-Arrestins scaffold cofilin with chronophin to direct localized actin filament severing and membrane protrusions downstream of protease-activated receptor-2. *J Biol Chem,* 285**,** 14318-29.